



THE UNIVERSITY  
*of* ADELAIDE

OXYGEN ISOTOPE RATIOS OF  
PHYTOLITHS AS A PROXY FOR  
PAST CLIMATES AND  
ENVIRONMENTS

Kimberley E. Edwards

Earth Sciences  
School of Physical Sciences  
University of Adelaide

This thesis is submitted in fulfilment of the requirements for  
the degree of Master of Philosophy



# Contents

Abstract.....	viii
<u>Originality Declaration</u> .....	x
<u>Acknowledgements</u> .....	xi
<b><u>Chapter 1: Introduction</u></b> .....	1
Abstract.....	2
1 Background information .....	2
1.1 Phytoliths.....	2
1.2 Oxygen isotope ratios.....	8
1.3 Knowledge gaps.....	12
2 Research Aims.....	15
3 Thesis outline .....	17
4 References .....	17
<b><u>Chapter 2: Phytolith extraction for oxygen isotope analysis: Method development</u></b> .....	25
Statement of Authorship .....	26
Abstract.....	28
1 Introduction .....	29
2 Methods and materials.....	32
2.1 Materials.....	32
2.2 Methods .....	33

2.3	Contamination assessment .....	44
3	Results and Discussion .....	46
3.1	Preparation of plant samples for phytolith extractions.....	46
3.2	Phytolith extractions .....	48
4	Conclusion.....	63
5	References .....	64

**Chapter 3: A revised method for the dehydroxylation of biogenic silica prior to oxygen**

<u>isotope analyses</u> .....	68
Statement of Authorship .....	69
Abstract.....	71
1 Introduction .....	72
2 Materials and methods.....	73
2.1 Materials.....	73
2.2 Dehydroxylation and IRMS comparison.....	74
2.3 Calculated oxygen yield.....	78
2.4 Oxygen isotope calibration.....	79
3 Results.....	79
3.1 Preliminary testing of the EAD method .....	79
3.2 EAD and IFD methods.....	80
3.3 $\delta^{18}\text{O}$ values of exchangeable oxygen .....	81
4 Discussion .....	82
4.1 Preliminary testing of the EAD method .....	82

4.2	Inaccuracies of both EAD and IFD methods .....	83
4.3	Online EAD versus offline IFD methods.....	84
4.4	Analysis of exchangeable oxygen .....	86
5	Conclusion.....	87
6	References .....	87
<b><u>Chapter 4: Oxygen isotope ratios of phytoliths from modern grasses and soil along a</u></b>		
<b><u>latitudinal transect of Australia and their correlation with climate.....</u></b>		
	Statement of Authorship .....	90
	Abstract.....	92
1	Introduction .....	94
2	Methods.....	96
2.1	Site locations .....	96
2.2	Materials for natural transect study .....	100
2.3	Phytolith extraction from plants .....	101
2.4	Phytolith extraction from soils along natural transect.....	101
2.5	Contamination assessment .....	102
2.6	Dehydroxylation and oxygen isotope analysis of phytoliths.....	103
2.7	Climate data.....	105
2.8	Phytolith oxygen isotope ratio modelling .....	105
2.9	Statistical analyses.....	107
3	Results.....	108
3.1	Plant phytolith oxygen isotope ratios .....	108

3.2	Plants vs climate .....	111
3.3	Soil phytolith oxygen isotope ratios.....	113
3.4	Soil vs climate .....	114
3.5	Plants vs soil .....	115
3.6	Modelled source water and phytolith $\delta^{18}\text{O}$ values .....	116
4	Discussion .....	121
4.1	Variability of plant phytolith oxygen isotope ratios within a site .....	121
4.2	Oxygen isotope ratios of phytoliths compared to climate along the transect ....	122
4.3	Phytolith oxygen isotope ratios from soil vs plant.....	127
4.4	Craig Gordon modelling and predicted phytolith $\delta^{18}\text{O}$ values. ....	128
5	Conclusions.....	131
6	References .....	131
	<b><u>Chapter 5: Conclusion</u></b> .....	136
	Conclusion.....	137
	Future research.....	140
1.	Extraction methods.....	140
2.	Dehydroxylation.....	141
3.	Phytolith oxygen isotope analysis .....	142
	Summary.....	143
	References .....	144
	<b><u>Appendix 1</u></b> .....	145

<u>Appendix 2</u> .....	153
<u>Appendix 3</u> .....	156

## Abstract

Past climate and vegetation records are essential to understand the natural range of environmental variability over timescales beyond the instrumental era. Tracers of past climate change are especially needed for arid regions, which are disproportionately sensitive to global climate warming, yet poorly represented in palaeoclimate archives. The oxygen isotope ratios ( $^{18}\text{O}/^{16}\text{O}$ ) of phytoliths (silica microfossils produced by plants) hold the potential to serve as a new proxy for past climates in dry environments, namely for temperature and relative humidity. To use this novel proxy, it is necessary to extract phytoliths of sufficient purity for oxygen isotope analysis and to have a deep understanding of the processes controlling the oxygen isotope signature of the phytoliths in sediments. The aims of this thesis are to improve the methods for extraction and analysis of oxygen isotope ratios of phytoliths, and to quantify the relationship between climate and the oxygen isotope ratios to interpret variations.

The oxygen isotope analysis of biogenic silica requires high purity samples. To improve and optimise phytolith extraction from plants and soils for oxygen isotope analysis, several methods were tested and compared to a novel approach using non thermal plasma ashing generated by radio frequency excitation of air under vacuum. Residual contamination was assessed using microscopy and Fourier Transform infrared-spectrometry modelling. Plasma ashing was found to have potential for organic material removal from plants, however the procedure is currently time consuming and requires further improvements to become a routine procedure. For extracting soil phytoliths, an added step of sulphuric acid and hydrogen peroxide (Piranha solution), normally reserved for extracting phytoliths from plants, produced samples with the required purity.



Biogenic silica (e.g., diatoms and phytoliths) contains exchangeable oxygen that can affect the accuracy of isotopic analysis. The processes to account for this exchangeable oxygen require specialised equipment that is not always available. A novel approach for silica dehydroxylation was developed, involving sample heating and fluorination in an Elemental Analyser, a common piece of isotope analysis equipment. In situ high temperature dehydroxylation was found to adequately replicate established oxygen isotope ratios for international silicate standards and can be used for silica samples as small as 600  $\mu\text{g}$ .

To be able to use phytolith oxygen isotope ratios as a palaeoclimate proxy, the impact of climate needs to be understood. To do this, measured phytolith oxygen isotope ratios from plants and soils from a transect across Australia were analysed. Modern plant phytolith oxygen isotope ratios did not exhibit the expected strong correlations with climate, but oxygen isotopes in soil phytoliths did, correlating strongly with mean warmest period relative humidity at the maximum temperature and the mean annual temperature. The oxygen isotope ratios of phytoliths from plants and soils could be successfully predicted using Craig Gordon leaf water modelling and temperature-dependant silica fractionation, indicating that the key environmental processes are well characterised. The oxygen isotope composition of fossilised plant phytoliths provides the potential to make qualitative inference of climate change. However, the influence of multiple climate variables means that the method would be best employed within a multi-proxy framework.



## Originality Declaration

I certify that this work contains no material which has been accepted for the award of any other degree or diploma in my name in any university or other tertiary institution and, to the best of my knowledge and belief, contains no material previously published or written by another person, except where due reference has been made in the text. In addition, I certify that no part of this work will, in the future, be used in a submission in my name for any other degree or diploma in any university or other tertiary institution without the prior approval of the University of Adelaide and where applicable, any partner institution responsible for the joint award of this degree.

The author acknowledges that copyright of published works contained within the thesis resides with the copyright holder(s) of those works.

I give permission for the digital version of my thesis to be made available on the web, via the University's digital research repository, the Library Search and also through web search engines, unless permission has been granted by the University to restrict access for a period of time.

I acknowledge the support I have received for my research through the provision of an Australian Government Research Training Program Scholarship.

## Acknowledgements

I would like to thank my official supervisors Francesca McInerney, Jonathan Tyler, and Alexander Francke. This was the dream team, with each supervisor having their own very different strengths and they all worked beautifully together and most importantly, with me. Cesca, what would I have done without you? Thank you for fighting to be my supervisor, believing in me, encouraging me and supporting me every single step of the way. Jon, thanks for stepping up last minute to jump on board as my supervisor. You replied to my emails way more than I was expecting but don't forget you still owe me a beer. Alex, thanks for being my go-to person to whinge to, I don't think this thesis would have been completed in time without your constant encouragement (and editing!).

To my unofficial supervisors, Robert Klæbe and Tony Hall. I thank you both for being there every time something went wrong and fixing it for me, for organising a lab for just me to work in, for finding me specialised safety gear that almost fit, and for constantly checking that I hadn't blown myself and the lab up.

Bryan Coad and Melanie Ford, thank you for introducing me to the most beautiful part of my research. The pink glow of plasma was the highlight of my research.

Wine time attendees, office mates, HDRs, and all the other Mawson building people, the insanity gave me sanity. Keep at it, you got this. #winetimeworks.

Family and friends, I don't know whether to curse you or thank you, either way, no matter the case, you all pushed me in the right direction – to becoming a mad scientist.

And to save the best for last, my husband Josh, without you I would not have achieved this.

It is not that I am not capable without you, but without your infectious enthusiasm for

science and your perseverance when things get tough, I wouldn't have even thought to pursue a career in science.



Chapter 1:  
Introduction

## Abstract

Understanding how recent and past climate has evolved is necessary to forecast future climate changes. A common means of inferring past climate is the analysis of oxygen isotope ratios, particularly in inorganic and biogenic carbonates, as well as in ancient ice and the organic remains of both plants and animals (Mann et al., 2008; Zielinski, 2000). Biogenic silica is a potential alternative to carbonate and organic materials as it is found in abundance in both marine and terrestrial sediments across the globe (Wallis, 2001). Of the types of biogenic silica, diatoms are the most abundant and studied, albeit restricted to aquatic environments (Leng and Barker, 2006). Phytoliths, passively produced silica structures in many higher plants, are also abundant silicate fossils, especially in dry regions such as the Australian arid zone, where they accumulate in wetland, fluvial and cave sediments (Baker, 1959; Hart, 1988; Jones, 1964). When plants decay, they leave behind phytoliths that can be preserved in sediments for millions of years (Currano et al., 2020; Prasad et al., 2005). Oxygen isotope analysis of phytolith silica therefore offers significant potential to be used as a proxy for changes in terrestrial ecosystems and environments. However, in order to realise this potential, it is necessary to first understand the modern processes that drive the oxygen isotope ratios in phytoliths.

## 1 Background information

### 1.1 Phytoliths

Phytoliths are silicate particles that precipitate inside many living plants. This can occur both inside cells and in intercellular spaces (Alexandre et al., 2012; Webb and Longstaffe, 2000). Phytoliths can range in size from 100 nm to over 500  $\mu\text{m}$  in size, are typically colourless and translucent, although they can be brown and opaque in appearance, and can have a range of densities from 1.5 to 2.3  $\text{g}/\text{cm}^3$  (Figure 1) (Nawaz et al., 2019; Piperno, 2006). The chemical



composition of phytolith silica is  $\text{SiO}_2 \cdot n\text{H}_2\text{O}$ , a hydrous opaline silica that can include occluded matter containing carbon, nitrogen, aluminium, and iron (Bartoli and Wilding, 1980).

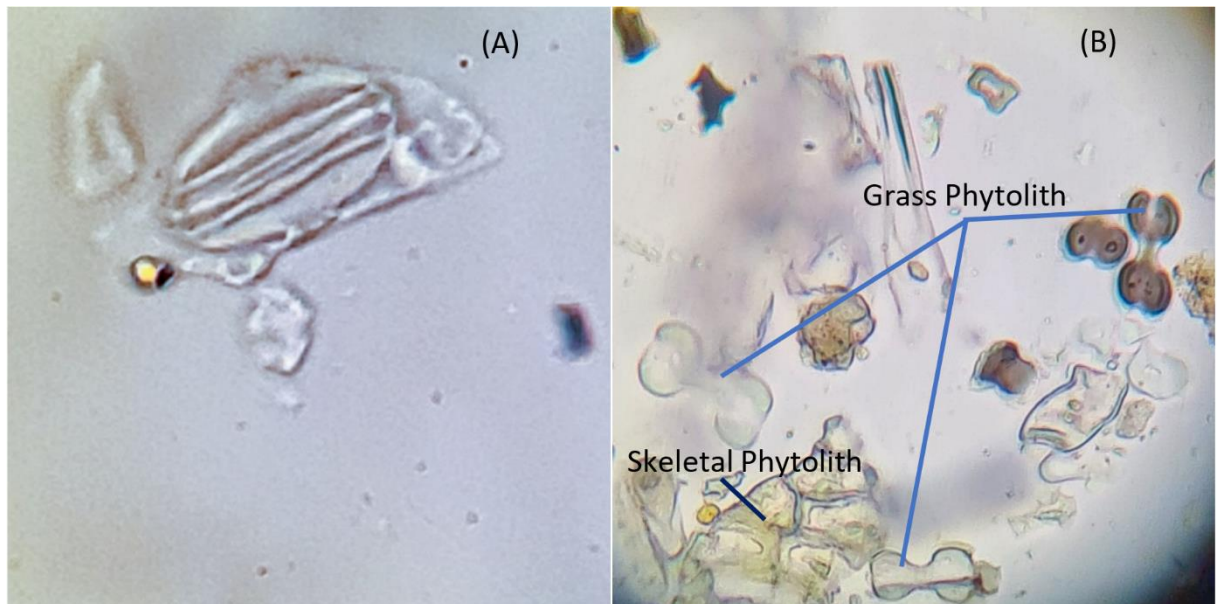


Figure 1 Preserved phytoliths from Australian topsoil. (A) Phytolith roughly 40 µm in size in the shape of a stomata. (B) Numerous phytoliths showing variation in colour, the grass phytoliths are approximately 15 µm long.

Phytoliths are found in many different groups of plants, but not all of them. Poaceae (grasses) are the most prolific producers of phytoliths, with all species synthesising phytoliths (Katz, 2014). However, other taxa are not so straightforward, with some species producing almost no phytoliths, and other species in the same genus producing almost as many as Poaceae (Katz, 2014). A study by An (2016) assessed phytoliths in 17 conifers and found that only 8 produced phytoliths, and there was no correlation with genus.

Plants do not need phytoliths, but studies have shown that they are beneficial. They can strengthen the plant by providing structural support, allowing it to grow taller and straighter (Law and Exley, 2011); they have a pesticidal effect by making it difficult for insects to attack the plant; they provide a physical barrier that prevents fungal infections (Datnoff and

Rodrigues, 2005); and they provide defence against herbivory as they make plants difficult to consume and digest (Garbuzov et al., 2011).

When a plant dies and decays, phytoliths are released into soils and following erosion and transportation, into sediments. Their chemical composition makes them resistant to dissolution and, under the right conditions, fossil phytoliths can be preserved for millions of years (Jones, 1964).

### *1.1.1 How phytoliths form*

The silica in phytoliths originates in soil. Monosilicic acid is leached into soil water, that is then transported into the plant via the roots and dispersed throughout the plant (Blackman and Parry, 1968; Shone, 1964). The silica from this acid is not used in any metabolic pathways, but there is evidence of genes directing silica to certain parts in some plants and causing it to precipitate before reaching saturation (Kumar et al., 2017; Law and Exley, 2011; Nawaz et al., 2019). Alternatively, silica builds up throughout the plant as silica gel, before precipitating as phytoliths at saturation (Exley, 2009; Kaufman et al., 1981; Sharma et al., 2019). It takes time for the silica gel to reach saturation, so phytoliths are usually produced in mature tissue near the end of a growing season. As more water is transpired through the stomata, water and silica are drawn up through the plant's roots into the transpiring tissue. The more water is transferred through the tissue, the more silica accumulates and precipitates as phytoliths, which results in more phytoliths being formed in transpiring tissue than in non-transpiring tissue (Hutton and Norrish, 1974; Kumar et al., 2017). Plants of the same species growing in low humidity produce more phytoliths than plants in high humidity as they draw up more silica and water (Santosh et al., 2017; Webb and Longstaffe, 2002). Silica can make up from 0.1% to over 10% of a plant's dry weight (Epstein, 1994).

Phytoliths can form anywhere in the plant where silica has accumulated, their shape and size are determined by where they have formed. If the phytolith precipitates out at the base of a hair follicle, then it will take that shape (Kealhofer and Piperno, 1998). If silica builds up in the plant and phytoliths form along the surface of several cells, then it will form a skeletal cast of those cells (Rosen, 1992). This means that many phytoliths will look the same across different species, as plant structures can be very similar. For example, stomata appear very similar across most plant species, so the phytoliths that fill stomata guard cells will look similar (Figure 1.A) (Kealhofer and Piperno, 1998). This also means that plants with unique traits can create unique phytoliths such as the bone-shaped phytoliths (Figure 1.B) produced in grasses (Geis, 1978). The morphology of unique phytoliths and assemblages of more common phytoliths are frequently studied (An, 2016; Hongyan et al., 2018; Novello et al., 2017; Rashid et al., 2019; Sharma et al., 2019; Strömberg, 2004).

### *1.1.2 Preservation of phytoliths*

Phytoliths can accumulate and be preserved in diverse sedimentary environments, including caves and rock shelters, lakes, wetlands, and marine sediments (Currano et al., 2020; Esteban et al., 2023; Jones, 1962; Jones, 1964; Jones et al., 1963; Strömberg et al., 2018). Many taphonomic processes affect the preservation of phytoliths, such as environment, soil type, pH, temperature, dissolution, and transport – both spatially and vertically (Borrelli et al., 2010; Hart, 2016; Nawaz et al., 2019; Prentice and Webb, 2016; Strömberg et al., 2018). Morphology also affects preservation, with small irregular-shaped phytoliths more likely to undergo dissolution, which in turn causes preservation bias. Small phytoliths are also likely to be transported through aeolian processes (Fishkis et al., 2010). Phytoliths are often abundant in soils where they can make up to 20% of the soil volume, though this often decreases with greater soil depth (Borrelli et al., 2010). The younger phytoliths are at the top

of the soil profile, and older phytoliths are found at greater depths (Hart and Humphreys, 2004).

In tropical environments, phytolith turnover in topsoil can be as short as 6-18 months, whereas in semiarid grasslands it can be as long as 250-1300 years (Borrelli et al., 2010). Taphonomic processes tend to favour the preservation of grass phytoliths over other phytoliths, which can be beneficial as phytoliths produced in grasses generally develop annually as opposed to tree phytoliths which form over much longer periods (Rashid et al., 2019). The variation in preservation makes it important to properly understand the depositional environment to be able to understand the phytolith record. Despite these issues, studies using morphology show that point sampling from the A-horizon still gives an accurate representation of phytoliths from local vegetation (Crifò and Strömberg, 2020).

### *1.1.3 Palaeo-research using phytolith morphology*

Most research on phytoliths has been in the fields of botany and archaeology, which have focused on the morphology of phytoliths (Hart, 2016; Hodson, 2016; Neumann et al., 2017; Piperno, 2006; Strömberg et al., 2018). Phytoliths have been used in palaeoenvironment reconstructions by using morphology, size, and abundance to reconstruct past climates and plant communities (Currano et al., 2020; Hongyan et al., 2018; Kealhofer and Piperno, 1998; Novello et al., 2017; Piperno, 2006; Rashid et al., 2019; Strömberg, 2004; Strömberg et al., 2018). This has been less successful in Australia, perhaps due to the native flora having fewer diverse and unique phytoliths, taphonomic processes moving phytoliths spatially, and a general lack of research conducted across Australia (Hart, 1988; Wallis, 2013).

Phytoliths, which are frequently found with human and animal remains (Neumann et al., 2017), have been used by archaeologists for many years to gain insight into human plant use

over time. In cave sediments, phytolith morphological studies have been conducted to understand the types of plants that were being used by human occupiers (Piperno, 2006). Dental calculus has been another source of phytoliths for researchers to assess the type of vegetation consumed (Henry et al., 2011). Baskets made of plant material have been analysed for phytoliths to reconstruct the types of plants used. Plant domestication has been investigated using various plants such as rice to see when different variants were farmed (Ball et al., 2016; Rashid et al., 2019; Strömberg et al., 2018). Additionally, phytoliths extracted from carbonised food residue on pottery were used to work out the expansion of maize in human food diets over the last 2500 years (Raviele, 2011). With regard to palaeo-environmental reconstructions, studies have used the morphological assemblages of phytoliths to infer changes in plant abundance and taxonomic composition over time (Crifò and Strömberg, 2020; Hongyan et al., 2018; Mercader et al., 2009; Mercader et al., 2019; Novello et al., 2017; Rashid et al., 2019; Strömberg, 2004; Thorn, 2004; Wallis, 2013).

There is developing interest in using the isotopic composition of phytolith silica and occluded organic matter for reconstructing past environments (Alexandre et al., 2012; Hodson, 2016; Hodson et al., 2008; Roy et al., 2020; Smith, 2004; Webb and Longstaffe, 2002). As technology has improved, smaller samples can be analysed more accurately and precisely, and as the equipment becomes more accessible, the number of publications focusing on the chemistry of phytoliths, in particular oxygen isotope ratios, has increased in recent years (Hodson, 2016; Roy et al., 2020; Sutton et al., 2018; Zancajo et al., 2019). Isotopes of silicon, oxygen, and carbon have been the main focus in phytoliths, both individually and in comparison, to each other (Hodson et al., 2008; Shahack-Gross et al., 1996). The carbon in occluded organic matter in phytoliths has proven useful for differentiating the grass type

that phytoliths found in sediments have come from (C<sub>3</sub> or C<sub>4</sub>) and for radiocarbon dating (Bird et al., 2020; McInerney et al., 2011; Roy et al., 2020; Smith, 2004).

<sup>18</sup>O/<sup>16</sup>O isotope ratios of phytoliths from modern plant material has been shown to correlate with relative humidity and temperature, providing potential for phytoliths to be used as a quantitative palaeoclimate proxy (Alexandre et al., 2018; Shahack-Gross et al., 1996; Webb and Longstaffe, 2002). In Australia, wood phytoliths in tropical Queensland soils were analysed for oxygen isotope ratios, including a novel investigation of oxygen-17 incorporation (Alexandre et al., 2012; Alexandre et al., 2019; Alexandre et al., 2018).

## 1.2 Oxygen isotope ratios

This thesis focuses on the application of oxygen isotope analyses to phytoliths. There are three stable oxygen isotopes: oxygen-16 (<sup>16</sup>O), oxygen-17 (<sup>17</sup>O), and oxygen-18 (<sup>18</sup>O). The lighter <sup>16</sup>O is the most abundant isotope, making up 99.76% of oxygen atoms. <sup>17</sup>O is the least abundant isotope with 0.04%, and the heavier <sup>18</sup>O has an abundance of 0.2%. The ratio of <sup>18</sup>O/<sup>16</sup>O is most commonly used in palaeoclimate research, commonly reported as δ<sup>18</sup>O (‰) values, calculated as:

$$\delta^{18}\text{O} = \frac{\left(\frac{^{18}\text{O}}{^{16}\text{O}} \text{ Sample}\right) - \left(\frac{^{18}\text{O}}{^{16}\text{O}} \text{ Standard}\right)}{\left(\frac{^{18}\text{O}}{^{16}\text{O}} \text{ Standard}\right)} \times 1000$$

(1)

### 1.2.1 Oxygen isotope fractionation before it is taken up by a plant

The oxygen in phytoliths originates as meteoric water. Rainfall infiltrates soils, and plants take up soil water via their roots (Webb and Longstaffe, 2003). Variability in the δ<sup>18</sup>O values of rainfall is affected by a range of processes, commonly linked to the progressive Rayleigh

distillation of water vapour between the evaporative source (predominantly ocean surface water) and the point of precipitation (Dansgaard, 1964). Variability in the  $\delta^{18}\text{O}$  of precipitation has been observed to correlate with latitude, altitude, distance from the coast, air temperature, precipitation amount, and changes in the source and trajectory of atmospheric circulation (Hollins et al., 2018; Munksgaard et al., 2012). Following precipitation, the  $\delta^{18}\text{O}$  values of surface meteoric water are further altered by evaporation, which in turn depends on surface water residence time, temperature, wind strength, and humidity (Allison et al., 1983; Barnes and Allison, 1983; Bowen et al., 2019). The extent to which soil waters are evaporated is strongly influenced by the infiltration rate and hence the permeability of the soil. The depth from which a plant draws up water through its root system also affects the  $\delta^{18}\text{O}$  value of the water it utilises (Von Freyberg et al., 2020).

### *1.2.2 Oxygen isotope fractionation within a plant*

Once the water is inside a plant, the  $\delta^{18}\text{O}$  value of the water is further fractionated. Most research on the stable  $\delta^{18}\text{O}$  values of phytoliths has focused on the fractionation process within plants, generally on grasses as they are fast growing and one of the biggest phytolith producers (Katz, 2014; Rashid et al., 2019). Research has shown that the  $\delta^{18}\text{O}$  values of stem water is similar to the  $\delta^{18}\text{O}$  values of soil water, but when water is relocated to transpiring parts of the plant, such as leaves, it becomes isotopically fractionated (Farris and Strain, 1978; Webb and Longstaffe, 2000). Water molecules with lighter oxygen isotopes ( $^{16}\text{O}$ ) are removed through transpiration (evaporation through stomata) more readily than those with heavier oxygen isotopes ( $^{18}\text{O}$ ), thus creating an enrichment of  $^{18}\text{O}$  in leaf water (Farris and Strain, 1978; Flanagan et al., 1991). Stem water  $\delta^{18}\text{O}$  values remain relatively stable while the pool of enriched water in a leaf or other transpiring tissue can change rapidly based on outside conditions, mainly due to changes in relative humidity (Alexandre et al., 2012;

Alexandre et al., 2018; Cernusak et al., 2016; Farris and Strain, 1978). Webb and Longstaffe (2000) found the  $\delta^{18}\text{O}$  value of leaf water in grasses can be as much as 28 ‰ higher than  $\delta^{18}\text{O}$  value of stem water and other studies have shown similar values in other families of plants, showing increasing degree of enrichment with decreasing relative humidity (Cernusak et al., 2022; Flanagan et al., 1993; Zhao et al., 2014).

Leaf water  $\delta^{18}\text{O}$  values can be predicted using a modified Craig and Gordon evaporation model (Cernusak et al., 2016; Craig and Gordon, 1965), which takes into consideration equilibrium and kinetic fractionation as well as relative humidity which is one of the main factors effecting the degree of enrichment of  $^{18}\text{O}$ . It has been observed that this model often produces a greater  $^{18}\text{O}$  enrichment than that observed in experiments (Barbour et al., 2000). This suggests that leaf water comes from two pools of water, one of which is enriched during transpiration and another of which is the same as stem water; therefore, leaf water is the mixture of the water it gets from these two sources (Farquhar and Lloyd, 1993).

### *1.2.3 Oxygen isotope composition of phytoliths*

The  $\delta^{18}\text{O}$  value of phytoliths is determined by the  $\delta^{18}\text{O}$  value of the plant water and the fractionation of oxygen isotopes between silicic acid and water, which varies with temperature with a coefficient between -0.2 and -0.4‰/°C (Alexandre et al., 2012; Clayton and Epstein, 1958; Juillet-Leclerc and Labeyrie, 1987; Shahack-Gross et al., 1996). The  $\delta^{18}\text{O}$  value of a phytolith is consequently dependent on where in the plant the phytolith is precipitated and temperature at the site of precipitation. Several studies of plants grown in controlled conditions show that the  $\delta^{18}\text{O}$  values of phytoliths formed in non-transpiring tissue such as roots and stems correlate with temperature (Shahack-Gross et al., 1996; Webb and Longstaffe, 2000). Phytoliths formed in transpiring tissue such as leaves, sheaths, and inflorescence have  $\delta^{18}\text{O}$  values which reflect a combination of temperature and relative



humidity. Phytoliths in transpiring tissue have been found to be enriched in  $^{18}\text{O}$  but are closer to  $^{18}\text{O}$  values of stem water rather than the highest values recorded in leaf water, which suggests that they record an average of the  $\delta^{18}\text{O}$  values of water over time (Alexandre et al., 2019; Alexandre et al., 2018; Webb and Longstaffe, 2000; Webb and Longstaffe, 2002, 2003; Webb and Longstaffe, 2006).

Relative humidity can affect the volume of phytoliths within plants. In general, the more evapotranspiration occurs, the more water and silica is acquired by the plant (Hutton and Norrish, 1974). Transpiring tissue is the “end of the line” for water flow through the plant, so more silica builds up and precipitates in transpiring tissue rather than non-transpiring tissue (Alexandre et al., 2019; Webb and Longstaffe, 2003). This process also causes isotopic fractionation in the transpiring tissue. As evapotranspiration draws water out of the leaves, it draws more  $^{16}\text{O}$  out than  $^{18}\text{O}$ . The degree of enrichment is controlled by relative humidity, with more enrichment at lower relative humidity. This fractionation occurs in line with the normal silica temperature fractionation process of  $^{16}\text{O}$  and  $^{18}\text{O}$  (Shahack-Gross et al., 1996). Webb and Longstaffe (2000) sampled grasses from a transect across Canada and showed it was possible to reconstruct the temperature from phytoliths from non-transpiring tissue of grasses growing in nature at the time of their growth. Webb and Longstaffe (2000) also showed that reconstructing climate from the phytoliths of transpiring tissue was not so simple, though there were clear trends of the  $\delta^{18}\text{O}$  values with the average relative humidity of the growing season. Numerous studies of the  $\delta^{18}\text{O}$  values of plant phytoliths have focused on phytoliths from different parts of the plants to better understand what is occurring in the different tissues (Alexandre et al., 2019; Alexandre et al., 2018; Outrequin et al., 2021; Shahack-Gross et al., 1996; Webb and Longstaffe, 2000).

In summary, it is to be expected that phytolith  $\delta^{18}\text{O}$  values reflect a combination of leaf water  $\delta^{18}\text{O}$  values, which in itself is largely a function of relative humidity, and the effect of temperature on silica-water oxygen isotope fractionation. This combination could provide significant value for palaeoenvironmental research however, there remains a need to empirically validate this interpretive framework. Therefore,  $\delta^{18}\text{O}$  values in phytoliths could be used as a proxy for both temperature and relative humidity (Alexandre et al., 2006; Alexandre et al., 2018; Webb and Longstaffe, 2000). At this stage, separating transpiring tissue phytoliths from non-transpiring tissue phytoliths when they have been mixed in sediments is not possible. Understanding the  $\delta^{18}\text{O}$  values of bulk phytoliths from soils is therefore key to using phytoliths as a climate proxy.

### 1.3 Knowledge gaps

There have been substantial efforts devoted to understanding phytolith production and variation in morphological assemblages for the application of studies in the palaeo-record (An, 2016; Geis, 1973; Geis, 1978; Katz, 2014; Mercader et al., 2009; Nawaz et al., 2019; Sharma et al., 2019; Wallis, 2003; Yang et al., 2015). Despite extensive research into phytolith morphology, there has been no consensus on a set of methods for extracting phytoliths from soils and plants, as no method developed yet can be used in every study. The most common methods involve acid digestion, dry ashing, or microwave digestion to remove organic material (Piperno, 2006; Roy et al., 2020). There are several issues with these methods, such as the use of hazardous chemicals, physical and chemical alteration and dissolution of the phytoliths or simply not being able to remove all organic matter or clay from the samples (Chapligin et al., 2011; Corbineau et al., 2013; Crespín et al., 2008; Evett and Cuthrell, 2017; Hart, 2016; Jakes and Mitchell, 1996; Lentfer and Boyd, 1999; Piperno, 2006; Roy et al., 2020; Zhao and Pearsall, 1998).

The methods for extracting phytoliths and other forms of biogenic silica (such as diatoms) from sediments are similar and often interchangeable. Many of the methods have been used for decades and were established when morphology and counting were the focus of the research. There has been a growing interest in the carbon isotope ratios of phytoliths as a dating tool in archaeological sites and for palaeoreconstruction which has resulted in some studies assessing extraction methods for the aim of carbon isotope ratio studies (Chapligin et al., 2011; Piperno, 2006; Roy et al., 2020; Saccone et al., 2007), but so far, no dedicated study has been done with the aim of developing and testing the extraction methods for oxygen isotope analysis.

Many of these methods are unsuitable for the oxygen analysis of biogenic silica as biogenic silica has exchangeable oxygen that at high temperatures (90 degrees or higher) will cause these weaker bonds to change to stronger bonds (Crespin et al., 2008; Tyler et al., 2017). Processes to remove the exchangeable oxygen, which need to be excluded during oxygen isotope analyses, are then unable to remove the now strongly bonded oxygen that could have exchanged with the environment since formation, thus permanently changing the isotopic ratios. For oxygen isotope studies, this excludes any methods that use high temperatures such as dry ashing. Standard chemical extraction methods for biogenic silica such as hydrogen peroxide can yield satisfying results of removing contaminants when carried out at high temperatures, but at lower temperatures fresher organic matter does not get fully digested (Mikutta et al., 2005). Plasma ashing has been suggested as a possible extraction method of phytoliths (Jakes and Mitchell, 1996) and has been used to clean diatoms (Jain et al., 2022; Saad et al., 2020). Bird et al. (2010) had success using oxygen plasma ashing as a pre-treatment on wood and charcoal for carbon isotope measurements instead of using chemicals to remove organic contaminants. A study on cleaning carbonate

for clumped isotopes showed that low temperatures of plasma ashing did not affect the  $\delta^{18}\text{O}$  values of the carbonate (Adlan et al., 2020) though this has not been tested to see if it effected the oxygen isotopes of silicates.

Other non-temperature related issues with extraction methods generally revolve around the fact that most phytolith research does not need a clean sample. Remnant quartz, clay, organic matter, and charcoal have no effect on the results of morphological analysis through a microscope, for example. This is not the case for isotope ratio studies where contamination of over 3% can not only alter the isotopic readings but could also result in damage to expensive analytical equipment (Leng and Barker, 2006).

The  $\delta^{18}\text{O}$  values of phytoliths and their correlation with climate parameters is a relatively new field, so much research is still needed to understand the basics. Studies have focused on the  $\delta^{18}\text{O}$  values in the phytoliths of specific tissues of living plants, and all have focused on one or two species of grasses only (Alexandre et al., 2019; Alexandre et al., 2018; Hodson et al., 2008; Outrequin et al., 2021; Shahack-Gross et al., 1996; Webb and Longstaffe, 2000; Webb and Longstaffe, 2002, 2003; Webb and Longstaffe, 2006). It is unknown if there are differences in  $\delta^{18}\text{O}$  values amongst different taxa. Plants that grow at the same location, at the same time may have a different  $\delta^{18}\text{O}$  value, which could confound the isotope signal seen in phytoliths in soils and sediments. Comparing the  $\delta^{18}\text{O}$  values of phytoliths from multiple species growing at the same time and location would reveal any variations. These variations could be attributed to fractionation among species or differences in  $\delta^{18}\text{O}$  values of the water resulting from water uptake at different soil depths. D'Agostini et al. (2022) showed that phytolith accumulation could be different among C4 plants, it is unknown if this could result in differences in the  $\delta^{18}\text{O}$  values of phytoliths in C3 and C4 plants grown at the same site.

Only Alexandre et al. (2012) and Alexandre et al. (2018) have investigated the oxygen isotopic composition of phytoliths in soils. Alexandre et al. (2012) focused on phytoliths in rainforest topsoil across a transect in tropical Queensland, Australia. The aim was to see if there was an altitudinal effect on the isotope ratios of phytoliths, so they focused on wood phytoliths, which were expected to record the  $\delta^{18}\text{O}$  value of stem water/soil water. It was found that there was a correlation between phytolith  $\delta^{18}\text{O}$  values and long-term relative humidity, indicating that there was still a significant amount of phytoliths from transpiring tissue in the samples. After accounting for grass phytoliths, which would mainly originate from transpiring tissue, thus recording relative humidity, they found phytolith assemblages from rainforests reflect changes in mean annual temperatures and  $\delta^{18}\text{O}$  value of precipitation (Alexandre et al. 2012). Alexandre et al. (2018) looked at phytolith  $\delta^{18}\text{O}$  values from soils across Africa, which showed no correlation with climate data. It was suggested that the lack of correlation was due to aeolian processes causing the mixing of phytoliths from different regions. However, a closer examination of the methods for extracting the phytoliths showed many of the samples had been treated at 90 degrees, which is known to affect the  $\delta^{18}\text{O}$  values (Alexandre et al., 1997; Alexandre et al., 2018; Bremond et al., 2005; Crespin et al., 2008). As such, these results should be treated with caution. The soil phytolith data from Alexandre et al. (2018) has also been used in Outrequin et al. (2021).

## 2 Research Aims

The central objective of this thesis is to assess the extent to which  $\delta^{18}\text{O}$  values of bulk phytoliths from topsoils reflect climate. However, in the process of preparing and analysing the phytoliths, it became apparent that established phytolith extraction methods were not suitable for the soil samples used in this study, despite them having been used for oxygen isotope analysis previously. As a result, a large focus of this thesis is dedicated to establishing

better methods for extracting phytoliths from soils and sediments for  $\delta^{18}\text{O}$  value analysis.

The research aims for improved extraction methods for oxygen isotope analysis of phytoliths are:

- To determine how to obtain phytolith extracts with minimal residual contamination to enable oxygen isotope analysis.
- To investigate if plasma ashing can be used to extract phytoliths with the required purity for oxygen isotope analysis.
- To establish a cheap, efficient, non-destructive way of testing for residual contamination in phytolith samples.

Furthermore, an alternative method for dehydrating and dehydroxylating biogenic silica in equipment readily accessible in standard isotope laboratories is investigated. This was prompted when the specialised equipment used for this process was inoperable while replacement parts were sourced. The research aims for the dehydroxylation study are:

- To develop and test a methodology for dehydroxylating biogenic silica than can be completed without expensive specialised equipment.
- To decrease the volume of biogenic silica required for oxygen isotope ratio analyses.

After the successful extraction and isotopic analysis of phytoliths from both plants and soils at locations along a latitudinal transect across Australia, the central objective of this thesis was able to be addressed. The research aims for assessing the extent to which  $\delta^{18}\text{O}$  values of bulk phytoliths from topsoils reflect climate are:

- To test whether phytoliths from different species of grass at the same location have similar  $\delta^{18}\text{O}$  values to one another.

- To investigate whether plant and soil phytolith  $\delta^{18}\text{O}$  values reflect the combined effects of relative humidity on leaf water isotope ratios and temperature on silica-water isotope fractionation during phytolith formation.
- To determine whether it is possible to use Craig-Gordon modelling of the environmental controls on leaf water  $\delta^{18}\text{O}$  value, combined with temperature-sensitive fractionation during silica precipitation to predict phytolith  $\delta^{18}\text{O}$  values in plants and soils.

### 3 Thesis outline

This thesis has five chapters.

This chapter: Introduction, including general background on phytoliths and oxygen isotopes in phytolith silica; research aims, thesis outline.

Chapter 2: Phytolith extraction for oxygen isotope analysis: Method development.

Chapter 3: A revised method for the dehydroxylation of biogenic silica prior to oxygen isotope analyses.

Chapter 4:  $\delta^{18}\text{O}$  values of phytoliths from modern grasses and soil along a latitudinal transect of Australia and their correlation with climate.

Chapter 5: Conclusion and future research.

### 4 References

- Adlan Q., Davies A. J. and John C. M. (2020) Effects of oxygen plasma ashing treatment on carbonate clumped isotopes. *Rapid Commun Mass Spectrom* **34**, e8802.
- Alexandre A., Meunier J.-D., Colin F. and Koud J.-M. (1997) Plant impact on the biogeochemical cycle of silicon and related weathering processes. *Geochim Cosmochim Acta* **61**, 677-682.
- Alexandre A., Crespin J., Sylvestre F., Sonzogni C. and Hilbert D. W. (2012) The oxygen isotopic composition of phytolith assemblages from tropical rainforest soil tops

- (Queensland, Australia): validation of a new paleoenvironmental tool. *Clim Past* **8**, 307-324.
- Alexandre A., Basile-Doelsch I., Sonzogni C., Sylvestre F., Parron C., Meunier J.-D. and Colin F. (2006) Oxygen isotope analyses of fine silica grains using laser-extraction technique: Comparison with oxygen isotope data obtained from ion microprobe analyses and application to quartzite and silcrete cement investigation. *Geochim Cosmochim Acta* **70**, 2827-2835.
- Alexandre A., Webb E., Landais A., Piel C., Devidal S., Sonzogni C., Couapel M., Mazur J.-C., Pierre M., Prié F., Vallet-Coulomb C., Outrequin C. and Roy J. (2019) Effects of leaf length and development stage on the triple oxygen isotope signature of grass leaf water and phytoliths: insights for a proxy of continental atmospheric humidity. *Biogeosciences* **16**, 4613-4625.
- Alexandre A., Landais A., Vallet-Coulomb C., Piel C., Devidal S., Pauchet S., Sonzogni C., Couapel M., Pasturel M., Cornuault P., Xin J., Mazur J.-C., Prié F., Bentaleb I., Webb E., Chalié F. and Roy J. (2018) The triple oxygen isotope composition of phytoliths as a proxy of continental atmospheric humidity: insights from climate chamber and climate transect calibrations. *Biogeosciences* **15**, 3223-3241.
- Allison G. B., Barnes C. J. and Hughes M. W. (1983) The distribution of deuterium and  $^{18}\text{O}$  in dry soils 2. Experimental. *Journal of Hydrology* **64**, 377-397.
- An X. (2016) Morphological characteristics of phytoliths from representative conifers in China. *Palaeoworld* **25**, 116-127.
- Baker G. (1959) Opal phytoliths in some Victorian soils and "red rain" residues. *Australian Journal of Botany* **7**, 64-87.
- Ball T., Chandler-Ezell K., Dickau R., Duncan N., Hart T. C., Iriarte J., Lentfer C., Logan A., Lu H., Madella M., Pearsall D. M., Piperno D. R., Rosen A. M., Vrydaghs L., Weisskopf A. and Zhang J. (2016) Phytoliths as a tool for investigations of agricultural origins and dispersals around the world. *J Archaeol Sci* **68**, 32-45.
- Barbour M. M., Schurr U., Henry B. K., Wong S. C. and Farquhar G. D. (2000) Variation in the Oxygen Isotope Ratio of Phloem Sap Sucrose from Castor Bean. Evidence in Support of the Pécelet Effect1. *Plant Physiology* **123**, 671-680.
- Barnes C. J. and Allison G. B. (1983) The distribution of deuterium and  $^{18}\text{O}$  in dry soils: 1. Theory. *Journal of Hydrology* **60**, 141-156.
- Bartoli F. and Wilding L. P. (1980) Dissolution of Biogenic Opal as a Function of its Physical and Chemical Properties. *Soil Sci Soc Am J* **44**, 873-878.
- Bird M. I., Charville-Mort P. D. J., Ascough P. L., Wood R., Higham T. and Apperley D. (2010) Assessment of oxygen plasma ashing as a pre-treatment for radiocarbon dating. *Quat Geochronol* **5**, 435-442.
- Bird M. I., Haig J., Hadeen X., Rivera-Araya M., Wurster C. M. and Zwart C. (2020) Stable isotope proxy records in tropical terrestrial environments. *Palaeogeography, Palaeoclimatology, Palaeoecology* **538**, 109445.
- Blackman E. and Parry D. W. (1968) Opaline Silica Deposition in Rye (*Secale cereale* L.). *Annals of Botany* **32**, 199-206.
- Borrelli N., Alvarez M. F., Osterrieth M. L. and Marcovecchio J. E. (2010) Silica content in soil solution and its relation with phytolith weathering and silica biogeochemical cycle in Typical Argiudolls of the Pampean Plain, Argentina—a preliminary study. *J Soil Sediment* **10**, 983-994.



- Bowen G. J., Cai Z., Fiorella R. P. and Putman A. L. (2019) Isotopes in the Water Cycle: Regional- to Global-Scale Patterns and Applications. *Annu Rev Earth Pl Sc* **47**, 453-479.
- Bremont L., Alexandre A., Peyron O. and Guiot J. (2005) Grass water stress estimated from phytoliths in West Africa. *Journal of Biogeography* **32**, 311-327.
- Cernusak L. A., Barbour M. M., Arndt S. K., Cheesman A. W., English N. B., Feild T. S., Helliker B. R., Holloway-Phillips M. M., Holtum J. A. M., Kahmen A., McInerney F. A., Munksgaard N. C., Simonin K. A., Song X., Stuart-Williams H., West J. B. and Farquhar G. D. (2016) Stable isotopes in leaf water of terrestrial plants. *Plant, Cell & Environment* **39**, 1087-1102.
- Cernusak L. A., Barbeta A., Bush R. T., Eichstaedt R., Ferrio J. P., Flanagan L. B., Gessler A., Martín-Gómez P., Hirl R. T., Kahmen A., Keitel C., Lai C.-T., Munksgaard N. C., Nelson D. B., Ogée J., Roden J. S., Schnyder H., Voelker S. L., Wang L., Stuart-Williams H., Wingate L., Yu W., Zhao L. and Cuntz M. (2022) Do  $2\text{H}$  and  $18\text{O}$  in leaf water reflect environmental drivers differently? *New Phytologist* **235**, 41-51.
- Chapligin B., Leng M. J., Webb E., Alexandre A., Dodd J. P., Ijiri A., Lücke A., Shemesh A., Abelmann A., Herzsich U., Longstaffe F. J., Meyer H., Moschen R., Okazaki Y., Rees N. H., Sharp Z. D., Sloane H. J., Sonzogni C., Swann G. E. A., Sylvestre F., Tyler J. J. and Yam R. (2011) Inter-laboratory comparison of oxygen isotope compositions from biogenic silica. *Geochim Cosmochim Acta* **75**, 7242-7256.
- Clayton R. N. and Epstein S. (1958) The Relationship between  $\text{O}18/\text{O}16$  Ratios in Coexisting Quartz, Carbonate, and Iron Oxides from Various Geological Deposits. *The Journal of Geology* **66**, 345-371.
- Corbineau R., Reyerson P. E., Alexandre A. and Santos G. M. (2013) Towards producing pure phytolith concentrates from plants that are suitable for carbon isotopic analysis. *Rev Palaeobot Palyno* **197**, 179-185.
- Craig H. and Gordon L. I. (1965) Stable isotopes in oceanographic studies and paleotemperatures. *V. Lischi e Figli, Pisa* **122**.
- Crespin J., Alexandre A., Sylvestre F., Sonzogni C., Paillès C. and Garreta V. (2008) IR Laser Extraction Technique Applied to Oxygen Isotope Analysis of Small Biogenic Silica Samples. *Analytical Chemistry* **80**, 2372-2378.
- Crifò C. and Strömberg C. A. E. (2020) Small-scale spatial resolution of the soil phytolith record in a rainforest and a dry forest in Costa Rica: applications to the deep-time fossil phytolith record. *Palaeogeography, Palaeoclimatology, Palaeoecology* **537**.
- Currano E. D., Jacobs B. F., Bush R. T., Novello A., Feseha M., Grímsson F., McInerney F. A., Michel L. A., Pan A. D., Phelps S. R., Polissar P., Strömberg C. A. E. and Tabor N. J. (2020) Ecological dynamic equilibrium in an early Miocene (21.73 Ma) forest, Ethiopia. *Palaeogeography, Palaeoclimatology, Palaeoecology* **539**, 109425.
- D'Agostini F., Vadez V., Kholova J., Ruiz-Pérez J., Madella M. and Lancelotti C. (2022) Understanding the Relationship between Water Availability and Biosilica Accumulation in Selected  $\text{C}4$  Crop Leaves: An Experimental Approach. *Plants* **11**, 1019.
- Dansgaard W. (1964) Stable isotopes in precipitation. *Tellus* **16**, 436-468.
- Datnoff L. E. and Rodrigues F. (2005) *The role of silicon in suppressing rice diseases*. The American Phytopathological Society, APSnet Features.
- Epstein E. (1994) The Anomaly of Silicon in Plant Biology. *Proceedings of the National Academy of Sciences of the United States of America* **91**, 11-17.

- Esteban I., Stratford D., Sievers C., Peña P. d. I., Mauran G., Backwell L., d'Errico F. and Wadley L. (2023) Plants, people and fire: Phytolith and FTIR analyses of the post-Howiesons Poort occupations at Border Cave (KwaZulu-Natal, South Africa). *Quaternary Sci Rev* **300**, 107898.
- Evelt R. R. and Cuthrell R. Q. (2017) Testing phytolith analysis approaches to estimate the prehistoric anthropogenic burning regime on the central California coast. *Quaternary International* **434**, 78-90.
- Exley C. (2009) Silicon in Life: Whither Biological Silicification? In *Biosilica in Evolution, Morphogenesis, and Nanobiotechnology: Case Study Lake Baikal* (eds. W. E. G. Müller and M. A. Grachev). Springer Berlin Heidelberg, Berlin, Heidelberg. pp. 173-184.
- Farquhar G. D. and Lloyd J. (1993) Carbon and Oxygen Isotope Effects in the Exchange of Carbon Dioxide between Terrestrial Plants and the Atmosphere. In *Stable Isotopes and Plant Carbon-water Relations* (eds. J. R. Ehleringer, A. E. Hall and G. D. Farquhar). Academic Press, San Diego. pp. 47-70.
- Farris F. and Strain B. R. (1978) The effects of water-stress on leaf H<sub>2</sub><sup>18</sup>O enrichment. *Radiation and Environmental Biophysics* **15**, 167-202.
- Fishkis O., Ingwersen J., Lamers M., Denysenko D. and Streck T. (2010) Phytolith transport in soil: A field study using fluorescent labelling. *Geoderma* **157**, 27-36.
- Flanagan L. B., Bain J. F. and Ehleringer J. R. (1991) Stable oxygen and hydrogen isotope composition of leaf water in C<sub>3</sub> and C<sub>4</sub> plant species under field conditions. *Oecologia* **88**, 394-400.
- Flanagan L. B., Marshall J. D. and Ehleringer J. R. (1993) Photosynthetic gas exchange and the stable isotope composition of leaf water: comparison of a xylem-tapping mistletoe and its host. *Plant, Cell and Environment* **16**, 623-631.
- Garbuzov M., Reidinger S. and Hartley S. E. (2011) Interactive effects of plant-available soil silicon and herbivory on competition between two grass species. *Annals of Botany* **108**, 1355-1363.
- Geis J. W. (1973) Biogenic Silica in Selected Species of Deciduous Angiosperms. *Soil Sci* **116**, 113-130.
- Geis J. W. (1978) Biogenic Opal in Three Species of Gramineae. *Annals of Botany* **42**, 1119-1129.
- Hart D. M. (1988) The Plant Opal Content in the Vegetation and Sediment of a Swamp at Oxford Falls, New South Wales, Australia. *Australian Journal of Botany* **36**, 159-170.
- Hart D. M. and Humphreys G. S. Distribution and mobility of spherical opaline phytoliths in a podzol (Podosol). *3rd Australian New Zealand soils conference*.
- Hart T. C. (2016) Issues and directions in phytolith analysis. *J Archaeol Sci* **68**, 24-31.
- Henry A. G., Brooks A. S. and Piperno D. R. (2011) Microfossils in calculus demonstrate consumption of plants and cooked foods in Neanderthal diets (Shanidar III, Iraq; Spy I and II, Belgium). *Proceedings of the National Academy of Sciences* **108**, 486.
- Hodson M. J. (2016) The development of phytoliths in plants and its influence on their chemistry and isotopic composition. Implications for palaeoecology and archaeology. *J Archaeol Sci* **68**, 62-69.
- Hodson M. J., Parker A. G., Leng M. J. and Sloane H. J. (2008) Silicon, oxygen and carbon isotope composition of wheat (*Triticum aestivum* L.) phytoliths: implications for palaeoecology and archaeology. *J Quaternary Sci* **23**, 331-339.
- Hollins S. E., Hughes C. E., Crawford J., Cendón D. I. and Meredith K. T. (2018) Rainfall isotope variations over the Australian continent – Implications for hydrology and isoscape applications. *Science of The Total Environment* **645**, 630-645.

- Hongyan L., Dongmei J., Lidan L., Zhuo G., Guizai G., Lianxuan S., Jixun G. and Zhihe Q. (2018) The Research on Phytoliths Size Variation Characteristics in *Phragmites communis* Under Warming Conditions. *Silicon* **10**, 445-454.
- Hsiao T. C. (1973) Plant responses to water stress. *Annual review of plant physiology* **24**, 519-570.
- Hutton J. T. and Norrish K. (1974) Silicon content of wheat husks in relation to water transpired. *Australian Journal of Agricultural Research* **25**, 203-212.
- Jain R., Dhali S., Nigam H., Malik A., Malik H. K. and Satyakam R. (2022) Recovery of diatom bio-silica using chemical, thermal, and plasma treatment. *Bioresource Technology Reports* **18**, 101035.
- Jakes K. and Mitchell J. (1996) Cold Plasma Ashing Preparation of Plant Phytoliths and their Examination with Scanning Electron Microscopy and Energy Dispersive Analysis of X-rays. *J Archaeol Sci* **23**, 149-156.
- Jones R. L. (1962) BIOGENETIC OPAL IN ILLINOIS SOILS. Ph.D., University of Illinois at Urbana-Champaign.
- Jones R. L. (1964) Note on Occurrence of Opal Phytoliths in Some Cenozoic Sedimentary Rocks. *Journal of Paleontology* **38**, 773-775.
- Jones R. L., Hay W. W. and Beavers A. H. (1963) Microfossils in Wisconsinan Loess and Till from Western Illinois and Eastern Iowa. *Science* **140**, 1222-1224.
- Juillet-Leclerc A. and Labeyrie L. (1987) Temperature dependence of the oxygen isotopic fractionation between diatom silica and water. *Earth and Planetary Science Letters* **84**, 69-74.
- Katz O. (2014) Beyond grasses: the potential benefits of studying silicon accumulation in non-grass species. *Frontiers in Plant Science* **5**, 376.
- Kaufman P. B., Dayanandan P., Takeoka Y., Bigelow W. C., Jones J. D. and Iler R. (1981) Silica in Shoots of Higher Plants. In *Silicon and Siliceous Structures in Biological Systems* (eds. T. L. Simpson and B. E. Volcani). Springer New York, New York, NY. pp. 409-449.
- Kealhofer L. and Piperno D. R. (1998) Opal phytoliths in Southeast Asian flora. *Smithsonian contributions to botany*.
- Kumar S., Soukup M. and Elbaum R. (2017) Silicification in Grasses: Variation between Different Cell Types. *Frontiers in Plant Science* **8**, 438.
- Law C. and Exley C. (2011) New insight into silica deposition in horsetail (*Equisetum arvense*). *BMC plant biology* **11**, 112.
- Leng M. J. and Barker P. A. (2006) A review of the oxygen isotope composition of lacustrine diatom silica for palaeoclimate reconstruction. *Earth-Science Reviews* **75**, 5-27.
- Lentfer C. J. and Boyd W. E. (1999) An Assessment of Techniques for the Deflocculation and Removal of Clays from Sediments Used in Phytolith Analysis. *J Archaeol Sci* **26**, 31-44.
- McInerney F. A., Strömberg C. A. E. and White J. W. C. (2011) The neogene transition from c3 to c4 grasslands in north america: Stable carbon isotope ratios of fossil phytoliths. *Paleobiology* **37**, 23-49.
- Mann M. E., Zhang Z., Hughes M. K., Bradley R. S., Miller S. K., Rutherford S. and Ni F. (2008) Proxy-based reconstructions of hemispheric and global surface temperature variations over the past two millennia. *Proceedings of the National Academy of Sciences* **105**, 13252-13257.
- Mercader J., Bennett T., Esselmont C., Simpson S. and Walde D. (2009) Phytoliths in woody plants from Miombo woodlands of Mozambique. *Annals of botany* **104**, 91-113.
- Mercader J., Clarke S., Bundala M., Favreau J., Inwood J., Itambu M., Larter F., Lee P., Lewiski-McQuaid G., Mollel N., Mwambwiga A., Patalano R., Soto M., Tucker L. and

- Walde D. (2019) Soil and plant phytoliths from the Acacia-Commiphora mosaics at Oldupai Gorge (Tanzania). *PeerJ* **7**, e8211.
- Mikutta R., Kleber M., Kaiser K. and Jahn R. (2005) Review. *Soil Sci Soc Am J* **69**, 120.
- Munksgaard N. C., Wurster C. M., Bass A. and Bird M. I. (2012) Extreme short-term stable isotope variability revealed by continuous rainwater analysis. *Hydrological Processes* **26**, 3630-3634.
- Nawaz M. A., Zakharenko A. M., Zemchenko I. V., Haider M. S., Ali M. A., Imtiaz M., Chung G., Tsatsakis A., Sun S. and Golokhvast K. S. (2019) Phytolith Formation in Plants: From Soil to Cell. *Plants (Basel)* **8**, 249.
- Neumann K., Chevalier A. and Vrydaghs L. (2017) Phytoliths in archaeology: recent advances. *Veg Hist Archaeobot* **26**, 1-3.
- Novello A., Barboni D., Sylvestre F., Lebatard A.-E., Paillès C., Bourlès D. L., Likius A., Mackaye H. T., Vignaud P. and Brunet M. (2017) Phytoliths indicate significant arboreal cover at Sahelanthropus type locality TM266 in northern Chad and a decrease in later sites. *Journal of Human Evolution* **106**, 66-83.
- Outrequin C., Alexandre A., Vallet-Coulomb C., Piel C., Devidal S., Landais A., Couapel M., Mazur J.-C., Peugeot C., Pierre M., Prié F., Roy J., Sonzogni C. and Voigt C. (2021) The triple oxygen isotope composition of phytoliths, a new proxy of atmospheric relative humidity: controls of soil water isotope composition, temperature, CO<sub>2</sub> concentration and relative humidity. *Clim Past* **17**, 1881-1902.
- Piperno D. R. (2006) *Phytoliths: a comprehensive guide for archaeologists and paleoecologists*. Academic Press, San Diego.
- Prasad V., Strömberg C. A. E., Alimohammadian Habib and Sahni A. (2005) Dinosaur Coprolites and the Early Evolution of Grasses and Grazers. *Science (American Association for the Advancement of Science)* **310**, 1177-1180.
- Prentice A. J. and Webb E. A. (2016) The effect of progressive dissolution on the oxygen and silicon isotope composition of opal-A phytoliths: Implications for palaeoenvironmental reconstruction. *Palaeogeography, Palaeoclimatology, Palaeoecology* **453**, 42-51.
- Rashid I., Mir S. H., Zurro D., Dar R. A. and Reshi Z. A. (2019) Phytoliths as proxies of the past. *Earth-Science Reviews* **194**, 234-250.
- Raviele M. E. (2011) Experimental assessment of maize phytolith and starch taphonomy in carbonized cooking residues. *J Archaeol Sci* **38**, 2708-2713.
- Rosen A. M. (1992) Preliminary Identification of Silica Skeletons from Near Eastern Archaeological Sites: An Anatomical Approach. In *Phytolith Systematics: Emerging Issues* (eds. G. Rapp and S. C. Mulholland). Springer US, Boston, MA. pp. 129-147.
- Roy B., Patra S. and Sanyal P. (2020) The carbon isotopic composition of occluded carbon in phytoliths: A comparative study of phytolith extraction methods. *Rev Palaeobot Palyno* **281**, 104280.
- Saad E., Pickering R., Shoji K., Hossain M., Glover T., Krause J. and Tang Y. (2020) Effect of cleaning methods on the dissolution of diatom frustules. *Marine Chemistry* **224**, 103826.
- Saccone L., Conley D. J., Koning E., Sauer D., Sommer M., Kaczorek D., Blecker S. W. and Kelly E. F. (2007) Assessing the extraction and quantification of amorphous silica in soils of forest and grassland ecosystems. *Eur J Soil Sci* **58**, 1446-1459.
- Santosh K., Yonat M., Yaniv B., Michael E. and Rivka E. (2017) Mechanism of silica deposition in sorghum silica cells. *The New Phytologist* **213**, 791-798.

- Shahack-Gross R., Shemesh A., Yakir D. and Weiner S. (1996) Oxygen isotopic composition of opaline phytoliths: Potential for terrestrial climatic reconstruction. *Geochim Cosmochim Acta* **60**, 3949-3953.
- Sharma R., Kumar V. and Kumar R. (2019) Distribution of phytoliths in plants: a review. *Geology, ecology, and landscapes* **3**, 123-148.
- Shone M. G. T. (1964) Initial Uptake of Silica by Excised Barley Roots. *Nature (London)* **202**, 314-315.
- Smith F. (2004) Modern calibration of phytolith carbon isotope signatures for C3/C4 paleograssland reconstruction. *Palaeogeography, Palaeoclimatology, Palaeoecology* **207**, 277-304.
- Strömberg C. A. E. (2004) Using phytolith assemblages to reconstruct the origin and spread of grass-dominated habitats in the great plains of North America during the late Eocene to early Miocene. *Palaeogeography, Palaeoclimatology, Palaeoecology* **207**, 239-275.
- Strömberg C. A. E., Dunn R. E., Crifò C. and Harris E. B. (2018) Phytoliths in Paleoecology: Analytical Considerations, Current Use, and Future Directions. In *Methods in Paleoecology: Reconstructing Cenozoic Terrestrial Environments and Ecological Communities* (eds. D. A. Croft, D. F. Su and S. W. Simpson). Springer International Publishing, Cham. pp. 235-287.
- Sutton J. N., André L., Cardinal D., Conley D. J., de Souza G. F., Dean J., Dodd J., Ehlert C., Ellwood M. J., Frings P. J., Grasse P., Hendry K., Leng M. J., Michalopoulos P., Panizzo V. N. and Swann G. E. A. (2018) A Review of the Stable Isotope Bio-geochemistry of the Global Silicon Cycle and Its Associated Trace Elements. *Front Earth Sc-Switz* **5**, 112.
- Thorn V. C. (2004) Phytolith evidence for C4-dominated grassland since the early Holocene at Long Pocket, northeast Queensland, Australia. *Quaternary Res* **61**, 168-180.
- Tyler J. J., Sloane H. J., Rickaby R. E. M., Cox E. J. and Leng M. J. (2017) Post-mortem oxygen isotope exchange within cultured diatom silica. *Rapid Communications in Mass Spectrometry* **31**, 1749-1760.
- Von Freyberg J., Allen S. T., Grossiord C. and Dawson T. E. (2020) Plant and root-zone water isotopes are difficult to measure, explain, and predict: Some practical recommendations for determining plant water sources. *Methods in Ecology and Evolution* **11**, 1352-1367.
- Wallis L. (2001) The History of Phytolith Researchers In Australia.
- Wallis L. (2003) An overview of leaf phytolith production patterns in selected northwest Australian flora. *Rev Palaeobot Palyno* **125**, 201-248.
- Wallis L. (2013) A comparative study of phytolith assemblages in modern sediments from the Kimberley, Western Australia. *Quaternary Australasia* **30**, 6-20.
- Webb E. A. and Longstaffe F. J. (2000) The oxygen isotopic compositions of silica phytoliths and plant water in grasses: implications for the study of paleoclimate. *Geochim Cosmochim Acta* **64**, 767-780.
- Webb E. A. and Longstaffe F. J. (2002) Climatic influences on the oxygen isotopic composition of biogenic silica in prairie grass. *Geochim Cosmochim Acta* **66**, 1891-1904.
- Webb E. A. and Longstaffe F. J. (2003) The relationship between phytolith- and plant-water  $\delta^{18}\text{O}$  values in grasses. *Geochim Cosmochim Acta* **67**, 1437-1449.
- Webb E. A. and Longstaffe F. J. (2006) Identifying the  $\delta^{18}\text{O}$  signature of precipitation in grass cellulose and phytoliths: Refining the paleoclimate model. *Geochim Cosmochim Acta* **70**, 2417-2426.

- Yang X., Song Z., Liu H., Bolan N. S., Wang H. and Li Z. (2015) Plant silicon content in forests of north China and its implications for phytolith carbon sequestration. *Ecol Res* **30**, 347-355.
- Zancajo V. M. R., Diehn S., Filiba N., Goobes G., Kneipp J. and Elbaum R. (2019) Spectroscopic Discrimination of Sorghum Silica Phytoliths. *Frontiers in Plant Science* **10**, 1571.
- Zhao L., Wang L., Liu X., Xiao H., Ruan Y. and Zhou M. (2014) The patterns and implications of diurnal variations in the  $\delta$ -excess of plant water, shallow soil water and air moisture. *Hydrol. Earth Syst. Sci.* **18**, 4129-4151.
- Zhao Z. and Pearsall D. M. (1998) Experiments for Improving Phytolith Extraction from Soils. *J Archaeol Sci* **25**, 587-598.
- Zielinski G. A. (2000) Use of paleo-records in determining variability within the volcanism–climate system. *Quaternary Sci Rev* **19**, 417-438.

## Chapter 2:

Phytolith extraction for oxygen isotope  
analysis: Method development

# Statement of Authorship

Title of Paper	Phytolith extraction for oxygen isotope analysis: Method development
Publication Status	<input type="checkbox"/> Published <input type="checkbox"/> Accepted for Publication <input type="checkbox"/> Submitted for Publication <input checked="" type="checkbox"/> Unpublished and Unsubmitted work written in manuscript style
Publication Details	

## Principal Author

Name of Principal Author (Candidate)	Kimberley Edwards		
Contribution to the Paper	Designed the study. Conducted sample processing and analysis. Conducted data analysis and interpretation. Wrote manuscript.		
Overall percentage (%)	75		
Certification:	This paper reports on original research I conducted during the period of my Higher Degree by Research candidature and is not subject to any obligations or contractual agreements with a third party that would constrain its inclusion in this thesis. I am the primary author of this paper.		
Signature		Date	31/01/2023

## Co-Author Contributions

By signing the Statement of Authorship, each author certifies that:

- i. the candidate's stated contribution to the publication is accurate (as detailed above);
- ii. permission is granted for the candidate to include the publication in the thesis; and
- iii. the sum of all co-author contributions is equal to 100% less the candidate's stated contribution.

Name of Co-Author	Dr Alexander Francke		
Contribution to the Paper	Supervised project. Provided input into study design, data analysis, interpretation and manuscript. Reviewed and edited final manuscript.		
Signature		Date	25/01/2023

Name of Co-Author	Dr Francesca McInerney
Contribution to the Paper	Supervised project. Provided input into study design, data analysis, interpretation and manuscript. Reviewed and edited final manuscript.



Signature		Date	31/01/2023
-----------	--	------	------------

Name of Co-Author	Dr Jonathan Tyler		
Contribution to the Paper	Supervised project. Provided input into study design, data analysis, interpretation and manuscript. Reviewed and edited final manuscript.		
Signature		Date	1/2/2023

Name of Co-Author	Dr Bryan Coad		
Contribution to the Paper	Provided input into plasma ashing study design. Reviewed final manuscript.		
Signature		Date	31/01/2023

Name of Co-Author	Dr Melanie Ford		
Contribution to the Paper	Provided input into plasma ashing study design. Reviewed final manuscript.		
Signature		Date	31/01/2023

## Abstract

The oxygen isotopic composition of phytoliths, composed of biogenic silica formed inside higher plants, has the potential to be used as a proxy to deduce past climates, particularly in depositional settings where other palaeoclimatic archives are sparse. However, several methodological challenges hinder isotope analysis of phytoliths in sediments. The standard phytolith extraction methods that are applied to soils and sediments involve high temperatures which can affect oxygen isotope ratios. Conversely, low temperature methods can be ineffective in removing organic and mineral contamination. This study investigates how residual contamination can be removed from soil samples using variations of chemical and density extraction methods, including the novel application of non-thermal plasma ashing generated by radio frequency (RF) excitation of air under vacuum. The purity of phytolith samples was evaluated using optical microscopy and Fourier transform infrared spectroscopy. A sequence of 5% hydrochloric acid, 30% hydrogen peroxide treatment, density separation using sodium polytungstate and nested cell filtration was not enough to remove all organic and clay matter from soil samples that were initially high in organic matter. A further treatment of sulfuric acid and hydrogen peroxide mixture (a.k.a. 'piranha solution') and a repeat of density separation and filtration was found to be most effective in removing residual organic and clay matter at temperatures <70 °C. These treatments are a combination of those previously applied to sediment-hosted and modern plant phytoliths. Non-thermal RF plasma ashing shows potential for future phytolith extraction from plants but was found to be time inefficient and so not currently applicable to large batches of samples.

## 1 Introduction

Understanding how recent and past climates have evolved is necessary to understand how future climate change may affect the biosphere (IPCC 2021). Oxygen isotope ratios are a commonly used proxy for past climates, particularly applied to carbonates, however many terrestrial and marine sedimentary archives lack suitable carbonate preservation. Biogenic silica is a potential alternative to carbonates as it is found in abundance across large tracts of the ocean floor, as well as in freshwater and acidic terrestrial lake and wetland sediments across the globe (e.g., Abrantes, 2003; Alexandre et al., 2018; Bremond et al., 2008; Rietti-Shati et al., 1998; Shemesh et al., 1992; Swann et al., 2010). Of the types of biogenic silica, diatoms are the most abundant and studied, however, phytoliths are also abundant, especially in dry regions such as Australia (Wallis, 2001).

Phytoliths are passively produced silica structures in many higher terrestrial plants. As they precipitate, their shape mimics that of the cell or intercellular void they fill (Piperno, 2006). This results in distinct shapes that can be used to differentiate species, though many cell shapes are shared by plant families and thus cannot be distinguished (Piperno, 2006; Strömberg et al., 2018). The amorphous silica of phytoliths is resistant to dissolution, which leads to accumulation in sedimentary environments (Baker, 1959b). This has led to many studies that use phytoliths as a proxy for climate and ecology (e.g., Cabanes and Shahack-Gross, 2015; Strömberg et al., 2018). There is a developing interest in using the isotope ratio of phytoliths as a climate proxy tool (e.g., Alexandre et al., 2018; Webb and Longstaffe, 2000), but existing phytolith extraction processes have posed methodological challenges.

Many of the extraction methods used in phytolith research are aimed at preparing phytoliths for morphological studies. In these studies minor contaminants such as organic matter, quartz, clay, and charcoal mixed into the phytoliths can be neglected (Katz et al., 2010;

Lentfer and Boyd, 1998, 1999; Zhao and Pearsall, 1998). Isotope analyses require a significantly lower level of contamination since oxygen released from clays or residual organic matter would affect the oxygen isotope ratios, so conventional phytolith extraction methods are unsuitable for isotope analyses (Leng and Barker, 2006). There have been several studies on how to clean phytoliths for carbon isotope analysis, targeting carbon trapped within the biogenic silica structure, but these methods are less suitable for oxygen isotopes due to the high temperatures applied during treatment (90 °C or higher), which have the potential to alter the oxygen isotopes (Corbineau et al., 2013; Crespin et al., 2008; Roy et al., 2020; Tyler et al., 2017).

Extracting phytoliths from plants for oxygen isotope analysis can be successfully conducted using a mixture of sulfuric acid and hydrogen peroxide with a ratio of 2:1, also known as “piranha solution”, due to its strong ability to dissolve organic matter at temperatures <70°C, a temperature not likely to affect oxygen isotopes (Crespin et al., 2008; Geis, 1973).

However, piranha solution is extremely hazardous due to it being highly oxidising, explosive and reactive with other potential sedimentary components and so is not normally used on soils or sediments (Piperno, 2006; Schmidt, 2022).

Extracting phytoliths from soils and sediments is more challenging than extracting them from plants. To obtain uncontaminated phytolith extracts from soils, purification methods need to remove organic material as well as any material that contains oxygen, such as quartz, carbonates, and clays. More gentle chemical extractions such as those using hydrogen peroxide at lower temperatures are often less effective at digesting organic matter (Pfeiffer and Fischer, 2020). Furthermore, organic matter tends to stick to other materials in sediments, so steps that target the removal of clays and quartz (such as density separation and filtration) are less successful if organic matter has not been removed first (Pfeiffer and Fischer, 2020; Piperno, 2006). Oxygen plasma ashing has been successfully used to remove

organic matter on non-silicate materials without effecting the carbon isotope ratios (Bird et al., 2010; Lebeau et al., 2014). It has also been utilized for removing leaf material from phytoliths and eliminating organics from diatoms (Jain et al., 2022; Jakes and Mitchell, 1996; Saad et al., 2020). Therefore, it presents a potential alternative method for removing organic matter during the extraction of phytoliths from plants and soils for oxygen isotope analysis. However, these setups have used high powered plasma which speeds up treatment but may heat up the sample and this needs to be considered. Once organic matter is removed, other contaminants such as quartz and clay can be removed through deflocculation, density separation and filtration (Piperno, 2006).

The main purpose of this study was to refine a technique to extract at least 1 mg of pure soil phytoliths whilst avoiding high temperature exposure. Phytoliths from soil samples (described in detail in Chapter 4) were extracted using the previously established method of Snelling et al. (2012) and assessed for residual contamination. These soil samples were then subjected to additional treatment steps in an effort to reduce contamination in preparation for oxygen isotope analysis. Steps to improve efficiency of soil phytolith extraction processes in preparation for oxygen isotope analysis were investigated, including the use of piranha solution, normally only applied to modern plant material. This study furthermore aimed to assess whether non-thermal RF plasma ashing could be used for organic removal for phytolith extractions by testing it on modern plant material.

To comprehensively test different pre-treatment and extraction methods and their suitability for subsequent oxygen isotope analyses, the following were tested:

(a) methods of preparing plant material for phytolith extractions (cutting vs. grinding), to determine if these influence the efficiency of the extraction.

(b) different chemical extraction methods for phytoliths in soils to determine which yields the cleanest extracted phytolith samples and additional treatments on samples treated with the method of Snelling et al. (2012) (Chapter 4) to assess the best way to remove residual contamination.

(c) qualitative (microscopy) and quantitative (Fourier Transform Infrared-spectroscopy and Inductively Coupled Mass Spectrometry) approaches to evaluating types and levels of contamination.

(d) non-thermal RF plasma ashing as an alternative extraction technique for separation of organic matter from phytoliths, replacing hazardous chemicals and/or high temperatures during treatment.

## 2 Methods and materials

### 2.1 Materials

#### 2.1.1 Plant material

Leaves of three distinct plant species were collected and used to evaluate preparation and extraction techniques. A naturally occurring Acacia growing in a shady area at the top of a river embankment in Adelaide, South Australia; a native Australian grass (*Pennisetum alopecuroides* (samples T5a-c and T13a)) grown in soil in a pot in direct sun, regularly watered with an automated watering system located in Adelaide; and barley (*Hordeum vulgare* cv. Golden Promise (samples T1-3 and T6-10) grown in soil in pots in a greenhouse at the School of Agriculture, Food and Wine, University of Adelaide. The greenhouse temperature was controlled at 20 °C during the day and turned off at night.

#### 2.1.2 Soil material

Three soil samples were selected from three locations to test extraction methods. Soil sample 1 (T4a-c) was an organic rich garden topsoil collected July 2021 from Munno Para,

South Australia. Soil sample 2 (NTAGFU0010) was a sandy clay topsoil containing charcoal collected May 2012 from Creswell, Northern Territory, Australia. Soil sample 3 (SATFLB0005) was organic rich, sandy topsoil sitting on a rocky substrate, collected in August 2012 in the Flinders Rangers, South Australia. The top 3 cm of topsoil at each location was collected. Soil samples 2 and 3 were collected by the Terrestrial Ecosystem Research Network (TERN) specifically for metagenomic and isotopic analysis (White et al., 2012).

## 2.2 Methods

### 2.2.1 Preparation of plant samples for phytolith extractions

Prior to further preparation, plant leaves (two samples of acacia, three samples of native grass, and nine samples of barley, each sample weighing approximately 100 mg) were submerged in Milli-Q water and sonicated for 30 minutes, then rinsed twice with Milli-Q water to remove any surface contaminants. The leaves were then dried in an oven at 40 °C for five days (Roy et al., 2020).

Plant phytolith extraction requires small aliquots of plant tissue material suitable for chemical treatment, and there is no standard method for preparing plant material prior to phytolith extractions (Corbineau et al., 2013; Roy et al., 2020). How plant preparation effects the efficiency of the extraction processes has yet to be studied. Prior to chemical treatment, three different pre-treatment methods were compared: cutting, ball-milling, and grinding with a mortar and pestle with the aid of liquid nitrogen.

One of the native grass samples was frozen with liquid nitrogen and then ground using a mortar and pestle. The other two native grass samples and six barley samples were cut into small pieces with clean scissors. The two Acacia samples were ball milled with stainless steel and ceramic balls, respectively. Five samples of barley were ball milled with stainless steel balls until they were finely powdered. Samples were weighed both before and after

extractions. All laboratory equipment was soaked in Decon-90 detergent, scrubbed, rinsed three times with tap water, rinsed three times with Milli-Q water, rinsed with ethanol then dried in fume cupboard in a beaker cleaned using the same process.

### 2.2.2 Extractions of phytoliths for oxygen isotope analysis

Four methods (Table 1) using chemical extraction and non-thermal plasma ashing generated by radio frequency (RF) excitation of air under vacuum (Michl et al., 2015) were compared for extraction of phytoliths from plants and soils in preparation for oxygen isotope analysis (Alexandre et al., 2012; Geis, 1973; Geis, 1978; Jakes and Mitchell, 1996; Piperno, 2006; Snelling et al., 2012). Chemical extraction method 1 (C1) is the most common chemical extraction method for extracting phytoliths from plant material (Piperno, 2006) but not soils. Chemical extraction methods very similar to methods two (C2) and three (C3) have previously been used to extract biogenic silica from soil samples (Alexandre et al., 2012; Snelling et al., 2012), however initial attempts to use these methods did not yield phytolith extractions clean enough for oxygen isotopic analysis (Leng and Barker, 2006). Consequently, the fourth chemical extraction methods were developed by testing two combinations of the previous methods, which is C4a (C2 followed by C1), and C4b (C3 followed by C1). These combined methods were used in attempt to obtain cleaner phytolith extracts from soils similarly to McInerney et al. (2011).



Table 1 Summary of samples and the methods tested on them. Methods include acids (H<sub>2</sub>SO<sub>4</sub> and HCl), oxidant (H<sub>2</sub>O<sub>2</sub>), dispersant (Sodium Hexametaphosphate, SHMP) and heavy liquid (Sodium Polytungstate, SPT).

Method	Material (number of samples)	Chemicals/treatments and order	Reference
Chemical 1 (C1) – (Piranha solution)	Plant (6)	H <sub>2</sub> SO <sub>4</sub> (30 ml, 98%) + H <sub>2</sub> O <sub>2</sub> (15 ml, 30%) (60 °C) → HCl (10 ml, 5%)	(Geis, 1973)
Chemical 2 (C2)	Soil (3)	HCl (10 ml, 5 %) → SHMP (10 ml, 10%) → SPT (4 ml) → H <sub>2</sub> O <sub>2</sub> (10 ml, 30%, 70 °C) → HCl (10 ml, 5%)	(Piperno, 2006; Snelling et al., 2012)
Chemical 3 (C3)	Soil (1)	HCl (10 ml, 5%) → SHMP (10 ml, 10%) → H <sub>2</sub> O <sub>2</sub> (10 ml, 30%, 70 °C) → SPT	(Alexandre et al., 2012)
Chemical 4a and 4b (C4a and C4b)	Soil (4)	Treated with C2 followed by C1 (for C4a), and C3 + C1 (for C4b)	(Piperno, 2006) or (Alexandre et al. 2012) followed by (Geis, 1973)
Plasma	Plant (4)	Plasma → HCl (10 ml, 5%)	Section 2.2.8

### 2.2.3 Chemical extraction method 1 (C1): Phytolith extraction on plants using Piranha solution

Phytolith extraction from plant material follows a modified protocol by Geis (1973). Five barley plant samples, two of which were ball milled and three of which were roughly cut into 1 cm long aliquots, were placed in glass beakers. Each beaker was filled with 20 ml of

concentrated sulfuric acid, ensuring that the samples were completely submerged by pushing floating material down with a glass stirrer. The two ball-milled samples were stirred with a glass stirrer to disperse the clumps that had formed. Each sample had its own stirrer, which was stored in a labelled conical flask to avoid cross-contamination. Samples were placed on a hot plate at 60 °C, a temperature which is thought to be cool enough not to affect  $\delta^{18}\text{O}$  values (Crespin et al., 2008). Samples were heated for two hours, and all samples turned to a consistent black sludge. After removing the samples from the hotplate, they were allowed to cool to room temperature. Using a pipette, 2 ml of cold hydrogen peroxide was added to each beaker and stirred with a glass stirrer. When the sample became transparent or reached a 2:1 ratio of sulfuric acid to hydrogen peroxide, all samples were allowed to settle until no visible reactions were occurring. Beakers were then placed back on a hot plate at 60 °C. Samples were stirred regularly. After two hours, the hotplate was turned off and the beakers were allowed to cool. Beakers were then covered with a watch glass and left to sit in the fume cupboard for 24 hours. Using pipettes, as much of the sulfuric acid and hydrogen peroxide solution as possible was siphoned off while not disturbing the solid material at the bottom. The samples were transferred to a 50 ml centrifuge tube, and the beakers were rinsed with Milli-Q water into the centrifuge tubes until they contained 50 ml of liquid. They were then centrifuged in an Eppendorf 5810 at 2000 RPM, acceleration 7, brake 0 for five minutes. The supernatant was removed using a pipette and the samples were rinsed with Milli-Q water, repeating three times. 10 ml of 10% HCl was added to each centrifuge tube and shaken, after which samples were rinsed in MQ water and centrifuged three times as before, to obtain a near-neutral pH. Phytolith extracts and remaining water were subsequently frozen and freeze dried.

Between sample extractions, Pyrex glass beakers, glass stirrers, glass watch plates, and conical flasks were cleaned with regular detergent, rinsed three times with tap water, and

then soaked for two hours in Decon-90 detergent diluted with hot water. The equipment was then rinsed with tap water and Milli-Q water three times. As a final rinse, ethanol was used, and the equipment was placed in a fume cupboard to dry.

#### 2.2.4 Chemical extraction method 2 (C2): Phytolith extraction from soils

An aliquot of each soil, approximately 10 g, was prepared using the method for extracting phytoliths from soil described in Piperno (2006), using suggested alternative chemicals at a lower temperature as was done in Snelling et al. (2012). Each sample was wet sieved at 2 mm using Milli-Q water to remove all large organic matter remains and gravel, then treated with 10% hydrochloric acid (HCl) overnight to remove carbonates and then rinsed with Milli-Q water and centrifuged three times. Next, sodium hexametaphosphate (SHMP) was used to deflocculate clay that inhibits organic removal (Mikutta et al., 2005; Tyner, 1940). 10 ml of 10% SHMP was added to each of the samples which were then shaken and left overnight. The next day, the supernatant was removed using a pipette. Each sample was rinsed three times with Milli-Q water and centrifuged to remove any residual SHMP at 1500 RPM, acceleration 7, brake 0 for five minutes.

Samples then underwent several gravity sedimentations to remove clay particles. Each sample was placed in a 500 ml beaker, filled with Milli-Q water, and left untouched for 1 hour at which time half the water was decanted. The first time, the decanted water was checked under a microscope to ensure no phytoliths were removed. This was repeated until the water was clear at the one-hour mark. Samples were centrifuged using Stoke's equation (taken from Graham, 2020) with the target to keep clays and fine silt up to 5  $\mu\text{m}$  up to a density of 1.4  $\text{g}/\text{cm}^3$  in suspension. Centrifuge settings were estimated to be RPM 600, acceleration 7, brake 0 for three minutes and ten seconds. Only half the supernatant was removed using pipette to ensure that no phytoliths were being removed. The vials were then

topped up with Milli-Q water and the procedure was repeated at least three times until supernatant was clear then all liquid was removed.

Samples then underwent heavy liquid density separation using sodium polytungstate (SPT) to separate the bulk of the clay, quartz and other mineral residual contaminants from the phytoliths that are estimated to have a density of less than  $2.3 \text{ g/cm}^3$  (Morley et al., 2004; Piperno, 2006). Four ml of SPT with a specific gravity of  $2.38 \text{ g/cm}^3$  was added to the samples and all samples were shaken and then centrifuged at 2500 RPM, acceleration 7, brake 0 for 20 minutes. The phytoliths and other residual contamination with a density lower than  $2.38 \text{ g/cm}^3$  floats to the top of the centrifuge tube. This float was removed to a new centrifuge tube using a plastic Pasteur pipette. The majority of the SPT was removed from the initial centrifuge tube and vacuum filtered at  $0.45 \mu\text{m}$  using a Polyethylene terephthalate (PET) cell filters in preparation to be recycled. The heavy density fraction ( $>2.38 \text{ g/cm}^3$ ) underwent SPT separation again to ensure that no phytoliths had been trapped in the residue. Both the initial and new floated materials were rinsed 3 times using Milli-Q water and centrifuged to wash out the SPT.

Hydrogen peroxide ( $\text{H}_2\text{O}_2$ ) was used to remove organic matter from the  $<2.38 \text{ g/cm}^3$  phytolith-rich fraction. The centrifuge tube was slowly filled with 10 ml of 30%  $\text{H}_2\text{O}_2$ , 1 ml at a time, and the samples were subsequently left untouched with the lid unscrewed and sitting lightly on top for several hours until the reaction had subsided. During this time, the samples were repeatedly shaken. The samples were then placed in a heating block with a thermometer and placed on a hot plate. The temperature was gradually raised to  $70 \text{ }^\circ\text{C}$ . Due to the intense reaction of  $\text{H}_2\text{O}_2$ , this may have taken several hours in some instances. The samples were kept at  $70^\circ\text{C}$  for an additional 6 days (for a total of 7 days in hydrogen peroxide), with frequent  $\text{H}_2\text{O}_2$  additions as it evaporated. During this time, the sample was continuously shaken. The samples were then cooled to room temperature, refilled with

38

Milli-Q water, and centrifuged for five minutes at 1500 RPM, acceleration 7, brake 0. The supernatant was removed using a pipette and the sample was then rinsed 3 times using Milli-Q water and centrifuged again with the same settings.

To remove carbonates from the samples, 10 ml of 5% HCl was added to the tubes, which was then shaken and left overnight at room temperatures. The supernatant was removed using a pipette and then the sample was rinsed three times using Milli-Q water and centrifuge (2000 RPM, acceleration 7, brake 0 for five minutes).

Finally, the samples were subjected to a repeat of the heavy density separation step to remove any clay particles that had been stuck to organic matter, using the same procedure as outlined above. After completion of the final density separation, the samples were refilled with Milli-Q water, and then centrifuged at 2000 RPM, acceleration 7, brake 0 for five minutes, vacuum-filtered at 10  $\mu\text{m}$  using a PET cell filter (with the  $> 10 \mu\text{m}$  being retained), and then freeze-dried.

#### 2.2.5 Chemical extraction method 3 (C3): Phytolith extraction from soils

A 2 g soil sample (Test sample) was used to test a phytolith extraction method described in Alexandre et al. (2012), which uses a slightly modified method from Piperno (2006) by applying the procedure in a different order and without the step targeting iron oxides. The new order after Alexandre et al. (2012) was as follows.

10 ml of 5% HCl was added to the sample tube, which was then shaken and left overnight. The supernatant was removed with a pipette and the sample rinsed three times with Milli-Q water and centrifuged at 1500 RPM, acceleration 7, brake 0 for five minutes.

In the next step, 10 ml of 10% SHMP was added to the sample, which was then shaken and left overnight. The next day, the supernatant was removed with a pipette. The sample was

rinsed three times with Milli-Q water and centrifuged at 1500 RPM, acceleration 7, brake 0 for five minutes.

10 ml of 30% H<sub>2</sub>O<sub>2</sub> was slowly added to the centrifuge tube 1 ml at a time, shaken in between. The sample was left for several hours with the lid sitting loosely on top until the reaction subsided. During this time, the sample was shaken repeatedly. The temperature was then gradually raised to 70 °C over the course of 24 hours to avoid vigorous sample reactions. The samples were shaken regularly during heating and the temperature was maintained for a further 6 days (a total of 7 days in H<sub>2</sub>O<sub>2</sub>) with frequent refills of H<sub>2</sub>O<sub>2</sub>. The samples were then cooled to room temperature, topped with Milli-Q water, and then centrifuged at 2000 RPM, acceleration 7, brake 0 for five minutes. Supernatant was removed using a pipette and then sample was rinsed 3 times using Milli-Q water and centrifuge to obtain a near-neutral pH.

Using the same procedures as described in method C2, samples underwent gravity sedimentation, centrifuge sedimentation using stokes equation, SPT density separation and finally freeze drying.

#### 2.2.6 Chemical treatment method 4 (C4a and C4b): Combination methods for extraction of phytoliths from soils

Organic matter was still present in soil samples that were extracted using methods C2 and C3. To address this, the samples were treated with Piranha solution. Though this method is typically used to remove fresh plant matter, a similar approach was used by McInerney et al. (2011) to purify previously extracted phytoliths from sediments for carbon isotope analysis. The samples previously treated with method C2 are referred to as being treated with method C4a, and the sample treated with C3 renamed to are referred to as being treated with method C4b.

The Piranha solution treatment was conducted following the procedure detailed in section 2.2.3. The soil samples then underwent a repeat of the SPT separation at 2.25 g/cm<sup>3</sup>, 2.16 g/cm<sup>3</sup> and 1.9 g/cm<sup>3</sup>, retaining the portion between 2.16-1.9 g/cm<sup>3</sup>. Following that, vacuum filtration was then completed using 85 µm, 20 µm, and 10 µm nested PET cell filters resulting in 4 fractions: <10 µm, 10 - 20 µm, 20 - 80 µm, and >80 µm (Urban et al., 2018) which were checked for residual contamination. The fractions 10 µm and higher were recombined and then samples were freeze-dried. Both of these extra steps were aimed at targeting any clays that had potentially been trapped within the organic matter. Assessing types of contaminants in soil phytoliths samples.

To better understand the types of contamination (charcoal, clay, quartz, or organic matter) that were still present in separated soil phytoliths samples, different density and size fractions of the separated phytoliths samples were investigated to test if only certain density and/or size fractions were affected by contamination, and if those density and/or size fractions show distinct enrichments in the various types of contamination (charcoal, clay, quartz, or organic matter remains). For this purpose, a 10 g soil sample (Test Sample) was subjected to extraction C2, but the SPT separation was performed only twice at a density of 2.32 g/cm<sup>3</sup> to ensure sufficient contamination for the purpose of contaminant identification. This sample then underwent further SPT separation steps to isolate density fractionations of 2.32 - 2.30 g/cm<sup>3</sup>, 2.29 - 2.25 g/cm<sup>3</sup>, 2.24 - 2.2 g/cm<sup>3</sup>, 2.1 - 2.16 g/cm<sup>3</sup>, 2.16 - 2.07 g/cm<sup>3</sup> and 2.07 - 1.9 g/cm<sup>3</sup>. These fractions were analysed under a microscope to assess residual contamination, as well as phytolith size and abundance in each density fraction.

The 1.9-2.07 g/cm<sup>3</sup> portion contained almost all of the phytoliths, and this fraction was subsequently vacuum filtered using 85 µm, 20 µm, and 10 µm nested cell filters resulting in 4 fractions: <10 µm, 10 - 20 µm, 20 - 80 µm, and >80 µm (Urban et al., 2018). Each portion was checked under a microscope for quantities of phytoliths and contamination.

### 2.2.7 Non-thermal plasma ashing

Acacia, barley, native grass, and soil samples were used to test non-thermal plasma ashing generated by radio frequency (RF) excitation of air under vacuum utilising a modified rotary evaporator with custom electrodes (Figure 1) (Michl et al., 2015). The vacuum is used to reduce the pressure of the air in the flask low enough that a plasma can be generated using radio frequency. For detailed information about the setup used in this study please see Ford (2022).

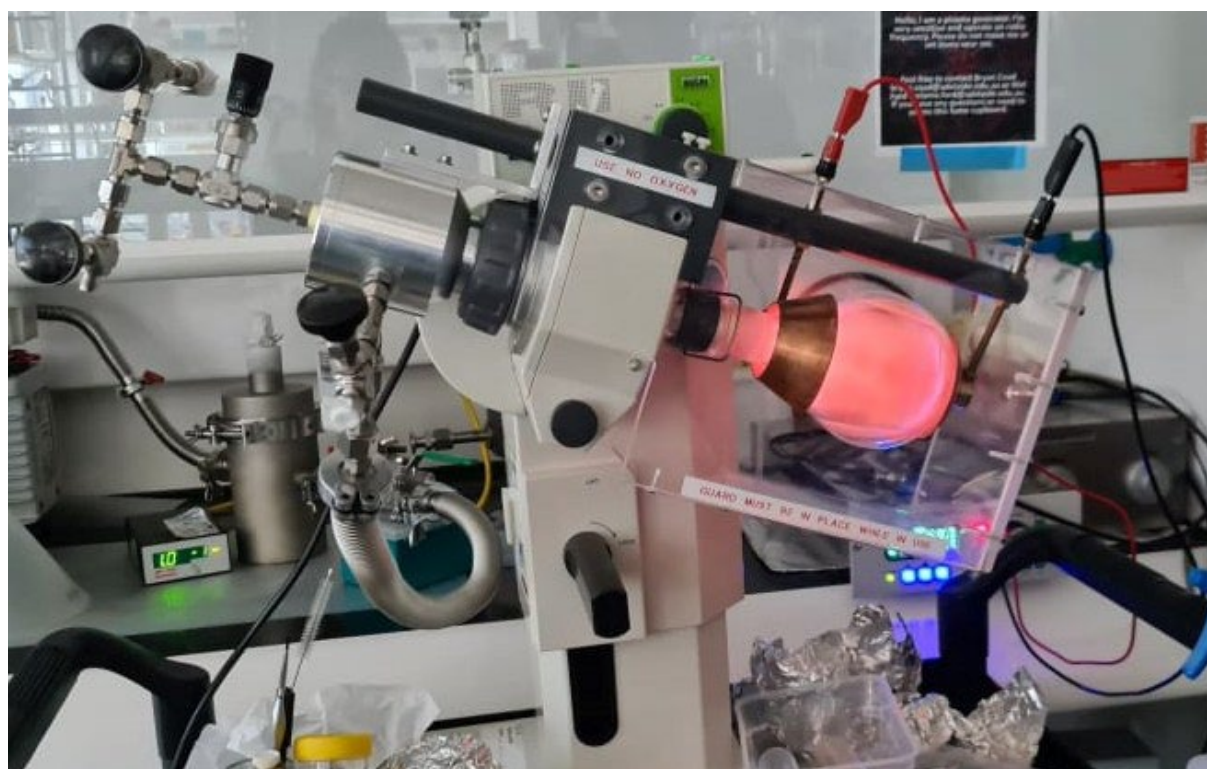


Figure 1 Plasma ashing Acacia ball milled sample.

A 500 ml round-bottomed, rotating glass flask with four internal baffles was used to facilitate sample mixing which allowed for lower power plasma to maintain lower temperatures. Two different methods were tested to create a seal around the neck of the flask. The interior neck of the glass flask was sealed with polytetrafluoroethylene tape and ethanol or vacuum grease. In the case of vacuum grease, the flask's neck was cleaned thoroughly with acetone,



ethanol, and a Kimwipe before the sample was removed from the flask. The treatments were performed using between 25 and 50 watts under a 100 mTorr vacuum with ambient air.

The plasma machine was in a climate-controlled room with the temperature set to 22 °C, in front of a fume cupboard with the booster turned on and the fume sash lowered.

This ensured that cool air from the ducted air system flowed past the inlet and helped to maintain cool plasma temperatures. Every 30 to 60 minutes, the temperature was measured externally using a laser thermometer aimed through the side of the glass at the centre of the large diode at the bottom of the flask. Comparing temperatures taken through the glass and then internally through the neck of the flask at the conclusion of each run revealed that the internal temperature was up to 10 °C hotter than the reading taken externally. If the externally measured temperature reached 24 °C, the plasma was turned off and the system was pressurised to allow the internal temperature to rapidly cool, and the system was restarted when the external temperature dropped to below 23 °C.

The two Acacia samples (T1) were run for 6 hours at 25 Watts (Table 2). After inspecting for contamination, it became clear that while most of the organic matter had been removed, a longer treatment time was required to remove all the organic matter (Bird et al., 2010; Lebeau et al., 2014). Due to the lack of phytoliths in the two Acacia samples, they were only used to evaluate preparation techniques. The treatment durations for the remaining samples were altered to 21-30 hours in 6- or 7-hour sessions. At the conclusion of the treatment, the flask's neck was cleaned, and the sample was transferred into centrifuged tubes using weighing paper. The flask was then rinsed with Milli-Q water into the centrifuge tubes to ensure the complete recovery of the sample. The samples were then centrifuged twice on an Eppendorf 5810 for five minutes at 2000 rpm, 7 acceleration, and 0 brake, and the supernatant was removed with a pipette.

To remove carbonates not targeted during plasma ashing, 10 ml of 10 percent hydrochloric acid (HCl) was added to samples. Samples were shaken before being centrifuged twice for five minutes at 2000 rpm, 7 acceleration, and 0 deceleration, with samples being shaken in between. After removing HCl with a pipette, samples were rinsed three times by filling centrifuge tubes to the 45 ml mark with Milli-Q water, shaken, centrifuged, and then liquid removed with a pipette. The rinses also assisted by removing soluble compounds such as sodium chlorite. Afterwards, samples were freeze-dried and weighed again.

After plasma ashing, one sample (cut native grass – T5) was a mix of clean phytoliths and whole pieces of grass, and these different materials were further subsampled and treated. At 15 hours some of the released phytoliths were removed to check under a microscope (subsample T5b). At the end of the plasma treatment (21 hours), the whole pieces of grass were removed with forceps and treated with piranha solution (subsample T5a), and then the rest (subsample T5c) was treated with HCl and freeze dried.

## 2.3 Contamination assessment

### 2.3.1 Microscopy

At various stages of chemical and plasma treatment, samples were inspected with wet mounts on an optical polarising microscope to determine the efficacy of the treatments. After freeze drying and completion of the extraction methods, all soil samples and selected plant samples were permanently mounted on microscope slides. A small amount of phytoliths were placed on a slide, dispersed with a drop of ethanol, and then allowed to dry. Norland optical adhesive was used to mount the phytoliths, followed by a cover slip, set under a UV light for approximately 30 min. Microscope slides were assessed using a compound microscope at 200 x magnification to check contaminant versus phytolith amounts and 400 x magnification to check organic matter still attached to the phytoliths.

Selected plant samples were examined with a scanning electron microscope (SEM) to determine contamination and whether phytoliths had been damaged by any of the extraction procedures (pitting, dissolution etc). Soil phytoliths were not checked as it was anticipated that soil phytoliths would already have undergone some dissolution naturally, and it would not be possible to distinguish between that caused by treatment and that which occurred naturally.

### 2.3.2 Fourier Transform Infrared Spectroscopy (FTIR) modelling

FTIR provides insight into the chemical structure of a sample. Covalent bonds have vibrations that consist of stretching and bending modes that can cause energy absorption at specific infrared wavelengths (Swann and Patwardhan, 2011). The absorbance of the infrared can be used to infer which chemical bonds are present in a given sample, for example, Si-O-Si asymmetric stretching vibrations show absorption at approximately  $1110\text{ cm}^{-1}$  (Musić et al., 2011). Phytolith extracts from each soil sample underwent FTIR spectrometry using the attenuated total reflectance method on a Shimadzu IRSpirit with a QATR-S accessory equipped with a diamond crystal. An aliquot of each sample was scanned 20 times within the wavelength region of 400- 3750 at a resolution of  $4\text{ cm}^{-1}$  using the Happ-Genzel function. A background scan was carried out before each sample.

MATLAB was used to create a model based after Swann and Patwardhan (2011) to assess the contamination of the phytolith samples by comparing the sample IR spectra to two endmember spectra that represented contamination and pure biogenic silica. Contaminant end members were prepared by leaching phytoliths from soil samples from each location using 1.0 M sodium hydroxide heated to  $80\text{ }^{\circ}\text{C}$  (Greenberg and Price, 1957). The pure biogenic silica endmembers were the UK Natural Environment Research Council (NERC) Isotope Geosciences Laboratory diatom standard "BFC" which originated from a lacustrine deposit in California, and "G95", which was created by extracting phytoliths from grass

(Chapligin et al., 2011; Hut, 1987; Leng et al., 2001; Leng and Sloane, 2008; Webb and Longstaffe, 2002). Baseline corrections and normalisations were carried out to the FTIR results of all samples, contaminant endmembers and clean biogenic silica endmembers. Following the procedure of Swann and Patwardhan (2011) only wavelengths between 700 and 1300 were retained for endmember modelling. This interval shows the main peaks for biogenic silica and common contaminants such as clays and cellulose. A mass-balance model was then created so that the sample was compared to its contaminant endmember and the pure endmember to work out the similarity to each of the endmembers. These were then averaged and used to estimate the relative contribution of each endmember. The model was run twice for each soil sample to compare against both pure endmembers.

### 2.3.3 Inductively coupled plasma mass spectrometry (ICP-MS)

One clay rich soil sample (NTAGFU0010) treated with method C2 underwent ICP-MS to check for aluminium contamination (indicative of clay) and compared to four biogenic silica standards. This was carried out to test how well the initial extraction method removes clays, and to test if the FTIR contamination modelling was accurate. There were insufficient phytoliths from the soil samples to do this on all samples.

## 3 Results and Discussion

Plant and soil samples were treated and evaluated in terms of the suitability of different techniques for a) preparation of plant material, b) chemical extraction of phytoliths with minimal contamination c) evaluation of the quantity and type of contaminants and d) employing plasma ashing to extract phytoliths from plants.

### 3.1 Preparation of plant samples for phytolith extractions

Of the three different methods of preparing the plant samples, the ball mill and cutting both worked well for preparing samples for extraction. Due to the fibrous nature of the grass, the

liquid nitrogen was incapable of breaking up the plant material into lengths suitable for extraction processes, so this method was abandoned.

It initially seemed that cutting samples resulted in a faster removal of organic matter by all extraction methods, as more organic matter was removed in the initial chemical extraction steps. When using the piranha solution treatment, cut plant samples appeared to dissolve more uniformly and rapidly in sulfuric acid than samples from the ball mill experiments. Samples that were ball-milled clumped together and needed to be stirred frequently to allow the sulfuric acid to dissolve the organic matter. However, when hydrogen peroxide was added to remove the dissolved organic matter, the cut plant sample solution took longer to turn clear than the ball-milled samples. Additional hydrogen peroxide was required to obtain a clear solution with the cut samples, indicating that the peroxide was not only removing dissolved carbon, but also reacting with undissolved organic matter.

During plasma ashing, all samples adhered to the glass of the rotating flask. The cut grass samples had larger pieces of grass knock the pieces of sample stuck to the flask, making them fall through the plasma. As a result, the samples had more contact with the electrons, ions, stable molecules, radicals, and photons produced by the plasma which was strongest in the centre of the flask making it more efficient at initial organic removal (Thiry et al., 2016). However, at 21 hours there was still a mixture of clean phytoliths, phytoliths with organic matter still attached, and complete grass fragments (Figure 2.B). The ball milled plant samples were free of organic matter at 21 hours, despite being adhered to the glass. The ball milled grass samples contained no visible organic matter under the microscope and appeared white compared to untreated ball milled leaf material after plasma treatment (Figure 2.D). The ball milling of the samples did result in crushed phytoliths, which could be an issue if morphology is of interest, cutting the plant sample would work best as it did not disrupt the skeletal phytoliths.

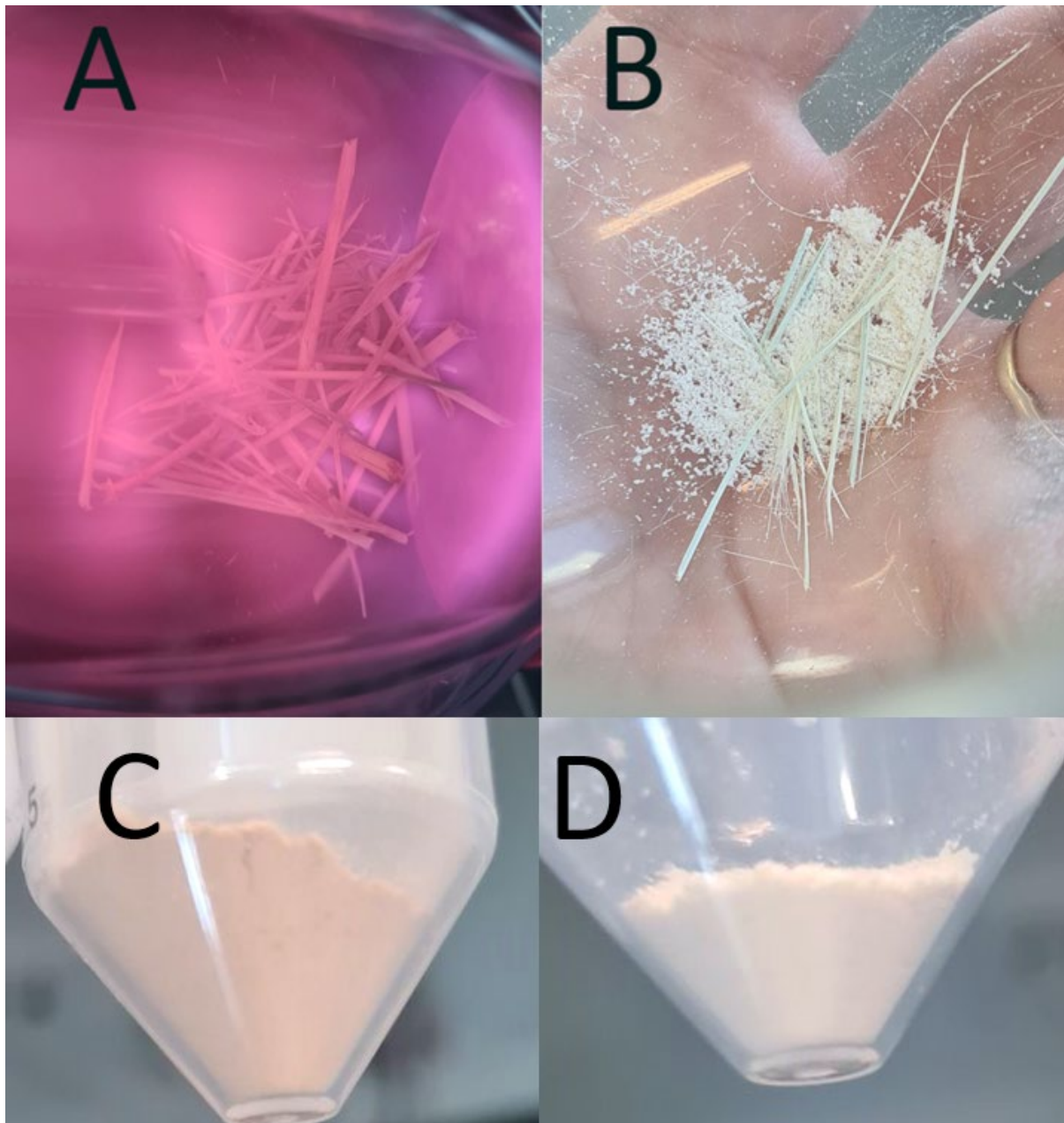


Figure 2 Cut native grass (T5) at the start of plasma treatment (A) and after 21 hours of plasma treatment (B). Untreated ball milled barley (T3) leaf material prior to plasma treatment (C) and after 21 hours of plasma treatment (D).

### 3.2 Phytolith extractions

#### 3.2.1 Chemical extraction methods for plant material

For plant samples, piranha solution was more efficient than plasma ashing with no contamination visible (Table 2). After the removal of pieces of grass from sample T5, the released phytoliths from cut grass (T5c) using the plasma ashing method showed no organic

matter under a polarising microscope and only small amounts of organic matter visible in crevices under SEM (Figure 3). The organic matter likely would have been removed if the sample had been either ball-milled first or had longer plasma treatment times.

Table 2 Results of assessment for contamination of phytoliths extracts from plants and soil using microscopy, ICP-MS and FTIR modelling.

Method	Preparation method	Material	Sample #	wt. (%) of phytoliths recovered	Visual observations (SEM and light microscope)	ICP-MS	FTIR modelled contamination - BFC endmember	FTIR modelled contamination - G95 endmember
<b>Chemical 1 (C1)</b>	Cut	Grass	T13a		Clean phytoliths with no visible organic matter			
	Ball mill	Barley	T6	0.13 %	Clean phytoliths with no visible organic matter			
	Ball mill	Barley	T7	0.07 %	Clean phytoliths with no visible organic matter			
	Cut	Barley	T8	0.14 %	Clean phytoliths with no visible organic matter			
	Cut	Barley	T9	0.10 %	Clean phytoliths with no visible organic matter			
	Cut	Barley	T10	0.07 %	Clean phytoliths with no visible organic matter			



Method	Preparation method	Material	Sample #	wt. (%) of phytoliths recovered	Visual observations (SEM and light microscope)	ICP-MS	FTIR modelled contamination - BFC endmember	FTIR modelled contamination - G95 endmember
<b>Chemical 2 (C2)</b>		Organic rich soil	T4a		Lots of organic matter, some visible clay			
		sandy clay	SATFLB0005		Some charcoal, lots of quartz, some organic matter, no visible clay		30 %	34 %
		Organic rich soil	NTAGFU0010		lots of charcoal and organic matter, no clay.	2 %	74 %	82 %
<b>Chemical 3 (C3)</b>		Organic rich soil	T4b	18.33 %	Lots of organic matter and some clay.			
<b>Chemical 4 (C4b)</b>		Organic rich soil	T4c	0.02 %	Clean phytoliths with no visible clay. Some charcoal but no other forms of organic matter visible			

Method	Preparation method	Material	Sample #	wt. (%) of phytoliths recovered	Visual observations (SEM and light microscope)	ICP-MS	FTIR modelled contamination - BFC endmember	FTIR modelled contamination - G95 endmember
(C4a)		sandy clay	SATFLB0005		some charcoal, lots of quartz, no visible organic or clay material		34 %	34 %
(C4a)		Organic rich soil	NTAGFU0010		Clean phytoliths with no visible clay. Lots of charcoal but no other forms of organic matter visible.		43 %	44 %
Plasma	Ball mill	Barley	T1 – 6 hour treatment		Lots of organic matter			
	Ball mill	Barley	T2 – 30 hour treatment	0.30 %	Clean			
	Ball mill	Barley	T3 – 21 hour treatment	0.26 %	Clean			
	Cut	Grass	T5c – 21 hour treatment		Some organic matter			

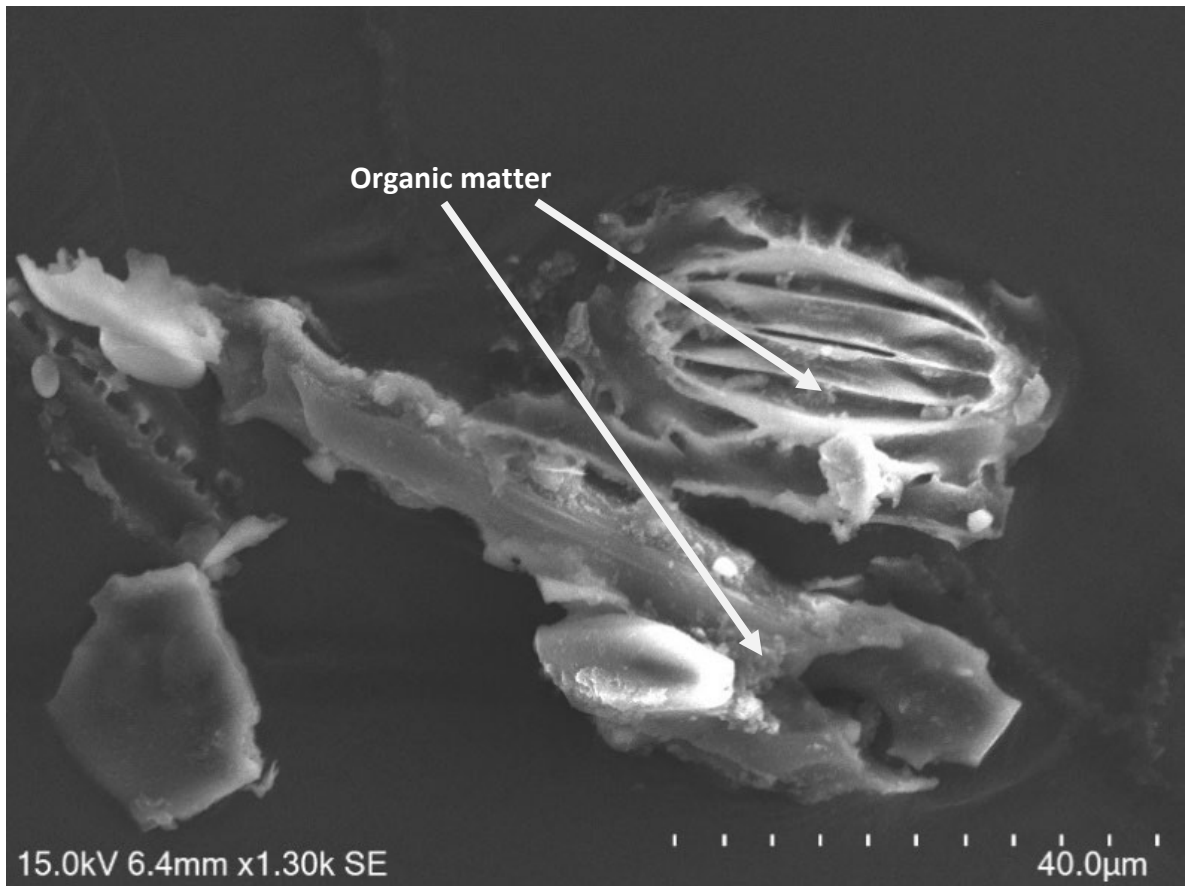


Figure 3 SEM image of extract after 21 hours of plasma on cut grass (T5c). Phytoliths from sample T5c show no damage caused by the plasma though there are small amounts of organic matter trapped in crevices.

### 3.2.2 Chemical extraction methods for soil material

Soil samples that were treated with methods C2 and C3 were all still contaminated with organic matter and charcoal. One sample (SATFLB0005) still had some quartz grains at the end of the treatments (Table 2). Quartz from the other samples were successfully removed during the SPT step. Residual contamination in samples treated with method C2 was only visible under a microscope but those treated with C3 had contamination that could be observed with the naked eye. Treatment temperatures of 90 °C or above during the organic removal steps may successfully result in a clean extract but that is not an option for phytoliths desired for oxygen isotopic analyses (Crespin et al., 2008). All extracts appeared to

have very low to no clay. No clay particles were visible under a polarising microscope. ICP-MS on the clay rich sample indicates the total amount of contamination of trace elements was 2.07% +/- 0.66. (Table 3). The two highest contaminating oxides were Fe<sub>2</sub>O<sub>3</sub> = 0.43% and Al<sub>2</sub>O<sub>3</sub> = 0.91% +/- 0.19. If further piranha solution treatment were applied, as in C4, it is expected that the final extracted sample would have even less contamination when examined with ICP-MS as the organic matter that binds clay would be removed, allowing steps targeting organic matter to be more successful (Piperno, 2006).

Table 3 ICP-MS results for sample NTAGFU0010 to assess contamination.

<b>SiO<sub>2</sub></b>	97.93% +/- 0.22
<b>Na<sub>2</sub>O</b>	0.16% +/- 0.03
<b>K<sub>2</sub>O</b>	0.12% +/- 0.03
<b>CaO</b>	0.23% +/- 0.05
<b>MgO</b>	0.098% +/- 0.02
<b>MnO</b>	0.04% +/- 0.01
<b>Fe<sub>2</sub>O<sub>3</sub></b>	0.43% +/- 0.09
<b>TiO<sub>2</sub></b>	0.04% +/- 0.01
<b>Al<sub>2</sub>O<sub>3</sub></b>	0.91% +/- 0.19
<b>P<sub>2</sub>O<sub>5</sub></b>	0.04% +/- 0.01
<b>Total trace elements</b>	2.07% +/- 0.66

Almost all soil samples contained at least some charcoal, and while the amount of charcoal in the samples decreased throughout the treatment, none of the methods comprehensively removed all charcoal. Further treatment with Piranha solution (C4) removed the organic

matter from these samples making them clean enough for oxygen isotope analysis, however there was still charcoal at the end of the treatment.

#### 3.2.2.1 Organic material

Extracts using C2 and C3 still had organic matter remaining, which can contain oxygen that would alter the measured values of phytolith  $\delta^{18}\text{O}$ . Organic matter also traps other contaminants in the sample, so this needs to be removed before oxygen isotope analysis, however removal can be inhibited by clay particles (Mikutta et al., 2005). Hydrogen peroxide removes the majority of organic matter but not all of it. Using sulfuric acid to breakdown organic matter, and then slowly adding hydrogen peroxide to remove the carbon by converting it to CO and CO<sub>2</sub> with by-products of H<sub>2</sub>O, O<sub>2</sub> and H<sub>2</sub>SO<sub>5</sub> was found to be faster and more effective. The caveat is, unlike plant material, sediments need to be pre-treated to remove the bulk of the other material, such as quartz, clay, and other minerals before using this solution otherwise there could be unknown reactions with other elements in the sediments (Bowman, 1989). There is evidence that the organic matter sticks to the other contamination, preventing the steps targeting clay and quartz from being successful (Piperno, 2006). This was supported by methods C2 and C3 having very different amounts of residual contamination even though the procedures used the same chemicals, just in different orders.

#### 3.2.2.2 Clay

While there was no visible clay in the samples, ICP-MS on the clay rich soil (NTAGFU0010) sample indicated there was nearly 1.5% aluminium and iron oxides in comparison to the other measured elements. This was done before piranha solution was used to clean the sample so it is assumed that it would be either the same or cleaner after being retreated. For the oxygen isotope analysis of biogenic silica, contamination needs to be under 3% of the mass of the sample (Leng and Barker, 2006). It has been suggested that clay sticks to the

organic matter, and this was probably a factor here as well. A combination of SPT and filtration at 10  $\mu\text{m}$  is sufficient to get rid of clay but organic matter needs to be removed before these steps otherwise the clay stays in the sample. Using piranha solution on soil samples requires SPT to be done twice. Once at a high density (denser than  $2.3 \text{ g/cm}^3$ ) to remove the bulk of the sediment before piranha treatment, and then again after piranha when the organics have been removed.

### 3.2.3 FTIR quantification of contamination

FTIR analysis on the clay rich soil sample (NTAGFU0010) indicated that there was not much contamination after method C2 and that there was a slight increase in contamination after C4 (Table 2, Figure 4.A, Figure 4.B). Absorbance for C2 (before piranha) and C4 (after piranha) (yellow and purple lines, Figure 4.A and Figure 4.B) are both more similar to the two biogenic silica end members (black lines) than the untreated endmember (blue line). There is more absorbance at approximately  $975 \text{ cm}^{-1}$  for the two treated samples (yellow and purple lines) compared to the two biogenic silica end members (black lines). After treatment with C4 (purple lines), there is a slight increase in absorbance at this location. This suggests that extracts using C4 had more OH groups attached to the phytoliths than extracts using in C2 for sample NTAGFU0010. This is not an issue for oxygen isotope analysis as the samples will undergo dehydroxylation to remove these before oxygen isotope analyses (Chapligin et al., 2010). The organic rich sample (SATFLB0005) FTIR results (Table 2, Figure 4.C and Figure 4.D) indicated a lot of residual contamination after treatment 2 (yellow line, Figure 4.C and Figure 4.D) and there was substantial improvement in phytolith purity after treatment with C4 (purple line). However, visual examination showed that SATFLB0005 extracts still had a lot of quartz after both treatments (Table 2).

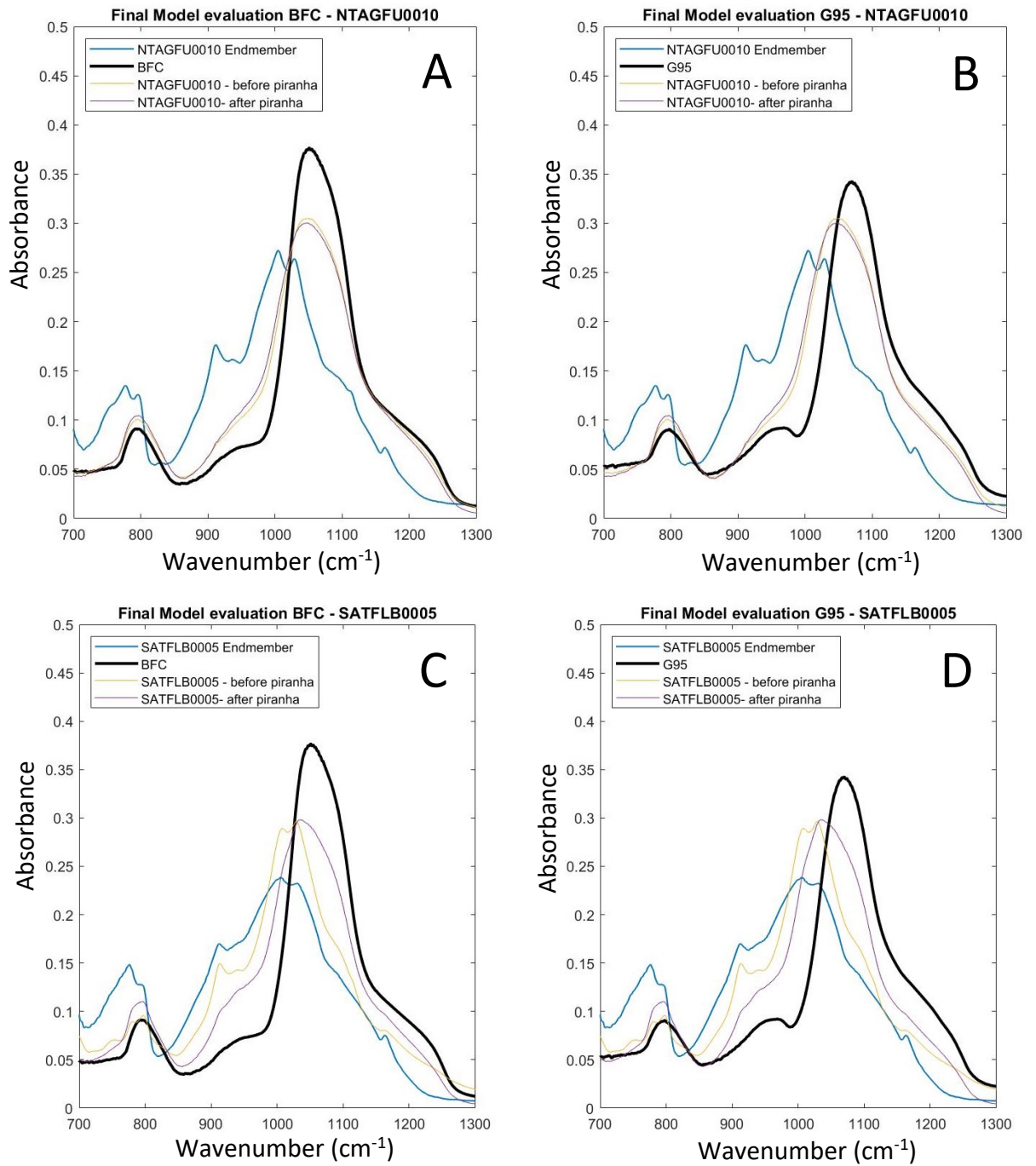


Figure 4 FTIR models for two sample endmembers compared against two biogenic silica standards (BFC (A and C) and G95 (B and D)) and two phytolith extracts from soils. Each plot shows the soil samples treated with C2 (yellow line) versus further treatment using piranha solution (C4) (purple line).

FTIR analyses and modelling suggested the final residual contamination for NTAGFU0010 was 43-44% and for SATFLB0005 34% (Table 2). However, NTAGFU0010 had no visible

contamination and ICP-MS indicated less than 2% contamination, so as a quantitative measure of contamination, the FTIR has clear room for improvement. To assess the types of residual contamination in biogenic samples, FTIR modelling provides a cheap and easy initial method that uses only small amounts of sample. While the modelling was able to pick up contamination of organic matter ( $900\text{ cm}^{-1}$ ) it did not pick up that sample SATFLB0005 (yellow lines of Figure 4.C and Figure 4.D) had a lot of residual quartz which should have resulted in higher absorbance at  $700\text{ cm}^{-1}$  which is visible in both soil endmembers (blue lines, Figure 4.A-D) (Meyer-Jacob et al., 2014). In theory this method is non-destructive, however, in this study, a small amount of each sample was lost in loading and recovery.

#### 3.2.4 Assessing density and size fractions of phytoliths from soils.

Density fractionations of the test soil showed that the portion denser than  $2.16\text{ g/cm}^3$  contained the occasional phytolith, but primarily consisted of quartz, organic matter, charcoal, and other unidentified contaminants. The fraction with a density between  $2.07\text{--}2.16\text{ g/cm}^3$  had some phytoliths, but contained much more organic contamination than phytoliths, and some charcoal. The least dense fraction ( $1.9\text{--}2.07\text{ g/cm}^3$ ) contained the majority of the phytoliths, some charcoal, and the occasional particulate of organic matter. The portion less dense than  $1.9\text{ g/cm}^3$  contained almost no particles, only the occasional clay and charcoal fragment. It is frequently claimed that the density of phytoliths ranges from  $1.5$  to  $2.3\text{ g/cm}^3$  (Jones and Beavers, 1963; Pearsall, 2015; Piperno, 2006; Rashid et al., 2019; Strömberg et al., 2018). However, this claim is based on Jones and Beavers (1963) which combined phytoliths of the size range  $20$  to  $50\text{ }\mu\text{m}$  from a number of sampling sites into one sample, and then separated this sample into aliquots using four different densities. The phytoliths were split into density fractions of less than  $1.74\text{ g/cm}^3$ ,  $1.74$  to  $1.89\text{ g/cm}^3$ ,  $1.89$  to  $2.04\text{ g/cm}^3$ ,  $2.04$  to  $2.12\text{ g/cm}^3$  and  $2.12\text{ g/cm}^3$  and higher. The authors (Jones and Beavers, 1963) concluded that because no phytoliths were found in densities higher than  $2.3$



g/cm<sup>3</sup> by previous studies, the phytoliths found in their study should have overall densities lower than 2.3 g/cm<sup>3</sup>. Consequently, all phytoliths in the fraction greater than 2.12 g/cm<sup>3</sup> (6% of all detected phytoliths) were reported to be between 2.12 and 2.3 (Jones and Beavers, 1963). This has been interpreted as some phytoliths have a density of 2.3, which has not actually been tested. All the study showed was that there were phytoliths with a density greater than 2.12 g/cm<sup>3</sup>. Two older papers reported phytoliths extracted from plants having a density of 2.10 and 2.15 g/cm<sup>3</sup> (Baker, 1959a; Kanno and Arimura, 1958). It may be time to reassess the density of phytoliths, and if very few phytoliths are above 2.2 g/cm<sup>3</sup>, it will be significantly easier to remove contaminants from phytoliths using a lower density solution than 2.3. For the scope of this study, sacrificing a small number of phytoliths in favour of achieving a higher level of sample purity is unlikely to significantly impact the results.

Nested cell filtration was used to isolate the phytoliths extracted from soil by size and there were few phytoliths bigger than 85 µm, but in terms of volume, this fraction made up a larger portion than the smaller fractions combined. The majority of the phytoliths were between 85 - 20 µm. While there were numerous phytoliths in the 20 – 10 µm portion, in terms of volume, this fraction contained very little biogenic silica. There were no visible phytoliths in the <10 µm portion. There was no visible clay in the fractions larger than 10 µm for any of the soil samples and minor organic matter through all fractions indicating that most of the residual contamination was in fraction with a density greater than 2.07 g/cm<sup>3</sup>.

### 3.2.5 Plasma ashing of plant material

The plasma set up used in this study successfully removed organic matter from plant material to extract phytoliths. Plasma extracted samples yielded higher weight percentage of phytoliths from grass than the piranha digested extracted samples, which suggests there was a loss of phytoliths during the chemical method.

Unfortunately, the method applied was inefficient and thus impractical for processing large batches of samples under the chosen conditions. Only one sample at a time can be plasma ashed and at an input power of 25 W, it took up to 30 hours for the complete organic removal from a ball-milled plant sample. The cut native grass samples were abandoned at 21 hours due to the amount of organic matter remaining. For morphology studies, a much shorter time at a high temperature could be applied as most of the organic matter is removed within the first few hours. With optimizing, non-thermal plasma ashing could be a viable option for extracting biogenic silica for oxygen isotope analysis as well. Higher power produces more heat, so some suggestions for optimisation for extracting phytoliths for oxygen isotope analysis are cooling the airflow as it comes in, cooling around the glass chamber, increasing airflow through the system to allow an increase in power as heat would be removed faster and this would enable faster processing time. Argon or pure oxygen could be tested to see if organic removal can be sped up. Initial organic matter was removed faster with the cut grass, likely due to particles sticking to the glass being knocked off by bigger pieces of grass, allowing them to fall through the plasma. Some sort of mechanism that could agitate the adhered particles, such as small glass beads, could be used.

It was noticed that the amount of organic matter being reacted affected the temperature of the plasma. The internal temperature of the flask rises quite quickly during the initial few hours of plasma ashing, but once the bulk of the organic matter is removed, the temperature decreases. The bulk of the organic matter in the ground samples was removed in 6 hours while the remaining organic matter was removed more slowly. During the removal of this remaining organic matter, the plasma temperature was only 2 °C warmer than the room temperature. A potential change could be to treat with plasma at low power to start, and then, after most of the organic matter has been removed, increase the power so that more energetic plasma is generated.

For the cut grass, the residual pieces of grass (T5a) were digested using piranha solution and there were few phytoliths extracted. Visually, the residue contained significantly less phytoliths than the initial “fall out” indicating that the phytoliths are accumulating closer to the surface rather than deeper into the leaf and stem and as the surface layer of the grass is removed via plasma first, they were released. These are similar findings to Jakes and Mitchell (1996) where phytoliths “fell” out of the leaf material as the material was plasma ashed at high temperature. This could create an opportunity for partial removal of phytoliths for morphological investigation or to assess isotopic differences within different parts of leaves of a plant. If there is a difference in  $\delta^{18}\text{O}$  values between the phytoliths that fall out at the start vs those that do not, it is more likely that it is the phytoliths from transpiring tissue are falling out providing a record of relative humidity and temperature, while phytoliths from non-transpiring tissue are still in the plant, which records primarily the temperature. So, this could potentially be a quick way to isolate transpiring tissue phytoliths for oxygen isotope ratios for relative humidity studies or isolating the temperature and relative humidity signals from each other.

### 3.2.6 Future soil phytolith extractions using chemicals

An optimised method for future extractions of phytoliths from soils or organic rich sediments is proposed on the basis of the experimental results presented here (Figure 5, Appendix 1 for detailed steps). This method represents a streamlined and modified version of C2 with a change in the organic matter removal step from  $\text{H}_2\text{O}_2$  to piranha solution to remove organics and a reorganising of the steps to ensure that the organic matter is removed before clay removal is attempted and to limit undesirable reactions with soil material (Piperno, 2006; Schmidt, 2022). This method needs future testing but should result in cleaner samples with fewer steps than doing method 4a where there is repetition in steps due to it being one extraction method following another.

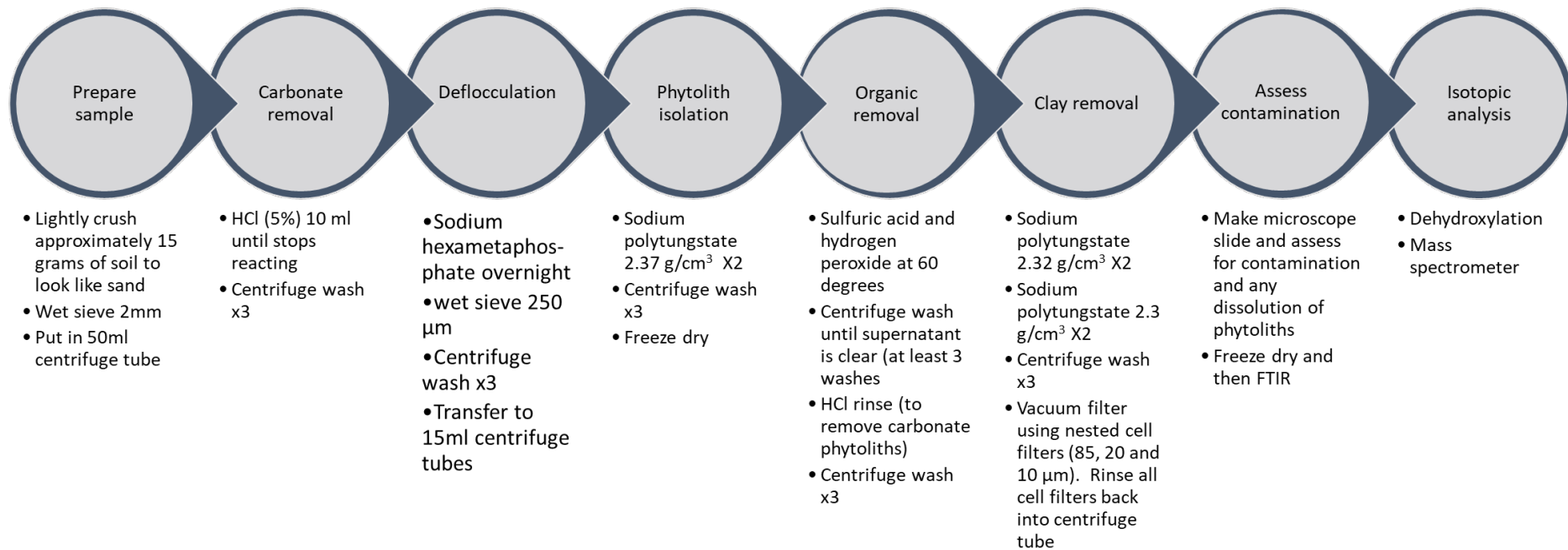


Figure 5 Proposed steps for extracting phytoliths from soils for oxygen isotope analyses. Detailed procedure in Appendix 1

## 4 Conclusion

This study examined a range of chemical and physical methods for purifying phytoliths from plants and soils for oxygen isotope analysis. Methods using piranha solution (C1 and C4) or plasma ashing both extracted phytoliths to a standard suitable for subsequent oxygen isotope analysis, while other chemical extraction methods without piranha solution (C2 and C3) did not. For phytolith samples that contain residual contamination, piranha solution followed by density separation and filtration can result in suitably clean samples for oxygen isotope determination. Chemical extractions allow for multiple phytolith samples to be extracted at the same time, while plasma ashing using the equipment described here can only extract one sample at a time. This low extraction throughput, combined with the long processing time for a plasma ashed sample, makes this process very inefficient for processing large batches of samples, however this could be greatly optimised in the future. The plasma ashing as it stands, would be better for targeted studies focusing on morphology.

## 5 References

- Abrantes, F. (2003) A 340,000 year continental climate record from tropical Africa – news from opal phytoliths from the equatorial Atlantic. *Earth and Planetary Science Letters* 209, 165-179.
- Alexandre, A., Crespin, J., Sylvestre, F., Sonzogni, C. and Hilbert, D.W. (2012) The oxygen isotopic composition of phytolith assemblages from tropical rainforest soil tops (Queensland, Australia): validation of a new paleoenvironmental tool. *Climate of the Past* 8, 307-324.
- Alexandre, A., Landais, A., Vallet-Coulomb, C., Piel, C., Devidal, S., Pauchet, S., Sonzogni, C., Couapel, M., Pasturel, M., Cornuault, P., Xin, J., Mazur, J.-C., Prié, F., Bentaleb, I., Webb, E., Chalié, F. and Roy, J. (2018) The triple oxygen isotope composition of phytoliths as a proxy of continental atmospheric humidity: insights from climate chamber and climate transect calibrations. *Biogeosciences* 15, 3223-3241.
- Baker, G. (1959a) A contrast in the opal phytolith assemblages of two Victorian soils. *Australian Journal of Botany* 7, 88-96.
- Baker, G. (1959b) Opal phytoliths in some Victorian soils and "red rain" residues. *Australian Journal of Botany* 7, 64-87.
- Bird, M.I., Charville-Mort, P.D.J., Ascough, P.L., Wood, R., Higham, T. and Apperley, D. (2010) Assessment of oxygen plasma ashing as a pre-treatment for radiocarbon dating. *Quaternary Geochronology* 5, 435-442.
- Bowman, R.A. (1989) A Sequential Extraction Procedure with Concentrated Sulfuric Acid and Dilute Base for Soil Organic Phosphorus. *Soil Science Society of America Journal* 53, 362-366.
- Bremond, L., Alexandre, A., Wooller, M.J., Hély, C., Williamson, D., Schäfer, P.A., Majule, A. and Guiot, J. (2008) Phytolith indices as proxies of grass subfamilies on East African tropical mountains. *Global and Planetary Change* 61, 209-224.
- Cabanes, D. and Shahack-Gross, R. (2015) Understanding Fossil Phytolith Preservation: The Role of Partial Dissolution in Paleoecology and Archaeology. *PLOS ONE* 10, e0125532.
- Chapligin, B., Leng, M.J., Webb, E., Alexandre, A., Dodd, J.P., Ijiri, A., Lücke, A., Shemesh, A., Abelmann, A., Herzsuh, U., Longstaffe, F.J., Meyer, H., Moschen, R., Okazaki, Y., Rees, N.H., Sharp, Z.D., Sloane, H.J., Sonzogni, C., Swann, G.E.A., Sylvestre, F., Tyler, J.J. and Yam, R. (2011) Inter-laboratory comparison of oxygen isotope compositions from biogenic silica. *Geochimica et Cosmochimica Acta* 75, 7242-7256.
- Chapligin, B., Meyer, H., Friedrichsen, H., Marent, A., Sohns, E. and Hubberten, H.W. (2010) A high-performance, safer and semi-automated approach for the delta18O analysis of diatom silica and new methods for removing exchangeable oxygen. *Rapid Commun Mass Spectrom* 24, 2655-2664.
- Corbineau, R., Reyerson, P.E., Alexandre, A. and Santos, G.M. (2013) Towards producing pure phytolith concentrates from plants that are suitable for carbon isotopic analysis. *Review of Palaeobotany and Palynology* 197, 179-185.
- Crespin, J., Alexandre, A., Sylvestre, F., Sonzogni, C., Paillès, C. and Garreta, V. (2008) IR Laser Extraction Technique Applied to Oxygen Isotope Analysis of Small Biogenic Silica Samples. *Analytical Chemistry* 80, 2372-2378.
- Ford, M.N. (2022) Investigating the Effects of Non-thermal Air Plasma on Five Grains and Their Economically Important Pathogens. University of Adelaide.
- Geis, J.W. (1973) Biogenic Silica in Selected Species of Deciduous Angiosperms. *Soil science* 116, 113-130.

- Geis, J.W. (1978) Biogenic Opal in Three Species of Gramineae. *Annals of Botany* 42, 1119-1129.
- Graham, J. (2020) *Biological centrifugation*. Garland Science.
- Greenberg, S.A. and Price, E.W. (1957) The Solubility of Silica in Solutions of Electrolytes. *The Journal of Physical Chemistry* 61, 1539-1541.
- Hut, G. (1987) Stable isotope reference samples for geochemical and hydrological investigations. Consultant Group Meeting IAEA, Vienna, 16–18 September 1985, Report to the Director General. International Atomic Energy Agency, Vienna 42.
- Jain, R., Dhali, S., Nigam, H., Malik, A., Malik, H.K. and Satyakam, R. (2022) Recovery of diatom bio-silica using chemical, thermal, and plasma treatment. *Bioresource Technology Reports* 18, 101035.
- Jakes, K. and Mitchell, J. (1996) Cold Plasma Ashing Preparation of Plant Phytoliths and their Examination with Scanning Electron Microscopy and Energy Dispersive Analysis of X-rays. *Journal of Archaeological Science* 23, 149-156.
- Jones, R.L. and Beavers, A.H. (1963) Some mineralogical and chemical properties of plant opal. *Soil science* 96, 375-379.
- Kanno, I. and Arimura, S. (1958) Plant Opal in Japanese soils. *Soil Science and Plant Nutrition* 4, 62-67.
- Katz, O., Cabanes, D., Weiner, S., Maeir, A.M., Boaretto, E. and Shahack-Gross, R. (2010) Rapid phytolith extraction for analysis of phytolith concentrations and assemblages during an excavation: an application at Tell es-Safi/Gath, Israel. *Journal of Archaeological Science* 37, 1557-1563.
- Lebeau, O., Busigny, V., Chaduteau, C. and Ader, M. (2014) Organic matter removal for the analysis of carbon and oxygen isotope compositions of siderite. *Chemical Geology* 372, 54-61.
- Leng, M., Barnker, P., Greenwood, P., Roberts, N. and Reed, J. (2001) Oxygen isotope analysis of diatom silica and authigenic calcite from Lake Pinarbasi, Turkey. *Journal of Paleolimnology* 25, 343-349.
- Leng, M.J. and Barker, P.A. (2006) A review of the oxygen isotope composition of lacustrine diatom silica for palaeoclimate reconstruction. *Earth-Science Reviews* 75, 5-27.
- Leng, M.J. and Sloane, H.J. (2008) Combined oxygen and silicon isotope analysis of biogenic silica. *Journal of Quaternary Science* 23, 313-319.
- Lentfer, C.J. and Boyd, W.E. (1998) A Comparison of Three Methods for the Extraction of Phytoliths from Sediments. *Journal of Archaeological Science* 25, 1159-1183.
- Lentfer, C.J. and Boyd, W.E. (1999) An Assessment of Techniques for the Deflocculation and Removal of Clays from Sediments Used in Phytolith Analysis. *Journal of Archaeological Science* 26, 31-44.
- McInerney, F.A., Strömberg, C.A.E. and White, J.W.C. (2011) The Neogene transition from C3 to C4 grasslands in North America: stable carbon isotope ratios of fossil phytoliths. *Paleobiology* 37, 23-49.
- Meyer-Jacob, C., Vogel, H., Boxberg, F., Rosén, P., Weber, M.E. and Bindler, R. (2014) Independent measurement of biogenic silica in sediments by FTIR spectroscopy and PLS regression. *Journal of Paleolimnology* 52, 245-255.
- Michl, T.D., Coad, B.R., Hüsler, A., Vasilev, K. and Griesser, H.J. (2015) Laboratory Scale Systems for the Plasma Treatment and Coating of Particles. *Plasma Processes and Polymers* 12, 305-313.
- Mikutta, R., Kleber, M., Kaiser, K. and Jahn, R. (2005) Review. *Soil Science Society of America Journal* 69, 120.

- Morley, D.W., Leng, M.J., Mackay, A.W., Sloane, H.J., Rioual, P. and Battarbee, R.W. (2004) Cleaning of lake sediment samples for diatom oxygen isotope analysis. *Journal of Paleolimnology* 31, 391-401.
- Musić, S., Filipović-Vinceković, N. and Sekovanić, L. (2011) Precipitation of amorphous SiO<sub>2</sub> particles and their properties. *Brazilian journal of chemical engineering* 28, 89-94.
- Pearsall, D.M. (2015) *Paleoethnobotany, Third Edition : A Handbook of Procedures*, 3rd ed. Left Coast Press, Walnut Creek.
- Pfeiffer, F. and Fischer, E.K. (2020) Various Digestion Protocols Within Microplastic Sample Processing—Evaluating the Resistance of Different Synthetic Polymers and the Efficiency of Biogenic Organic Matter Destruction. *Frontiers in Environmental Science* 8.
- Piperno, D.R. (2006) *Phytoliths: a comprehensive guide for archaeologists and paleoecologists*. Academic Press, San Diego.
- Rashid, I., Mir, S.H., Zurro, D., Dar, R.A. and Reshi, Z.A. (2019) Phytoliths as proxies of the past. *Earth-Science Reviews* 194, 234-250.
- Rietti-Shati, M., Shemesh, A. and Karlen, W. (1998) A 3000-Year Climatic Record from Biogenic Silica Oxygen Isotopes in an Equatorial High-Altitude Lake. *Science* 281, 980-982.
- Roy, B., Patra, S. and Sanyal, P. (2020) The carbon isotopic composition of occluded carbon in phytoliths: A comparative study of phytolith extraction methods. *Review of Palaeobotany and Palynology* 281, 104280.
- Saad, E., Pickering, R., Shoji, K., Hossain, M., Glover, T., Krause, J. and Tang, Y. (2020) Effect of cleaning methods on the dissolution of diatom frustules. *Marine Chemistry* 224, 103826.
- Schmidt, H.G. (2022) Safe Piranhas: A Review of Methods and Protocols. *ACS Chemical Health & Safety* 29, 54-61.
- Shemesh, A., Charles, C.D. and Fairbanks, R.G. (1992) Oxygen isotopes in biogenic silica: global changes in ocean temperature and isotopic composition. *Science* 256, 1434-1436.
- Snelling, A.M., Swann, G.E.A., Leng, M.J. and Pike, J. (2012) A Micro-manipulation Technique for the Purification of Diatoms for Isotope and Geochemical Analysis. *Silicon* 5, 13-17.
- Strömberg, C.A.E., Dunn, R.E., Crifò, C. and Harris, E.B. (2018) Phytoliths in Paleoecology: Analytical Considerations, Current Use, and Future Directions, in: Croft, D.A., Su, D.F., Simpson, S.W. (Eds.), *Methods in Paleoecology: Reconstructing Cenozoic Terrestrial Environments and Ecological Communities*. Springer International Publishing, Cham, pp. 235-287.
- Swann, G.E.A., Leng, M.J., Juschus, O., Melles, M., Brigham-Grette, J. and Sloane, H.J. (2010) A combined oxygen and silicon diatom isotope record of Late Quaternary change in Lake El'gygytgyn, North East Siberia. *Quaternary Science Reviews* 29, 774-786.
- Swann, G.E.A. and Patwardhan, S.V. (2011) Application of Fourier Transform Infrared Spectroscopy (FTIR) for assessing biogenic silica sample purity in geochemical analyses and palaeoenvironmental research. *Climate of the Past* 7, 65-74.
- Thiry, D., Konstantinidis, S., Cornil, J. and Snyders, R. (2016) Plasma diagnostics for the low-pressure plasma polymerization process: A critical review. *Thin Solid Films* 606, 19-44.
- Tyler, J.J., Sloane, H.J., Rickaby, R.E.M., Cox, E.J. and Leng, M.J. (2017) Post-mortem oxygen isotope exchange within cultured diatom silica. *Rapid Communications in Mass Spectrometry* 31, 1749-1760.
- Tyner, E.H. (1940) The use of sodium metaphosphate for dispersion of soils for mechanical analysis. *Proceedings. Soil Science Society of America*, 1939 4, 106-113.



- Urban, M.A., Romero, I.C., Sivaguru, M. and Punyasena, S.W. (2018) Nested cell strainers: An alternative method of preparing palynomorphs and charcoal. *Review of Palaeobotany and Palynology* 253, 101-109.
- Wallis, L. (2001) *The History of Phytolith Researchers In Australia*.
- Webb, E.A. and Longstaffe, F.J. (2000) The oxygen isotopic compositions of silica phytoliths and plant water in grasses: implications for the study of paleoclimate. *Geochimica et Cosmochimica Acta* 64, 767-780.
- Webb, E.A. and Longstaffe, F.J. (2002) Climatic influences on the oxygen isotopic composition of biogenic silica in prairie grass. *Geochimica et Cosmochimica Acta* 66, 1891-1904.
- White A., Sparrow B., Leitch E., Foulkes J., Flitton R., Lowe A. and Caddy-Retalic S. (2012) *Ausplots rangelands survey protocols manual*, V. 1.2.9 ed. The University of Adelaide Press, Adelaide, South Australia.
- Zhao, Z. and Pearsall, D.M. (1998) Experiments for Improving Phytolith Extraction from Soils. *Journal of Archaeological Science* 25, 587-598.

## Chapter 3:

A revised method for the dehydroxylation  
of biogenic silica prior to oxygen isotope  
analyses

# Statement of Authorship

Title of Paper	Dehydroxylation of biogenic silica		
Publication Status	<input type="checkbox"/> Published	<input type="checkbox"/> Accepted for Publication	<input checked="" type="checkbox"/> Unpublished and Unsubmitted work written in manuscript style
Publication Details			

## Principal Author

Name of Principal Author (Candidate)	Kimberley Edwards		
Contribution to the Paper	Designed the study. Conducted sample processing and analysis. Conducted data analysis and interpretation. Wrote manuscript.		
Overall percentage (%)	85		
Certification:	This paper reports on original research I conducted during the period of my Higher Degree by Research candidature and is not subject to any obligations or contractual agreements with a third party that would constrain its inclusion in this thesis. I am the primary author of this paper.		
Signature		Date	31/01/2023

## Co-Author Contributions

By signing the Statement of Authorship, each author certifies that:

- i. the candidate's stated contribution to the publication is accurate (as detailed above);
- ii. permission is granted for the candidate to include the publication in the thesis; and
- iii. the sum of all co-author contributions is equal to 100% less the candidate's stated contribution.

Name of Co-Author	Dr Robert Klæbe		
Contribution to the Paper	Provided input into the study design. Reviewed and edited final manuscript		
Signature		Date	31/01/2023

Name of Co-Author	Dr Jonathan Tyler		
Contribution to the Paper	Provided input into study design. Reviewed and edited final manuscript.		

Signature		Date	1/2/2023
-----------	--	------	----------

Name of Co-Author	Dr Alexander Francke		
Contribution to the Paper	Reviewed and edited manuscript.		
Signature		Date	25/01/2023

Name of Co-Author	Dr Francesca McInerney		
Contribution to the Paper	Reviewed and edited manuscript.		
Signature		Date	31/01/2023

## Abstract

The oxygen isotope composition of biogenic silica, such as diatoms and phytoliths, is often used as a proxy for determining past climate. However, some of the silica-bonded oxygen is in the form of silanol, with loosely bound hydroxyl groups that exchange oxygen with surrounding water, both in the sedimentary environment and in the laboratory.

Palaeoclimate applications therefore only target the oxygen trapped within tetrahedrally bonded siloxane silica, requiring that oxygen bound in hydroxyl groups be accounted for by either removal or controlled exchange with oxygen of a known isotopic composition prior to mass spectrometry. Several methods exist to undertake dehydroxylation efficiently, however they all require specialised equipment in addition to the mass spectrometer and silica preparation device. In addition, most of the established methods do not provide the means to determine the amount and oxygen isotope composition of hydroxyl-bonded oxygen within a sample.

A new method for dehydroxylating biogenic silica was developed using a HEKAtech high temperature oxygen analyser (TC) coupled to a EuroVector Euro elemental analyser (EA) and a Nu Instruments Perspective Isotope Ratio Mass Spectrometer (IRMS) operated in continuous flow mode. The same instruments were used to subsequently extract and measure oxygen isotope ratios from the residual siloxane, thus avoiding the need for additional peripheral devices or double handling of samples. This method was tested on reference material of known isotopic composition and yielded the expected isotope ratios. In addition, for two samples of phytoliths extracted from soils, the new method provided

equivalent or better precision to results from samples prepared using offline inert gas flow thermal dehydroxylation (IFD). While the new method is slower than IFD, which can be performed in batches, it enables the analysis of smaller sample sizes (600 µg compared to 2000 µg) and provides the potential for analysing the oxygen isotope ratios of the silanol-bound oxygen being removed as well as the targeted siloxane silica.

## 1 Introduction

Growing interest in using the  $\delta^{18}\text{O}$  values of biogenic silica as a proxy for past climates has created the need for more accessible and reproducible analytical methods. Biogenic silica contains up to 12% exchangeable oxygen in the form of water and hydroxyl molecules within silanol (Si-OH) (Knauth, 1973). As a consequence, the exchangeable oxygen needs to be removed or exchanged with oxygen of a known isotopic composition before the oxygen isotope composition of structurally stable, tetrahedrally bonded silica (siloxane, Si-O-Si) is analysed as a proxy for past climates and environments (Chapligin et al., 2011). Several different methods exist for silica dehydroxylation as well as subsequent oxygen isotope analysis, including stepwise fluorination (Leng et al., 2001; Leng and Sloane, 2008) low intensity laser fluorination (Dodd and Sharp, 2010) and inductively coupled high temperature reduction (Lücke et al., 2005), as well as controlled isotope exchange (Crespin et al., 2008; Juillet-Leclerc and Labeyrie, 1987). At the University of Adelaide, exchangeable oxygen is removed from biogenic silica using inert gas flow thermal dehydroxylation (IFD) in an offline tube furnace following Chapligin et al. (2010). Silica samples are loaded into nickel capsules and heated to 1100°C under a stream of either helium or argon gas. The samples are then cooled to room temperature and transferred for analysis by microfluorination thermal conversion elemental analyser isotope ratio mass spectrometry (TC/EA-IRMS) following Menicucci et al. (2013). Microfluorination is accomplished via heating in the

presence of Polytetrafluoroethylene (PTFE; aka Teflon®) that degrades to hydrofluoric acid at high temperature and break the Si-O-Si bonds to release CO gas for online isotope ratio analysis (Menicucci et al. 2013). Offline IFD preparation offers distinct advantages, namely that it can be conducted with batches of samples relatively quickly. However, IFD also has disadvantages, notably the need to purchase and maintain an additional piece of equipment, as well as a lack of any ability to monitor the dehydroxylation of individual samples. With this in mind, we explored the potential for performing dehydroxylation online, using the same TC/EA-IRMS apparatus that is subsequently used to measure oxygen isotope ratios.

A new method was explored, referred to as the EA dehydroxylation method (EAD), whereby loosely bonded water and hydroxyl oxygen is released by heating to 1450°C (a higher temperature than IFD) in the absence of fluorine, without ramp degassing (slowly heating the sample so that the oxygen is slowly released), sample cooling, or additional handling of the sample after dehydroxylation. This new method is tested on silica reference material of known isotopic composition as well as on two samples of phytoliths extracted from soil to compare the isotopic results from EAD method with those using IFD.

## 2 Materials and methods

### 2.1 Materials

Three silica standards were used to test a new EAD method for dehydrating and dehydroxylating biogenic silica. The  $\delta^{18}\text{O}$  values of the tested standards expressed relative to Vienna Standard Mean Ocean Water (VSMOW) are  $9.57 \pm 0.3 \text{ ‰}$  for quartz standard NBS-28,  $29.0 \pm 0.3 \text{ ‰}$  for diatomite standard BFC and  $36.6 \pm 0.8 \text{ ‰}$  for phytolith standard G95-25-CL (Chapligin et al., 2011; Hut, 1987; Leng and Sloane, 2008; Webb and Longstaffe, 2002). All three standards have been assessed for cleanliness and reproducibility previously in Chapligin et al. (2011).

Two samples of phytoliths extracted from topsoils (S1 - NTADAC0001 and S17 - SATFLB0012) were also used to compare the EAD method with the IFD method. The purification of phytoliths from soil is described in detail in Chapter 4, but briefly, samples were treated with hydrogen peroxide, sulphuric acid, hydrochloric acid, and sodium hexametaphosphate and then underwent density separation using sodium polytungstate and nested cell filtration. Samples were checked for contamination using microscopy and Fourier transform infra-red (FTIR) analysis (see Chapter 2 and 4 for more details).

## 2.2 Dehydroxylation and IRMS comparison

### 2.2.1 TC/EA-IRMS setup

All oxygen isotope measurements of silica, whether prepared by EAD or IFD method, were measured using the same TC/EA-IRMS set up. The reaction column of the TC/EA furnace was packed with glassy carbon chips and nickelised carbon powder, heated and maintained at 1450°C under a continuous helium flow at approximately 80 ml/min. At this temperature, oxygen is released from hydroxyl bonded to biogenic silica, which then reacts with carbon to form carbon monoxide which is analysed by the IRMS. The helium flow is used to carry carbon monoxide through the TC/EA into the IRMS via a water trap, a liquid nitrogen trap, a calcium metal trap, and silver wool before being introduced to the IRMS for oxygen isotope analysis. The liquid nitrogen traps any resultant silicon tetrafluoride and water molecules, and needs to be baked and purged regularly to prevent blockage (Menicucci et al., 2013). This is done manually between analyses while the trap is set to waste using a heat gun to heat up the trap to at least 100 degrees to vaporise the water.

### 2.2.2 Preliminary testing of the EAD method.

During preliminary trials of the EAD method (Supplementary information S.2, Appendix 2), it was noted that unlike in Menicucci et al. (2013), PTFE runs used to clear the column



frequently returned readings the same or close to the  $\delta^{18}\text{O}$  value of the sample analysed previously. As a result, a small trial was run to see if it was possible to get more than 1 reading from each replicate by analysing multiple PTFE + graphite mix additions. BFC was finely ground and 250  $\mu\text{g}$  weighed into a silver capsule and crimped. The capsule was then introduced into the reaction column of the TC/EA and left for 20 minutes to dehydroxylate. Then 10 silver capsules of 1000  $\mu\text{g}$  of PTFE + graphite mix (ratio of 1000:85) were analysed. The peak area, which represents the amount of signal the mass spec is analysing, was recorded to test if the amount of signal had any correlation with the recorded isotope values of the biogenic silica.

### 2.2.3 EAD method

Prior to analyses, each sample was finely ground to ensure homogeneous samples and to maximise sample surface area. Four to five subsamples (150  $\mu\text{g}$  +/- 10 %) of each sample were weighed into silver capsules and crimped. Analysis was conducted in a series of four to five subsamples (replicates). The first replicate was used as a column conditioner. It was introduced into the reaction column of the oxygen analyser and held for 20 minutes under continuous helium flow at approximately 80 ml/min (Figure 1). Loosely bound hydroxyl and water groups are carried away by the carrier gas and analysed as a measure of the exchangeable oxygen. After 20 minutes, 2000  $\mu\text{g}$  of PTFE + graphite mix weighed into a silver capsule was introduced into the reaction column of the oxygen analyser with the sample introduced previously (Menicucci et al., 2013). The PTFE, once heated, reacts with the silica sitting in the column, breaking the silicon-oxygen bonds and allowing silicon to bond to fluorine (F), producing waste silicon tetrafluoride (Menicucci et al., 2013). The released oxygen bonds with the carbon from the graphite and the carbon column to form carbon monoxide. The result from the initial conditioning sample is discarded, following Menicucci

et al. (2013). The following three to four replicates in the analytical suite were repeated in the same way except by analysing two PTFE + graphite mixes after the sample instead of one (Figure 1). After each set of replicates were analysed, the column of the oxygen analyser was flushed of remaining silica by analysing 4 silver capsules with at least 2 mg of PTFE, ensuring that blank CO peak readings had returned to background levels before proceeding with subsequent samples.

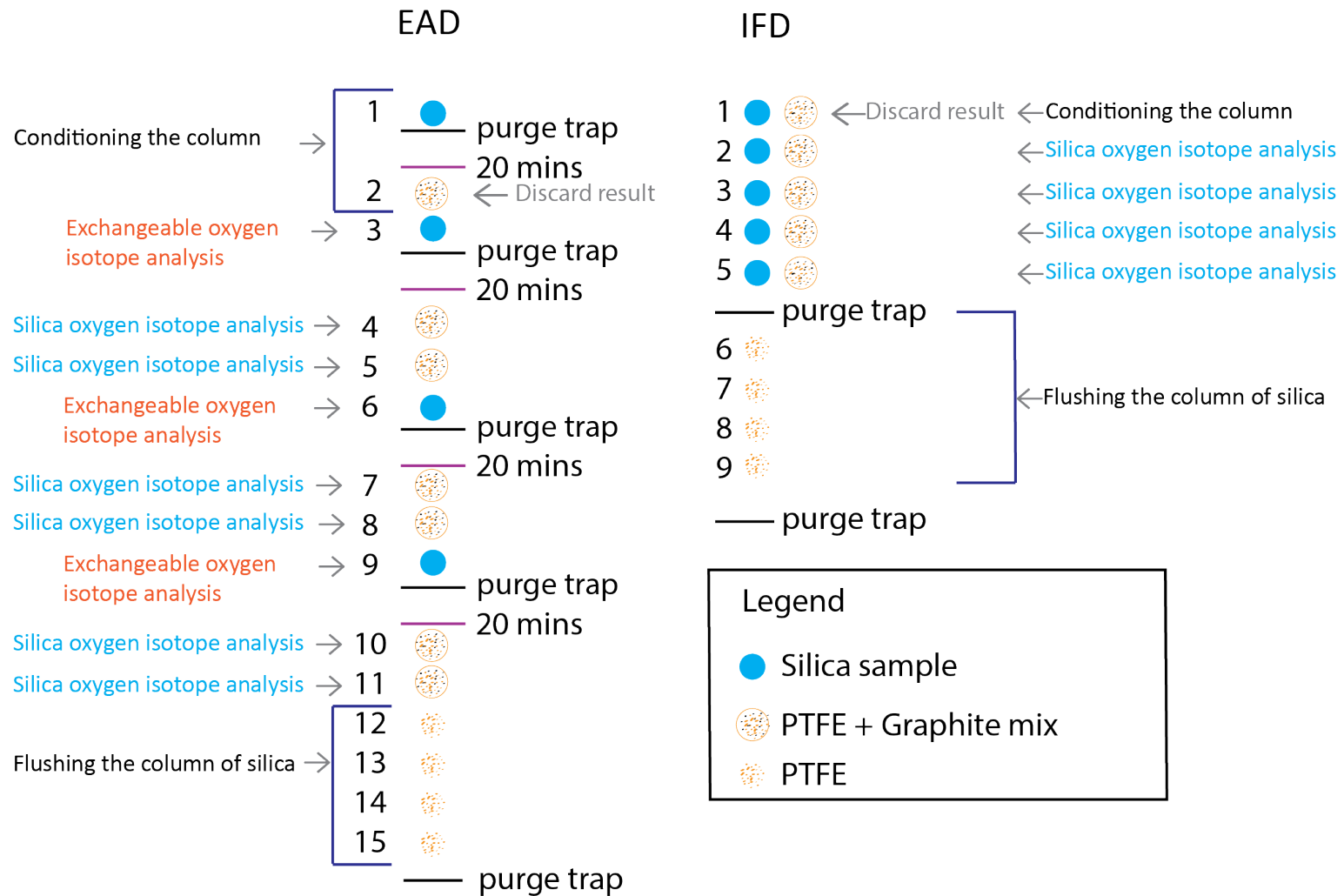


Figure 1 Comparison of analytical suites using the EAD and IFD methods, with line numbers indicating an analysis.

#### 2.2.4 IFD method

The Chaplignin et al. (2010) IFD method was used to prepare phytolith samples for comparison to  $\delta^{18}\text{O}$  values obtained with the EAD method. At least 2000  $\mu\text{g}$  of each sample was loaded into nickel capsules then placed into a tube furnace under argon gas flow of 5L/minute (Menicucci et al., 2020; Menicucci et al., 2017). The tube furnace was heated to 1100°C over two hours and held at this temperature for one hour, allowing weak oxygen bonds to break, and oxygen removal via the gas flow. The temperature was then allowed to return to room temperature under the reduced gas flow of 2L/minute. Samples were removed from tube furnace and stored in a desiccator.

Each sample was crushed to a fine powder, and then 200  $\mu\text{g}$  +/- 10 % of sample was weighed into silver capsules preloaded with 2000  $\mu\text{g}$  of PTFE + Graphite mix and crimped. In Menicucci et al. (2013) 390–410  $\mu\text{g}$  of silica (~200  $\mu\text{g}$  of oxygen) is used for each of the five replicates totalling 2000  $\mu\text{g}$  total for a single sample analysis. The sensitivity of the Nu Perspective IRMS at the University of Adelaide used in this study allowed for a smaller mass to be analysed, as little as 50  $\mu\text{g}$  of oxygen which is approximately 100  $\mu\text{g}$  of silica. Each analysis was completed using the same TC/EA- IRMS setup with the same instrument settings as used in the EAD method. Five replicates were analysed consecutively without any delay (Figure 1). The first replicate result was discarded, and the remaining analyses were kept, following the protocol of (Menicucci et al., 2013).

#### 2.3 Calculated oxygen yield

Different masses of sucrose standard were used to develop a linear regression between the IRMS CO peak areas and oxygen yield. This linear regression was then used to calculate the percentage of oxygen being released from one of the soil phytolith samples.

## 2.4 Oxygen isotope calibration

All the results are expressed in ‰ relative to VSMOW. An in-house sucrose standard (+35.48 ‰ SD 0.27), was run before and in between each set of replicates and used to normalise values. This standard has been calibrated to certified reference materials NBS127 (barium sulfate) and silver phosphate (Elemental Microanalysis) as well as reference standards CBS, a Caribou Hoof Standard, KHS (Kudu Horn Standard) (Qi et al., 2011). Menicucci et al. (2013) noted an offset in the  $\delta^{18}\text{O}$  value of silica resulting from the micro-fluorination process and applied a correction for this, but this was not observed in this study, so a correction was not required.

## 3 Results

### 3.1 Preliminary testing of the EAD method

The first  $\delta^{18}\text{O}$  value from the ten analyses of PTFE + graphite mix, run after dehydroxylating BFC in the reaction column of the TC/EA, was 30.1‰, the following two  $\delta^{18}\text{O}$  values were 29.2‰ and 29.3‰. The expected value was 29.0 ‰ (SD 0.3). From the fourth analysis the  $\delta^{18}\text{O}$  values consistently decreased in value (Figure 2). The peak area for each analysis varied greatly, with the largest peak being greater than double the size of the smallest peak. There was no trend with the peak area size and the measured  $\delta^{18}\text{O}$  values of the silica (Figure 2).

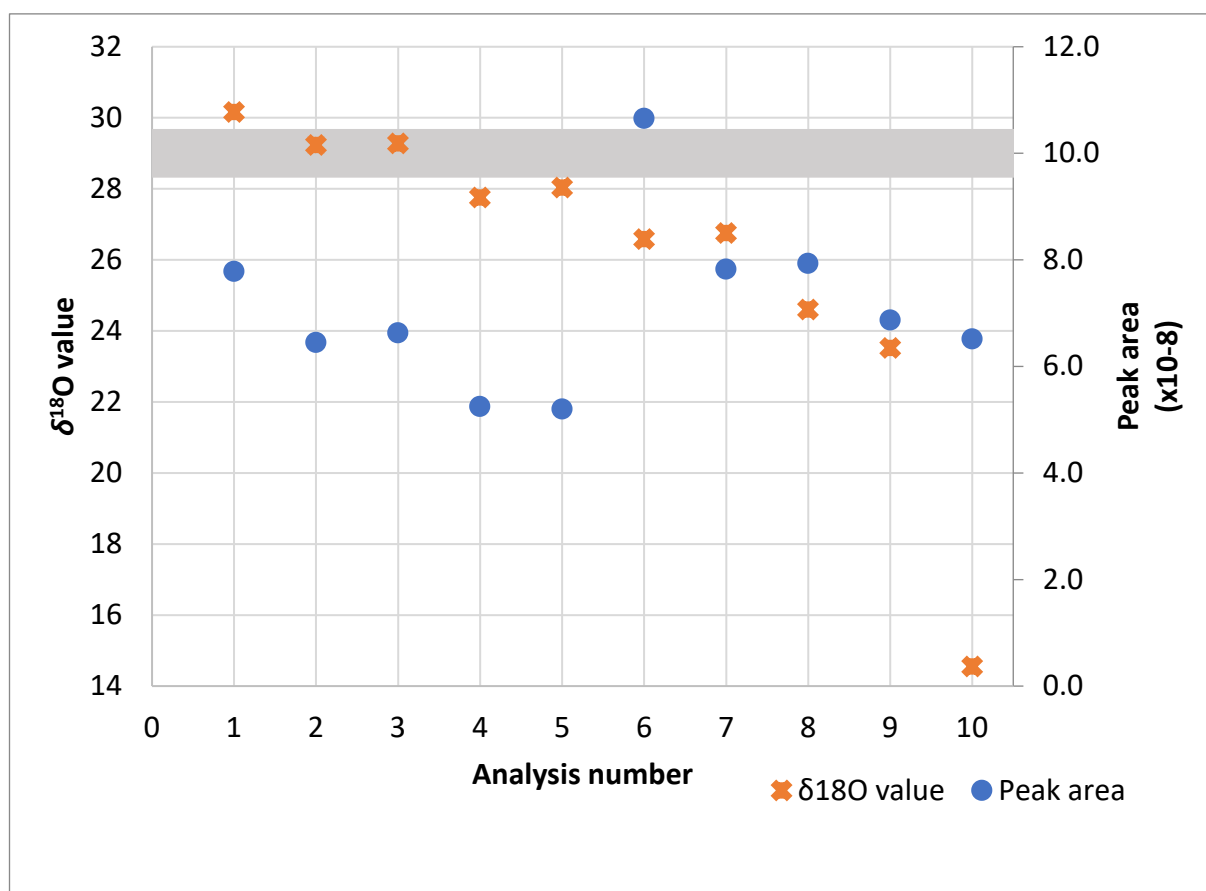


Figure 3. The  $\delta^{18}\text{O}$  values of PTFE and graphite analyses (orange crosses) and the peak area (blue circles) for each analysis. The grey line indicates published values for BFC (29.0  $\pm$  0.3).

### 3.2 EAD and IFD methods

The silica standards dehydroxylated using the EAD method had  $\delta^{18}\text{O}$  values (Table 1) within error of those reported by Chaplignin et al. (2011). Each replicate value is reported in Supplementary information S.3, Appendix 2.

Table 1 Comparison of published  $\delta^{18}\text{O}$  values of silicate standards from Chaplignin et al. (2011) and measured  $\delta^{18}\text{O}$  values using the EAD method.

Sample name	Accepted value (‰)	SD	Mean measured (‰)	SD	Number of analyses	Min $\delta^{18}\text{O}$ (‰)	Max $\delta^{18}\text{O}$ (‰)
BFC	29.0	0.3	28.9	0.3	22	28.4	29.4
G95	36.6	0.8	36.7	0.5	5	35.9	37.3
NBS-28	9.6		9.6	0.3	23	9.2	10.2

The two soil phytolith samples where the EAD and IFD methods were compared also return values which were identical within analytical uncertainty for each sample (Table 2).

Table 2 Comparison of measured  $\delta^{18}\text{O}$  values from bulk soil phytoliths using the EAD method and the IFD method (Chaplignin et al. 2011).

Method:	EAD					IFD				
Sample	Mean measured	SD	No	min	max	Mean measured	SD	No	min	max
S1	29.7	0.3	4	29.4	29.9	29.2	0.9	4	28.5	30.4
S17	39.7	0.4	5	39.2	40.1	39.6	0.6	4	39.2	40.5

### 3.3 $\delta^{18}\text{O}$ values of exchangeable oxygen

The isotope composition of exchangeable oxygen removed from the biogenic silica was analysed to test if liberated oxygen yields constant values. It was found that though the results were variable with a standard deviation between 1.1 and 2.5 ‰ the values for each replicate of a sample were somewhat consistent (Table 3). The soil phytolith samples, which were extracted in the same batch, had similar  $\delta^{18}\text{O}$  values of  $\sim 13.5$  ‰. The mass being

removed from the phytolith soil sample during dehydroxylation indicated that 8% of the total oxygen was removed.

Table 3  $\delta^{18}\text{O}$  values of the exchangeable oxygen coming off the silica during the dehydroxylation process.

Sample	Mean measured		Number of analyses	Min $\delta^{18}\text{O}$	Max $\delta^{18}\text{O}$
	$\delta^{18}\text{O}$	SD			
BFC	3.8	1.1	16	2.7	5.9
S1	13.3	1.5	5	10.3	15.7
S17	13.8	2.4	4	12.0	15.6

## 4 Discussion

### 4.1 Preliminary testing of the EAD method

The number of precise readings obtainable from analysis of a single sample through repeated addition of PTFE + graphite mix while using the EAD method was tested. As in Menicucci et al. (2013) the first analysis of PTFE + graphite mix was slightly offset from the expected value (Figure 3). The following two analyses were accurate and subsequent readings gave values below the expected value. This was consistent even when trialling different weights of sample (100  $\mu\text{g}$ -1000  $\mu\text{g}$ ), PTFE + graphite mix (1000  $\mu\text{g}$ - 2000  $\mu\text{g}$ ), and while attempting to clear the column of silica by analysing PTFE only. This raises the question why one large sample followed by 5-10 PTFE + graphite mix produce inaccurate results while 5 small replicates and 1-2 PTFE mix analysed after each replicate gives accurate results. When the sample size was increased to 1 mg significantly more PTFE was needed to clear out the tube, so it is not a problem of all silica being used up. Like Menicucci et al. (2013), increasing the amount of PTFE dropped at once did not speed up the purging of the column, it was better to drop four 1000  $\mu\text{g}$  PTFE capsules instead of one 5000  $\mu\text{g}$  PTFE capsule. This



indicates that only a certain amount of PTFE and silica can react at one time, perhaps due to the residence time of the fluorine in the column, which is being carried by the gas.

During initial trials it was observed that despite the larger samples of silica remaining in the tube, there was no carry over, even when running samples with a variation of over 20 %.

The newest introduced silica falls on top of the older silica, so it is likely the fluorine is reacting with only the fresher silica on top and not the older silica. For best practise, the column is cleared out in between each sample.

#### 4.2 Inaccuracies of both EAD and IFD methods

In both methods, it was found that the first replicate frequently gave inaccurate values, and it was observed that this occurred more frequently with the IFD method. Increasing ratios of sample to PTFE and graphite mix or increasing sample size did not improve accuracy or precision. The micro-fluorination process involves instant combustion of the PTFE which releases fluorine that then reacts with the silica as it flows through the column to form CO and SiF<sub>4</sub> (Menicucci et al., 2013). While using the IFD method, where the sample and PTFE + Graphite mix are combined, the PTFE turns to gas instantly as it enters the reaction column, and fluorine is released while the silica is still in a solid form. The gaseous fluorine may not have time to react properly with the falling silica before it is carried away by the carrier gas. On subsequent replicates, there is leftover silica from the previous analyses sitting on top of the column, so the fluorine has two opportunities to react, firstly with the replicate sample it is mixed into, and then the replicate sitting at the top of the column. In the EAD method, the silica is already sitting in the column when the first PTFE is added. Frequently, the reported value of the first analyse was accurate, but when it was not, the peak area was generally low. The first analysis of biogenic silica had only 150 µg of hydrated silica, the column is quite wide in comparison to the amount of sample. It is hypothesised that the results that were

inaccurate or where the peak area too small, are a result of the fluorine not colliding with the bulk of the silica, a narrower column, or a funnel at the top of the column to direct both the sample and gas to the same spot may result in more consistent readings.

#### 4.3 Online EAD versus offline IFD methods

The analyses of the biogenic silica dehydroxylated using the EAD method gave  $\delta^{18}\text{O}$  values in-line with those reported in other studies (Table 1), indicating this method successfully removed the exchangeable oxygen without effecting the  $\delta^{18}\text{O}$  values of the non-exchangeable oxygen. A comparison of the EAD and IFD methods using phytoliths extracted from soils showed that there was some difference in the measured  $\delta^{18}\text{O}$  values. Menicucci et al. (2013) tested masses of silica samples between 100  $\mu\text{g}$  to 1500  $\mu\text{g}$  with the micro-fluorination method and found that masses of below 200  $\mu\text{g}$  produced lower  $\delta^{18}\text{O}$  values than larger sample sizes. Both soil samples (200  $\mu\text{g}$  used for each replicate during analyses) dehydroxylated in the IFD method showed mean  $\delta^{18}\text{O}$  values lower than the samples in the EAD method. However, the maximum  $\delta^{18}\text{O}$  value reported from the replicates for each of these samples (Table 2) is higher than the maximum  $\delta^{18}\text{O}$  value for the samples dehydroxylated in the EAD method. The same study (Menicucci et al. (2013) also reported a “PTFE offset” suggesting that using PTFE as a source of fluorine caused offsets of +0.3 to +1.6‰ in silicate samples. The biogenic silica isotope ratios in this study were normalised to a non-silica standard (sucrose) and the resulting values were the same as reported values (Table 1), so no “PTFE offset” was observed in this study. While Menicucci et al. (2013) did not use a tube furnace to dehydroxylate samples, they used a similar process but with a muffle furnace. The process of cooling down samples may lead to a small isotopic exchange that is not noticeable in larger volumes of sample. This could explain their “PTFE offset” and this study's lower mean  $\delta^{18}\text{O}$  values for the samples dehydroxylated in the tube furnace

(Table 2). Perhaps lower mean  $\delta^{18}\text{O}$  values for the two soil samples results from a combination of the dehydration process and insufficient homogenisation. Because the sample volumes used in this study are so small and micro-fluorination does not entirely reduce the entire sample in one analysis, heterogeneity of the sample can affect the results if it is not sufficiently homogenised. Normally 400  $\mu\text{g}$  of sample is used for each replicate when using microflourination to combat this issue, while only 200  $\mu\text{g}$  was used in this study for the IFD method and 150  $\mu\text{g}$  for the EAD dehydration method (Menicucci et al., 2013; Menicucci et al., 2020; Menicucci et al., 2017).

There are some benefits for using the EAD method over the IFD method. The need for an expensive tube furnace and nickel capsule holder are eliminated, allowing for a cost-efficient access to this type of analysis. A further disadvantage of the IFD method is that the samples are stored in a desiccator since samples must be dehydroxylated in large batches to allow for time-effective sample processing. This, however, possess the risk of oxygen from the atmosphere starting to attach to the biogenic silica again (Chapligin et al., 2010). As the EAD method analyses the samples immediately after dehydroxylation, there is no risk of the samples re-hydroxylating. Masses of 150  $\mu\text{g}$  of hydroxylated sample were successfully run, this was partly due to the IRMS being able to analyse as little as 50  $\mu\text{g}$  of oxygen, but also the peak areas were larger and more consistent with the PTFE being added later instead of in the same step as is done in the IFD method (Menicucci et al., 2013). An investigation into adding the PTFE into the reactor column after the tube dehydroxylated sample instead of with it should be tested to see if it could give better results.

While both dehydroxylation methods performed well, the IFD method requires less maintenance of equipment (e.g., column changes and purging the liquid nitrogen trap) and faster analyse time on the IRMS. Samples dehydroxylated using the tube furnace take

approximately 1 hour to analyse on the IRMS, including baking and purging of the liquid nitrogen trap, purging the column of silica, and running standards to check that the linearity had not changed. This same process using the TC/EA to remove the exchangeable oxygen the samples took around 2.5 hours per sample. The carbon packing in the column needed to be changed more frequently with the EAD method as more material is passing through the column (the removed hydroxyl and water molecules). The liquid nitrogen trap needed to be flushed after each replicate instead of after each run of a sample (4-5 replicates) or the trap would block up. All of which makes the IFD method more efficient if large sample numbers are processed, whilst the EAD method is beneficial for small sample aliquots.

#### 4.4 Analysis of exchangeable oxygen

It is possible to analyse the exchangeable oxygen being removed from the sample with the EAD method. The mass being removed from the dehydroxylation process, indicating the amount of exchangeable oxygen, was quantifiable. The phytolith soil sample, gave a result of 8% of the oxygen molecules being removed, which falls in the expect range of 1%-12% for biogenic silica (Knauth, 1973). The  $\delta^{18}\text{O}$  values of the exchangeable oxygen for each replicate of a sample had variations up to 5.4 ‰ (Table 5). The TC/EA-IRMS setup traps water, and that would affect the results as both OH and water molecules are being removed from the biogenic silica. The readings from the samples are likely to be from laboratory water used during the extraction process, and the fact that the two soil phytolith values are so similar adds weight to this conclusion. Much research has been done regarding exchangeable oxygen in biogenic silica, mostly on diatoms, and being able to easily measure the exchangeable oxygen being removed may help with our understanding of this exchange process and should be explored further (Akse et al., 2020; Menicucci et al., 2017; Tyler et al., 2017).

## 5 Conclusion

This study presents a new method for determining the  $\delta^{18}\text{O}$  values of biogenic silica that requires as little as 600  $\mu\text{g}$  of sample (four replicates of 150  $\mu\text{g}$  each) as compared to the IFD method that requires at least 2000  $\mu\text{g}$  of sample. The new EAD method demonstrated that biogenic silica can reliably be dehydroxylated, micro-fluorinated and analysed for  $\delta^{18}\text{O}$  values using an TC/EA and IRMS setup. This eliminates the need for expensive specialised equipment and makes the analyses of biogenic silica available to the wider research community. This new EAD method of dehydroxylation, with some minor modifications, could allow for easy analyse of the released oxygen during the dehydroxylation process. This could aid in understanding the effect of laboratory cleaning procedures on  $\delta^{18}\text{O}$  ratios.

## 6 References

- Akse S. P., Middelburg J. J., King H. E. and Polerecky L. (2020) Rapid post-mortem oxygen isotope exchange in biogenic silica. *Geochim Cosmochim Acta* **284**, 61-74.
- Chapligin B., Meyer H., Friedrichsen H., Marent A., Sohns E. and Hubberten H. W. (2010) A high-performance, safer and semi-automated approach for the delta18O analysis of diatom silica and new methods for removing exchangeable oxygen. *Rapid Commun Mass Spectrom* **24**, 2655-2664.
- Chapligin B., Leng M. J., Webb E., Alexandre A., Dodd J. P., Ijiri A., Lücke A., Shemesh A., Abelmann A., Herzsich U., Longstaffe F. J., Meyer H., Moschen R., Okazaki Y., Rees N. H., Sharp Z. D., Sloane H. J., Sonzogni C., Swann G. E. A., Sylvestre F., Tyler J. J. and Yam R. (2011) Inter-laboratory comparison of oxygen isotope compositions from biogenic silica. *Geochim Cosmochim Acta* **75**, 7242-7256.
- Crespin J., Alexandre A., Sylvestre F., Sonzogni C., Paillès C. and Garreta V. (2008) IR Laser Extraction Technique Applied to Oxygen Isotope Analysis of Small Biogenic Silica Samples. *Analytical Chemistry* **80**, 2372-2378.
- Dodd J. P. and Sharp Z. D. (2010) A laser fluorination method for oxygen isotope analysis of biogenic silica and a new oxygen isotope calibration of modern diatoms in freshwater environments. *Geochim Cosmochim Acta* **74**, 1381-1390.
- Hut G. (1987) Stable isotope reference samples for geochemical and hydrological investigations. Consultant Group Meeting IAEA, Vienna, 16–18 September 1985, Report to the Director General. *International Atomic Energy Agency, Vienna* **42**.
- Juillet-Leclerc A. and Labeyrie L. (1987) Temperature dependence of the oxygen isotopic fractionation between diatom silica and water. *Earth and Planetary Science Letters* **84**, 69-74.
- Knauth L. P. (1973) Oxygen and hydrogen isotope ratios in cherts and related rocks. California Institute of Technology.

- Leng M., Barnker P., Greenwood P., Roberts N. and Reed J. (2001) Oxygen isotope analysis of diatom silica and authigenic calcite from Lake Pinarbasi, Turkey. *J Paleolimnol* **25**, 343-349.
- Leng M. J. and Sloane H. J. (2008) Combined oxygen and silicon isotope analysis of biogenic silica. *J Quaternary Sci* **23**, 313-319.
- Lücke A., Moschen R. and Schleser G. H. (2005) High-temperature carbon reduction of silica: A novel approach for oxygen isotope analysis of biogenic opal. *Geochim Cosmochim Ac* **69**, 1423-1433.
- Menicucci A. J., Matthews J. A. and Spero H. J. (2013) Oxygen isotope analyses of biogenic opal and quartz using a novel microfluorination technique. *Rapid Communications in Mass Spectrometry* **27**, 1873-1881.
- Menicucci A. J., Thunell R. C. and Spero H. J. (2020) 220 Year Diatom  $\delta^{18}\text{O}$  Reconstruction of the Guaymas Basin Thermocline Using Microfluorination. *Paleoceanography and Paleoclimatology* **35**, e2019PA003749.
- Menicucci A. J., Spero H. J., Matthews J. and Parikh S. J. (2017) Influence of exchangeable oxygen on biogenic silica oxygen isotope data. *Chem Geol* **466**, 710-721.
- Qi H., Coplen T. B. and Wassenaar L. I. (2011) Improved online  $\delta^{18}\text{O}$  measurements of nitrogen- and sulfur-bearing organic materials and a proposed analytical protocol. *Rapid Communications in Mass Spectrometry* **25**, 2049-2058.
- Tyler J. J., Sloane H. J., Rickaby R. E. M., Cox E. J. and Leng M. J. (2017) Post-mortem oxygen isotope exchange within cultured diatom silica. *Rapid Communications in Mass Spectrometry* **31**, 1749-1760.
- Webb E. A. and Longstaffe F. J. (2002) Climatic influences on the oxygen isotopic composition of biogenic silica in prairie grass. *Geochim Cosmochim Ac* **66**, 1891-1904.

## Chapter 4:

Oxygen isotope ratios of phytoliths from modern grasses and soil along a latitudinal transect of Australia and their correlation with climate

# Statement of Authorship

Title of Paper	Oxygen isotope ratios of phytoliths from modern grasses and soil along a latitudinal transect of Australia and their correlation with climate
Publication Status	<input type="checkbox"/> Published <input type="checkbox"/> Accepted for Publication <input type="checkbox"/> Submitted for Publication <input checked="" type="checkbox"/> Unpublished and Unsubmitted work written in manuscript style
Publication Details	

## Principal Author

Name of Principal Author (Candidate)	Kimberley Edwards		
Contribution to the Paper	Designed the study. Conducted sample processing and analysis. Conducted data analysis and interpretation. Wrote manuscript.		
Overall percentage (%)	75		
Certification:	This paper reports on original research I conducted during the period of my Higher Degree by Research candidature and is not subject to any obligations or contractual agreements with a third party that would constrain its inclusion in this thesis. I am the primary author of this paper.		
Signature		Date	31/01/2023

## Co-Author Contributions

By signing the Statement of Authorship, each author certifies that:

- i. the candidate's stated contribution to the publication is accurate (as detailed above);
- ii. permission is granted for the candidate to include the publication in the thesis; and
- iii. the sum of all co-author contributions is equal to 100% less the candidate's stated contribution.

Name of Co-Author	Dr Francesca McInerney		
Contribution to the Paper	Supervised project. Co-conceived research idea, provided input into study design, data analysis, interpretation and manuscript. Reviewed and edited manuscript.		
Signature		Date	31/01/2023

Name of Co-Author	Dr Jonathan Tyler
Contribution to the Paper	Supervised project. Co-conceived research idea, provided input into study design, data analysis, interpretation and manuscript. Reviewed and edited final manuscript.



Signature		Date	1/2/2023
-----------	--	------	----------

Name of Co-Author	Dr Alexander Francke		
Contribution to the Paper	Supervised project. Provided input into study design, data analysis, interpretation and manuscript. Reviewed and edited manuscript.		
Signature		Date	25/01/2023

Name of Co-Author	Dr Robert Klæbe		
Contribution to the Paper	Provided input into data analysis. Reviewed and edited final manuscript.		
Signature		Date	31/01/2023

## Abstract

Phytoliths, microscopic biogenic silica structures in plants, are translocated to soils and sediments after plant decomposition. The oxygen isotope composition of the phytoliths is thought to provide a record of plant water isotope ratios and the temperature at the time of formation. A better understanding of the processes controlling the phytolith oxygen isotope signal transfer from plant to soil may help to untangle the temperature and relative humidity signal. Towards this aim, the oxygen isotope ratios of phytoliths extracted from grasses and soils from across a latitudinal transect of Australia were analysed, compared to each other and to climate data. The oxygen isotope ratios of phytoliths extracted from grasses at the same sites were compared to test if they have similar values. Climate data was compared to the oxygen isotope ratios of the grass and soil phytoliths. The oxygen isotope values from the phytoliths in grasses were then compared to those from the phytoliths extracted from the soil to examine how the signal from plants is transferred to soil. To test our understanding of the main processes controlling the oxygen isotopic ratios, modelling using the oxygen isotopes of precipitation, relative humidity, and temperature data was used to predict the oxygen isotopic ratios of phytoliths from plants and soils at our sites. The results show that the oxygen isotopes of phytoliths extracted from grasses at the same site exhibited large variability which may be attributed to age variations in the plants. The oxygen isotopes of phytoliths extracted from both grasses and soils correlated with long term temperature and the relative humidity at the maximum temperature of the warmest period. The oxygen isotope values in phytoliths from grasses were lower than the oxygen isotope values in phytoliths from soils which may be because the samples were collected during a La Niña event where the oxygen isotope ratios of precipitation may have been significantly lower than normal. The predicted isotope values of phytoliths in plants and soils

were in good agreement with the measured values indicating the main processes controlling the isotope ratios can be modelled.

## 1 Introduction

The oxygen isotope ratios of phytoliths (microscopic silica structures precipitated in plants) offer the potential to be used as a climate proxy in dry environments, which often have fewer proxy archives (Shahack-Gross et al., 1996). To be able to use the oxygen isotopes as a climate proxy, the processes controlling the oxygen isotope ( $\delta^{18}\text{O}$ ) ratios of phytoliths need to be better characterised. During formation, phytoliths record the plant water stable oxygen isotope ratios, which are heavily influenced by relative humidity (RH) (Shahack-Gross et al., 1996). Additionally, there is a temperature dependent fractionation of the oxygen isotopes relative to plant water during the formation of phytoliths (Alexandre et al., 2012; Alexandre et al., 2018). Previous research has attempted to reconstruct temperature and relative humidity from phytoliths deposited in soil, with limited success (Alexandre et al., 2012; Alexandre et al., 2018).

Most research on the  $\delta^{18}\text{O}$  values of phytoliths has focused on their precipitation and location within a plant to better understand the process of formation (Alexandre et al., 2012; Alexandre et al., 2019; Alexandre et al., 2018; Outrequin et al., 2021; Shahack-Gross et al., 1996; Webb and Longstaffe, 2000; Webb and Longstaffe, 2002, 2003). This has resulted in some key findings. First, there is a quantifiable temperature dependent fractionation of the oxygen during phytolith formation (Kita et al., 1985; Shahack-Gross et al., 1996; Shemesh et al., 1992). Second, the  $\delta^{18}\text{O}$  values of phytoliths within a plant are heterogenous both throughout a plant, and within the same tissue (Alexandre et al., 2019; Webb and Longstaffe, 2000; Webb and Longstaffe, 2003). This is because phytoliths in transpiring tissue have higher  $\delta^{18}\text{O}$  values than phytoliths in non-transpiring tissue due to the effect of relative humidity on the  $\delta^{18}\text{O}$  values of plant water, which the phytoliths are recording (Webb and Longstaffe, 2003). The  $\delta^{18}\text{O}$  values of phytoliths from transpiring tissue correlate best with

the relative humidity of the summer months (Webb and Longstaffe, 2003). The  $\delta^{18}\text{O}$  values of phytoliths in leaves increase from the base of a leaf to the tip as does the  $\delta^{18}\text{O}$  values of leaf water (Alexandre et al., 2019). Phytolith  $\delta^{18}\text{O}$  values in non-transpiring tissue are not affected by relative humidity and therefore can be used as a record of temperature (Alexandre et al., 2012; Webb and Longstaffe, 2000). This has led to the question: can the  $\delta^{18}\text{O}$  value of phytoliths found in sediment be used to reconstruct past climate? The issue is that when phytoliths are deposited in sediments, they are mixed, and it is not possible to separate phytoliths formed in transpiring tissue (isotope signature controlled by relative humidity and temperature) from those formed in non-transpiring tissue (isotope signature controlled by temperature). The measured  $\delta^{18}\text{O}$  values of phytoliths in various parts of plants (roots, stems, leaves, etc.) and the percentage each group contributed to the plant's total phytolith weight were used to model the  $\delta^{18}\text{O}$  values of phytoliths found in soil (Webb and Longstaffe, 2000). The results indicated soil phytoliths should have a  $\delta^{18}\text{O}$  values approximately halfway between transpiring and non-transpiring tissue. This remains to be tested.

Modern day Australia has extremely dry environments, and thus provides a good location to test whether the  $\delta^{18}\text{O}$  of phytoliths in sediments can be used as a climate proxy. Northern Australia has a monsoonal wet season characterised by relative high humidity, temperature, and rainfall during the peak growing period for plants (Kottek et al., 2006). Central Australia has low relative humidity and high temperatures during peak growth periods, and while southern Australia has high humidity and low temperatures during peak growth (Kottek et al., 2006). This gives a good combination of different temperatures and humidity levels to test if  $\delta^{18}\text{O}$  values of phytoliths in both plants and topsoil record these climate parameters. If it is better understood what the phytoliths in topsoils are recording, then the  $\delta^{18}\text{O}$  values of

phytoliths in depositional environments such as wetlands and caves could be used to reconstruct past climates.

To explore the potential of phytoliths as a proxy for climate, this study measures the oxygen isotope ratios of phytoliths from plants and soils from a latitudinal transect of Australia (Figure 1) to test the following hypotheses:

H1: Phytoliths from different species of grass at the same location will have similar  $\delta^{18}\text{O}$  values to one another.

H2:  $\delta^{18}\text{O}$  values of phytoliths from plants and bulk topsoil will reflect the combined effects of relative humidity on leaf water  $\delta^{18}\text{O}$  values and temperature on silica-water isotope fractionation during phytolith formation.

H3: Phytoliths from grasses will have similar  $\delta^{18}\text{O}$  values to those of topsoil at the same location.

H4: Craig-Gordon modelling of the environmental controls on leaf water  $\delta^{18}\text{O}$  values, combined with an understanding of temperature-sensitive fractionation during silica precipitation can be used to predict phytolith  $\delta^{18}\text{O}$  values in plants and soils.

## 2 Methods

### 2.1 Site locations

Australia's Terrestrial Ecosystem Research Network (TERN) provided plant and soil samples collected from 20 locations (Figure 1) using the AusPlots Rangelands survey procedure (White et al., 2012). These locations are on a latitudinal transect of Australia encompassing a variety of climates and seven different Australian bioregions.

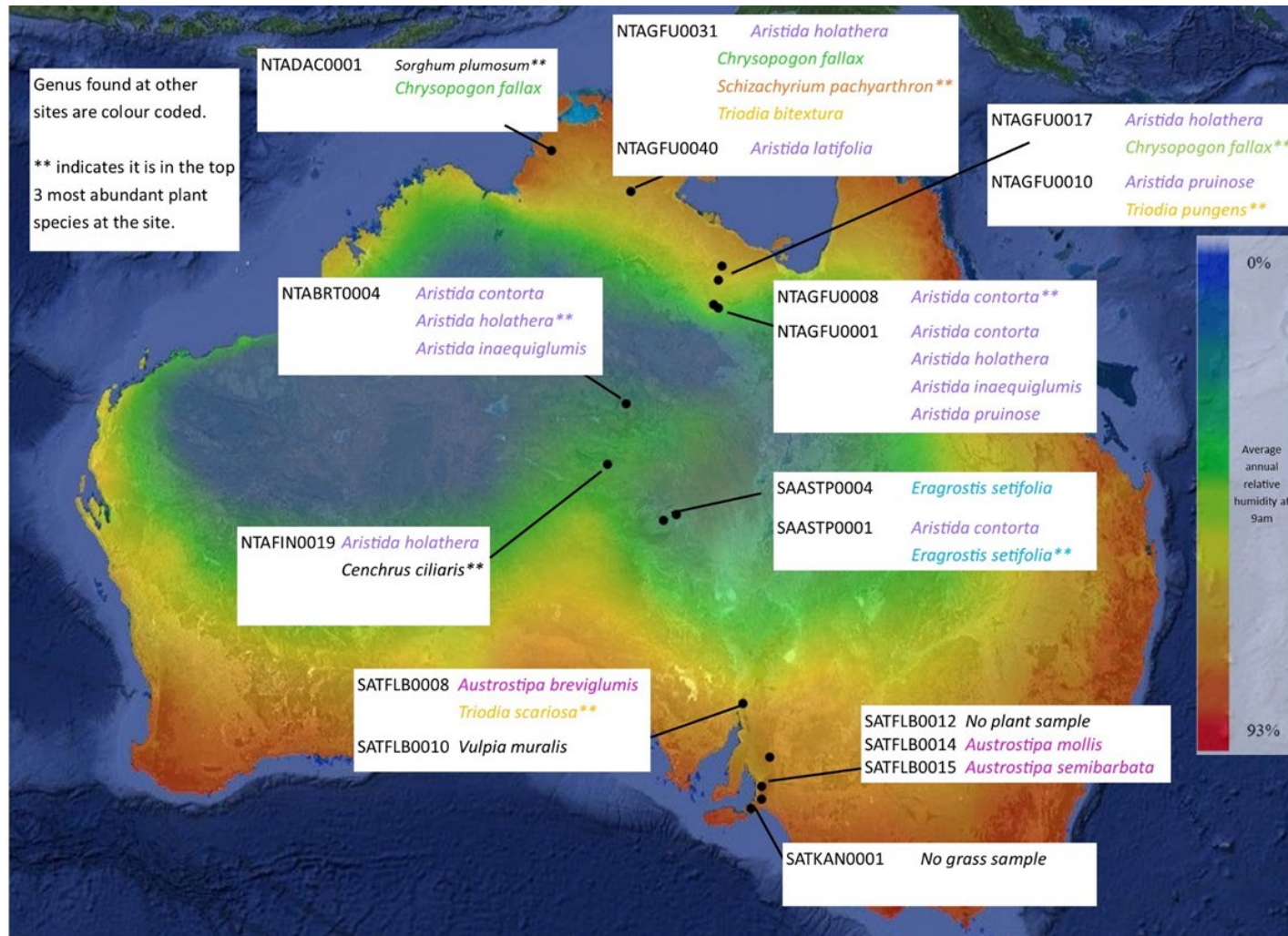


Figure 1 Site locations and plant species selected at each site. Genera found at multiple sites are colour coded in the same colours.

Table 1 Site information. Mean annual temperature (MAT), mean annual precipitation (MAP), and mean annual relative humidity (RH) extracted from ANUCLIM 6.1 layers of a 1960–2014 average climate information for each location through the Atlas of Living Australia spatial portal ([www.ala.org.au](http://www.ala.org.au))(Xu and Hutchinson, 2013). Köppen Climate Classification also extracted through Atlas of Living Australia spatial portal (Peel et al., 2007). Samples collected by TERN from Northern Territory (NT) and South Australia (SA), Australia.

Site	Location	State	Latitude	Longitude	Collection date	Köppen Climate Classification	RH (%)	MAP (mm)	MAT(°C)
NTADAC0001	Litchfield National Park	NT	-13.16	130.778	28/05/2013	Tropical: savanna	78.3	1465	26.5
NTAGFU0031	Wongalara Reserve	NT	-14.13	134.387	6/07/2012	Tropical: savanna	75.9	899	27.3
NTAGFU0040	Moroak Station	NT	-14.67	133.845	15/07/2012	Tropical: savanna	73.2	828	27.7
NTAGFU0017	Calvert Hills Station	NT	-17.35	137.158	17/05/2012	Grassland: hot (winter drought)	70.9	702	25.6
NTAGFU0010	Benmara Station	NT	-17.90	137.101	9/05/2012	Grassland: hot (winter drought)	69.0	580	25.7
NTAGFU0008	Mittiebah Station	NT	-18.79	136.865	20/04/2012	Grassland: hot (winter drought)	66.2	430	25.5
NTAGFU0001	Alexandria Station	NT	-18.91	137.069	12/04/2012	Grassland: hot (winter drought)	65.4	424	25.7



NTABRT0004	Pine Hill Station	NT	-22.29	133.616	23/01/2012	Grassland: hot (persistently dry)	59.8	287	22.7
NTAFIN0019	Henbury Station	NT	-24.36	132.936	1/12/2011	Desert: hot (persistently dry)	62.0	232	21.9
SAASTP0004	Hamilton Station	SA	-26.09	135.452	1/07/2012	Desert: hot (persistently dry)	59.8	157	22.7
SAASTP0001	Hamilton Station	SA	-26.28	134.999	27/06/2012	Desert: hot (persistently dry)	60.2	172	22.2
SATFLB0008	Dutchman's Stern Conservation Park	SA	-32.32	137.954	23/08/2012	Grassland: warm (persistently dry)	73.2	390	15.1
SATFLB0010	Mount Remarkable National Park	SA	-32.83	138.033	25/08/2012	Grassland: warm (persistently dry)	73.8	338	17.3
SATFLB0014	Tothill Range	SA	-34.00	138.959	20/11/2012	Temperate: no dry season (warm summer)	77.3	497	14
SATFLB0012	Black Hill Conservation Park	SA	-34.88	138.708	16/11/2012	Temperate: distinctly dry (and warm) summer	76.9	603	15.8
SATKAN0001	Deep Creek Conservation Park	SA	-35.61	138.261	21/08/2012	Temperate: distinctly dry (and warm) summer	82.3	644	14

## 2.2 Materials for natural transect study

### 2.2.1 Modern grasses

Above ground plant samples were collected by TERN, minimising skin contact, and placed each sample in separate synthetic tea bags, which were sealed and labelled. Bagged samples were then placed in a sealable container containing a 1 cm layer of a mix of indicator silica granules and non-indicator silica granules. A separate container is used for each location. Silica granules were replaced when indicator granules change colour indicating saturation of moisture (White et al., 2012).

Plant material was chosen from the Poaceae (grasses) family as these are the most abundant producers of phytoliths so their phytoliths are expected to make up the bulk of phytoliths found in topsoils in non-rainforest sites (Alexandre et al., 2012). As there is large variability in climate from the locations chosen in this study, there is no one species or genus found across all sites. In total 41 grass specimens (Figure 1) from several species and genera were selected that cover:

- The most abundant grass/es at each location (Howard et al., 2018).
- One genus (*Austrostipa*) collected at three sites in the southern part of Australia.
- One genus (*Aristida*) collected at nine sites across much of Australia.
- Nine sites have at least two different grass species for comparison of the isotopic signal in different species at the same site.

### 2.2.2 Modern topsoils

Soil for metagenomic and isotopic analysis were collected by TERN using the protocol outlined in White et al. (2012). This involved collecting approximately 200 g of the surface layer up to three centimetres deep. Soil samples are placed in individual calico bags,

labelled, and then placed inside individual large Ziplock bags with half a cup of silica granules. Silica granules were replaced regularly until the indicator silica granules did not change colour. Soil samples from each location were then stored together in a large calico bag.

The 20 soil samples had previously been used as part of Howard et al. (2018) study on *n*-alkanes. As part of that research the samples were sieved at 1000 and 250  $\mu$ m to remove remaining plant material and underwent mid-infrared particle size analysis.

### 2.3 Phytolith extraction from plants

Transpiring tissue was targeted as this is expected to give the highest isotopic value due to its being enriched in  $^{18}\text{O}$  during transpiration. Approximately 80 mg of grass was rinsed in Milli-Q water to remove any debris or silica dust from the desiccant granules, and then cut and put into Pyrex beakers and left to dry in a fume cupboard. Phytoliths were extracted using a standard chemical extraction method for plants (Chemical 1, Chapter 2) (Piperno, 2006). Grass was dissolved in 40 ml of 98% sulphuric acid heat to 60 °C for two hours, then cooled to room temperature before 20 ml of 30% hydrogen peroxide was slowly. The residue was recovered using centrifugation and triple rinsed with Milli-Q water. Plant samples were then treated with 10 ml of 5% hydrochloric acid to remove carbonates and then triple rinsed again (Geis, 1973). Plant samples were then checked for contamination via microscopy (see section 2.5.1) and then freeze-dried.

### 2.4 Phytolith extraction from soils along natural transect

Phytoliths were extracted from soil using the same chemical extraction method as suggested in Piperno (2006), though using the suggested alternative chemicals (Snelling et al., 2012) (Chemical 2, Chapter 2). Each chemical step was followed by three rinses of Milli-Q water in

a centrifuge at 2000 RPM, acceleration 7, brake 0 for 5 minutes. Soils were prepared by lightly crushing using a mortar and pestle then sieved at 250  $\mu\text{m}$ . Phytoliths were then extracted using 5% hydrochloric acid, sodium hexametaphosphate (SHMP), gravity separation using stokes equation, sodium polytungstate (SPT) for density separation, and hydrogen peroxide at 70 degrees for seven days with frequent top ups. Two additional steps were then applied. The first involved the use of nested cell strainers under vacuum to separate phytoliths into different size classes (250–85, 85–20, and 20–10  $\mu\text{m}$ ) which allowed for better filtration as large phytoliths did not clog the smaller sized filters, trapping clay particles (Urban et al., 2018). These portions were then recombined so that the final size fraction was 10  $\mu\text{m}$  – 250  $\mu\text{m}$ . The soils still had some clay and organic matter so were treated with the same method as the plants (Chemical 1, Chapter 2, with the entire extraction process termed Chemical 4a, Chapter 2) and then underwent SPT separation again. Based on results from chapter 2, SPT was used with densities of 2.25  $\text{g}/\text{cm}^3$ , 2.16  $\text{g}/\text{cm}^3$  and 1.9  $\text{g}/\text{cm}^3$ , and the portion between 2.16-1.9  $\text{g}/\text{cm}^3$  was retain, re-filtered, and freeze-dried.

## 2.5 Contamination assessment

### 2.5.1 Microscopy

At various stages of extraction, the samples were wet mounted on a microscope slide and assessed through an optical polarizing microscope at 400x magnification to check that the organic, clay and quartz material were being removed. After the extracted phytolith samples were freeze dried, permanent microscope slides of each sample were prepared, excluding a few plant samples that had very small yields of phytoliths. Slides were made using ethanol to disperse phytoliths in the slides, and Norland optical adhesive was used with a UV light to

permanently mount them. Several plant samples underwent SEM to ensure that they were clean, and no dissolution occurred during the piranha solution treatment.

#### 2.5.2 Fourier Transform Infrared Spectroscopy (FTIR) analysis

The phytoliths from each of the soil samples were assessed for contamination using the same FTIR analysis as described in chapter two. This was completed twice, once after the first extraction attempt, and then again after the Piranha solution treatment to assess that the residual contamination had been removed.

#### 2.6 Dehydroxylation and oxygen isotope analysis of phytoliths

Both the elemental analyser dehydroxylation (EAD) and offline inert gas flow thermal dehydroxylation (IFD) methods were used to remove the exchangeable oxygen from the phytoliths (See chapter 3 for detailed information).

The EAD dehydroxylation method combines the removal of exchangeable oxygen, fluorination of the biogenic silica to release the non-exchangeable oxygen, and the isotopic analysis of the non-exchangeable oxygen in one procedure. This was done on a HEKAtech high temperature oxygen analyser (TC) coupled with a EuroVector Euro elemental analyser (EA) in-line with a Nu Instruments Perspective Isotope Ratio Mass Spectrometer (IRMS) operated in continuous flow mode. Essentially, by conducting an analysis sequence without adding a reagent, the biogenic silica is held in the reaction tube of the EA under a gas flow of helium at 1450°C. At this temperature and gas flow, the exchangeable oxygen is removed. 20 minutes after the sample entered the reaction column, the reagents, a silver capsule of Polytetrafluoroethylene (Teflon) and graphite, was added to the reaction tube. When the Teflon enters the reaction tube, it vaporises and releases fluorine which reacts with the silica to reduce it. The silica and fluorine combine to form silicon tetrafluoride and the released

oxygen combines with the graphite to form carbon monoxide, which is then analysed by the IRMS.

The IFD method has a preparatory step where the exchangeable oxygen is removed in a tube furnace following a method designed by Chaplignin et al. (2010). Biogenic silica is loaded into nickel capsules and then placed into a tube furnace. The samples are slowly heated to 1100 °C degrees under an argon gas flow. They are maintained at this temperature for 1 hour and then allowed to cool to room temperature. The samples are then stored in a desiccator until the samples are ready to be weighed into silver capsules preloaded with Teflon and graphite. The samples are then analysed on the TC-EA-IRMS, where the biogenic silica and Teflon and graphite mix react as soon as they enter the reaction column.

Many of the phytolith samples were too small to use the IFD dehydroxylation method which requires approximately 2 mg of phytoliths (Chaplignin et al., 2010). Time constraints did not allow the slower EAD method to be used on all the samples (two to three samples a day versus six to seven). Several samples were run with both methods to make sure that the results were comparable (See Chapter 3). Initially samples were run using 5 replicates, with the first replicate being discarded, but after many analyses had been completed, it became evident that 4 replicates were enough to get an accurate and precise value (Menicucci et al., 2013; Menicucci et al., 2020). Thereafter, we continued with using only 4 replicate values, continuing to discard the first replicate. Replicate  $\delta^{18}\text{O}$  values can be seen in Supplementary Table S.6, Appendix 3. For samples dehydroxylated using both methods, all the results were combined to give one mean value.

For both methods, an in-house sucrose standard (+35.48‰, repeated measurements gave reproducibility better than 0.3‰) was run before and in between each set of replicates and

used to normalise values. This standard has been calibrated to certified reference materials NBS127 (barium sulfate) and silver phosphate (Elemental Microanalysis) as well as reference standards CBS, a Caribou Hoof Standard, KHS (Kudu Horn Standard) (Qi et al., 2011). The reaction column was cleared in between each set of replicates by analysing at least 4 silver capsules with a minimum of 2 mg of Teflon until CO peak readings had returned to normal background levels. All the results are expressed relative to VSMOW.

## 2.7 Climate data

Long term mean annual temperature ( $T_{\text{annual}}$ ) and mean annual relative humidity ( $RH_{\text{annual}}$ ) data was extracted from the Atlas of Living Australia spatial portal ([www.ala.org.au](http://www.ala.org.au)) (Table 1). These data are interpolated long term averages for 1960-2014 using ANUCLIM 6.1 (Xu and Hutchinson, 2013). The maximum daily temperature, and relative humidity at the maximum temperature, were extracted from the Scientific Information for Land Owners (SILO) database (Jeffrey et al., 2001). The relative humidity is derived by SILO from the Australian Bureau of Meteorology (BOM) measured vapour pressure at 9 am using the highest daily temperatures. Using these maximum daily temperatures and the derived relative humidity, mean annual maximum temperature ( $T_{\text{max}}$ ) and mean relative humidity at the peak temperature ( $RH_{T_{\text{max}}}$ ) were calculated for each site for 5, 2, 1, 0.5, 0.25 years and 1 month before each sample was collected, as well as the longer term of 1976-2013. The same was done again but using the warmest quarter data only (December – February). These have been defined as mean warmest quarter daily maximum temperature ( $T_{\text{max-warm}}$ ) and mean warmest quarter relative humidity at the daily maximum temperature ( $RH_{T_{\text{max-warm}}}$ )

## 2.8 Phytolith oxygen isotope ratio modelling

The  $\delta^{18}\text{O}$  values of phytoliths from both plants and soils at each site was predicted using a two endmember mixing model. To do this, two endmember  $\delta^{18}\text{O}$  values were created. The

first was phytoliths forming directly from precipitation, which was used to represent phytoliths from non-transpiring tissue. For this endmember, the annual average  $\delta^{18}\text{O}$  value of precipitation at each site was extracted from the Hollins et al. (2018) isoscapes and then a temperature dependent silica-water oxygen isotope fractionation equation (Equation 1; Shahack-Gross et al., 1996) was used with the 5 year  $T_{\text{max}}$  (Supplementary Table S.4, Appendix 3) for each site to estimate the  $\delta^{18}\text{O}$  values of the phytoliths that would be precipitating in equilibrium directly from precipitation.

$$\delta^{18}\text{O}_{\text{phytolith}} = ((T_{\text{max}} - 5.8) / - 2.8) + 40 + \delta^{18}\text{O}_{\text{precipitation}} \quad (1)$$

The second endmember represented phytoliths precipitating directly from leaf water which would be enriched in  $^{18}\text{O}$  relative to precipitation due to transpiration. For this endmember leaf water  $\delta^{18}\text{O}$  values were first modelled using the Craig-Gordon model (Cernusak et al., 2016) and then the temperature dependent fractionation equation (equation 1) was used substituting  $\delta^{18}\text{O}_{\text{leaf water}}$  in for  $\delta^{18}\text{O}_{\text{precipitation}}$ . The standard Craig-Gordon model was completed with the R code from McInerney et al. (2023) using the kinetic fractionation value of  $26.9 \pm 0.5 \text{ ‰}$  based on measurements of plants across Australia (Cernusak et al., 2016; Cernusak et al., 2022; Munksgaard et al., 2017). For the temperature and relative humidity inputs, the 5 year  $T_{\text{max}}$  and 5 year  $\text{RH}_{T_{\text{max}}}$  was used (Supplementary Table S.5, Appendix 3).

A standard two endmember mass balance model was then used to calculate for each measured phytolith  $\delta^{18}\text{O}$  value, the percentage of each endmember contribution needed to model the measured value. Once this was completed for each data point, the means were calculated for the plant samples and the soils samples. The means were then used to predict what the plant and soil phytolith  $\delta^{18}\text{O}$  values would be at each site.



## 2.9 Statistical analyses

Statistical analyses (Pearson's product-moment correlation coefficient, Q-Q plots, root mean square error (RMSE), residual and redundancy analyses) were completed using R 4.2.2 (R Core Team, 2021). Pearson's product-moment correlation coefficient was used to assess the relationships between measured  $\delta^{18}\text{O}$  values of phytoliths and modelled  $\delta^{18}\text{O}$  values of source waters with climate data. This was also used to assess the relationship between measured and predicted  $\delta^{18}\text{O}$  values of phytoliths. Results were considered significant if the  $p$ -value was below 0.05 and regression lines and statistics are only shown on plots when the  $p$ -value was statistically significant. Pearson's correlation coefficient values have been interpreted based on suggestions in Schober et al. (2018) (Table 2).

Table 2 Pearson's correlation coefficient values and the terms used to interpretate values when the  $P$ -value indicates it is statistically significant ( $p > 0.05$ )

<i>r</i> -value	Interpretation of <i>r</i> -value
0.00–0.10	Negligible correlation
0.10–0.39	Weak correlation
0.40–0.69	Moderate correlation
0.70–0.89	Strong correlation
0.90–1.00	Very strong correlation

Several different methods to test the model's validity were undertaken. Q-Q plots were used to check that the data had a normal distribution. Root mean square error (RMSE), scatterplots with a 1:1 line and graphical residual analysis was used to assess how well the modelled data fit with the measured data.

### 3 Results

#### 3.1 Plant phytolith oxygen isotope ratios

Oxygen isotope ratios were measured on 29 plant phytolith samples, while 15 plant samples could not be analysed for the isotopic composition due to insufficient phytolith quantities or equipment issues that resulted in loss of sample. Plant phytolith material showed very tiny amounts of organic matter trapped in crevices under SEM but not enough to interfere with measurement of oxygen isotope ratios, as it was well below 3% contamination. There was no dissolution noticeable in the SEM photos (Figure 2). Plant phytolith  $\delta^{18}\text{O}$  values had range of 9.8‰ with lowest value being 21.2‰ and the highest 31.0‰ (Table 3, individual readings - Supplementary Table S.6, Appendix 3). Nine sites had more than one species of grass analysed and the maximum within-site difference in  $\delta^{18}\text{O}$  values ranged from 1.6 to 4.1 ‰ (Table 3).

Table 3  $\delta^{18}\text{O}$  values of phytoliths from soils and plants, organised by latitude of sites.

SITE	$\delta^{18}\text{O}$ SOIL PHYTOLITHS	SD	NUMBER OF SOIL ANALYSES	IDENTIFIER	TERN CATALOG NUMBER	SPECIES	$\delta^{18}\text{O}$ PLANT PHYTOLITHS	SD	NUMBER OF PLANT ANALYSES
NTADAC0001	29.5	0.6	8	P24	NTA005877	<i>Sorghum plumosum</i>	28.0	0.3	8
				P25	NTA005870	<i>Chrysopogon fallax</i>	30.0	0.9	3
NTAGFU0031	31.3	0.4	8	P19	NTA003588	<i>Schizachyrium pachyarthron</i>	21.2	0.1	3
				P21	NTA003637	<i>Aristida holathera</i>	22.5	0.3	4
				P18	NTA003628	<i>Triodia bitextura</i>	25.0	0.1	3
				P20	NTA003631	<i>Chrysopogon fallax</i>	25.3	0.5	3
NTAGFU0040	34.3	0.2	3	P22	NTA003970	<i>Aristida latifolia</i>	24.1	0.2	3
				P23	NTA003995	<i>Heteropogon contortus</i>	27.2	0.4	3
NTAGFU0017	33.7	0.3	4	P38	NTA002610	<i>Chrysopogon fallax</i>	23.1	0.9	3
				P15	NTA002631	<i>Aristida holathera</i>	26.2	0.4	4
NTAGFU0008	32.0	0.6	4	P13	NTA002011	<i>Aristida contorta</i>	27.6	0.4	5
NTAGFU0010	30.8	0.3	3	N/A					
NTAGFU0001	33.1	0.7	6	P07	NTA001439	<i>Aristida holathera</i>	26.1	0.6	7
				P12	NTA001530	<i>Aristida inaequiglumis</i>	29.1	0.2	3
				P09	NTA001518	<i>Aristida contorta</i>	29.5	0.5	5
				P10	NTA001524	<i>Aristida pruinosa</i>	26.2	0.7	3
NTABRT0004	33.3	0.4	6	P41	NTA001318	<i>Aristida holathera</i>	28.6	0.5	6
				P06	NTA001324	<i>Aristida contorta</i>	30.3	0.3	7
				P05	NTA001316	<i>Aristida inaequiglumis</i>	31.0	0.4	7
NTAFIN0019	37.6	0.6	9	P02	NTA000760	<i>Aristida holathera</i>	26.2	0.2	4
				P01	NTA000754	<i>Cenchrus ciliaris</i>	24.4	0.4	4
SAASTP0004	33.6	0.4	9	P37	SAT 000070	<i>Eragrostis setifolia</i>	28.5	0.8	4

<b>SAASTP0001</b>	36.8	0.5	5	P32	SAA 000294	<i>Eragrostis setifolia</i>	27.8	0.6	3
				P31	SAA 000288	<i>Aristida contorta</i>	29.4	0.7	4
<b>SATFLB0008</b>	34.5	0.4	4	P30	SAT 000423	<i>Austrostipa breviglumis</i>	29.1	0.6	4
				P26	SAT 000424	<i>Triodia scariosa</i>	25.9	0.6	3
<b>SATFLB0010</b>	36.7	0.3	4	P36	SAT 000559	<i>Austrostipa sp.</i>	29.2	0.7	5
<b>SATFLB0014</b>	38.4	0.5	3	P27	SAT 000749	<i>Austrostipa mollis</i>	30.2	0.6	3
<b>SATFLB0012</b>	39.7	0.5	9	N/A					
<b>SATKAN0001</b>	31.8	0.5	9	N/A					

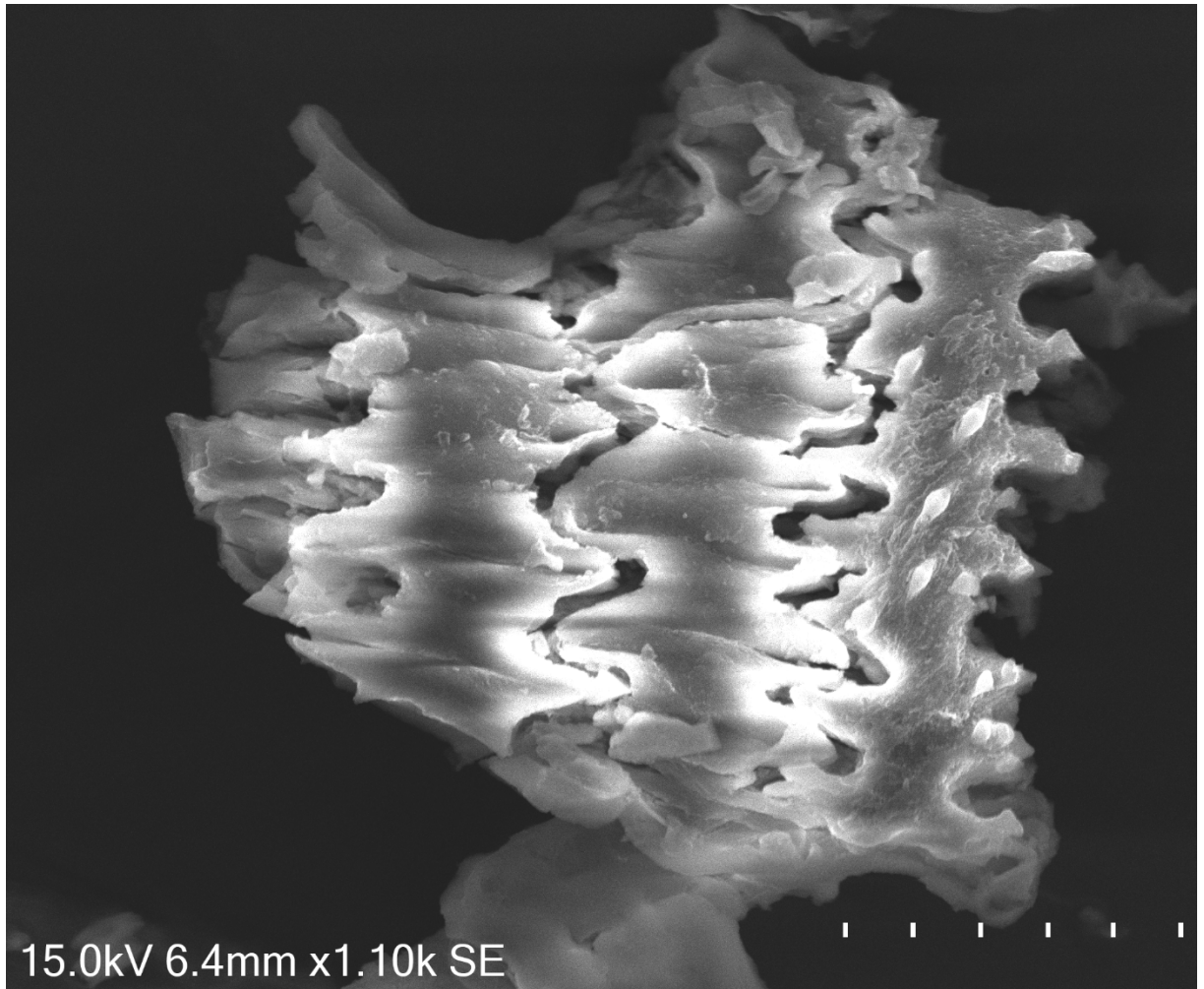


Figure 2 Sample P32 - *Eragrostis setifolia* Skeletal phytolith showing no pitting or noticeable dissolution.

### 3.2 Plants vs climate

The  $\delta^{18}\text{O}$  values of phytoliths extracted from grasses had no statistically significant correlation with the  $\text{RH}_{\text{annual}}$  ( $r: -0.33, p > 0.05$ ) (Figure 3.A, Supplementary Table S.7, Appendix 3) and a statistically significant, moderate negative correlation with the  $T_{\text{annual}}$  ( $r: -0.43, p = 0.03$ ) (Figure 3.B). The 2 year  $\text{RH}_{\text{Tmax-warm}}$  (Figure 3.C) and five year  $\text{RH}_{\text{Tmax-warm}}$  (Figure 3.D) showed the strongest correlations of all the relative humidity data. The 2 year  $\text{RH}_{\text{Tmax-warm}}$ , which had the highest  $r$  value had a moderately negative correlation ( $r = -0.42, p = 0.03$ ). Despite the large variation of  $\delta^{18}\text{O}$  values of phytoliths extracted from grasses of different taxa at the same sites, averaged values of the genus *Aristida* did show a strong

negative correlation with both the 2 year  $RH_{T_{max-warm}}$  and the 2 and 5 year  $RH_{T_{max-warm}}$  (Figure 3.B-D).

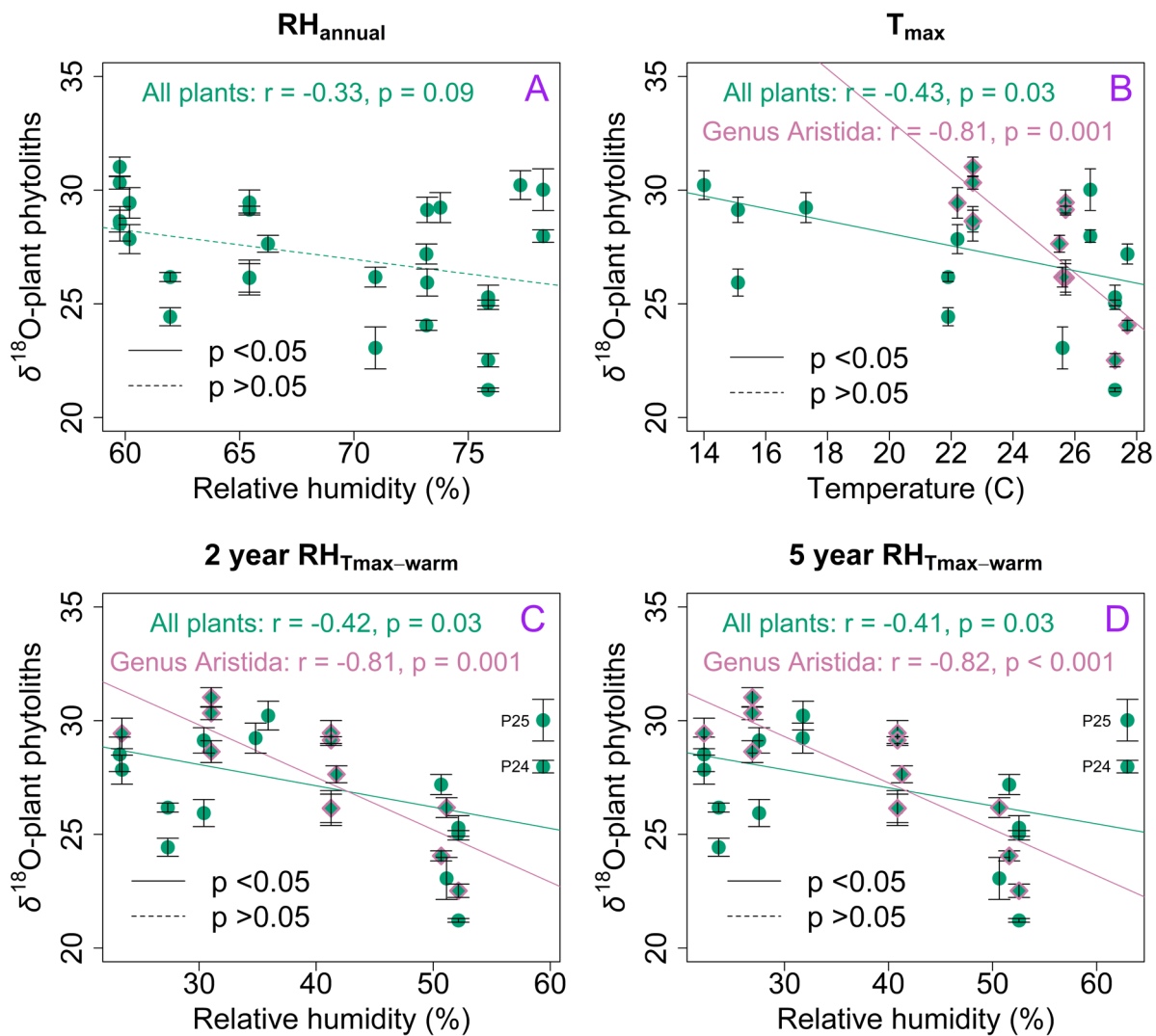


Figure 3 The  $\delta^{18}O$  values of phytoliths from plants versus (A) long term mean annual relative humidity ( $RH_{annual}$ ), (B) long term mean annual temperature ( $T_{max}$ ), (C) mean two year warmest quarter relative humidity at the daily maximum temperature (2 year  $RH_{T_{max-warm}}$ ), and (D) mean five year warmest quarter relative humidity at the daily maximum temperature (5 year  $RH_{T_{max-warm}}$ ). There were 27 grass samples from 13 sites, the  $\delta^{18}O$  values of phytoliths extracted from genus *Aristida* (13 samples from eight sites) are shown as diamonds and highlighted in pink with regressions shown in pink.

### 3.3 Soil phytolith oxygen isotope ratios

Three of the samples of phytoliths extracted from soils had contamination higher than 3%. Soil sample SATFLB0005 had approximately 10% contamination (determined by microscopy), which was mostly quartz grains which would not separate from the phytoliths. FTIR model for this sample (Figure 4.A) showed lower absorbance at  $1050\text{ cm}^{-1}$ , the wavenumber indicating biogenic silica, than samples that were deemed clean under the microscope (Figure 4.B), indicating significant contamination. As a result, this sample was analysed but results were discarded (Figure 4.A, Supplementary Table S.6, Appendix 3). Two soil samples had large amounts of charcoal: SATFLB0015 had approximately 20% charcoal and SATKAN0002 had over 70% charcoal. While charcoal can have large amounts of oxygen, previous research on the  $\delta^{18}\text{O}$  values of phytoliths has suggested charcoal should not be a problem for the  $\delta^{18}\text{O}$  values as high temperature charcoal contains little oxygen (Alexandre et al., 2019; Bird et al., 2014). As these samples were treated at high temperatures to remove the exchangeable oxygen, it was thought that the charcoal would be converted to high temperature charcoal with little oxygen, so these samples were still analysed. However, these two samples provided isotope results that were much lower than expected and had high standard deviations, so these samples were also removed from this study. Repeated analyses on these two soil samples to make sure that the issue was not due to insufficient homogenising of the samples or insufficient sample size was completed without improvement of precision or accuracy. Results for removed sample  $\delta^{18}\text{O}$  values can be seen in Supplementary Table S.6, Appendix 3. For the remaining samples, soil phytolith  $\delta^{18}\text{O}$  values had a range of  $10.22\text{‰}$  (Number of samples = 16) with lowest value being  $29.47\text{‰}$

and the highest 39.69‰ (Table 3, individual readings- see Supplementary Table S.6, Appendix 3).

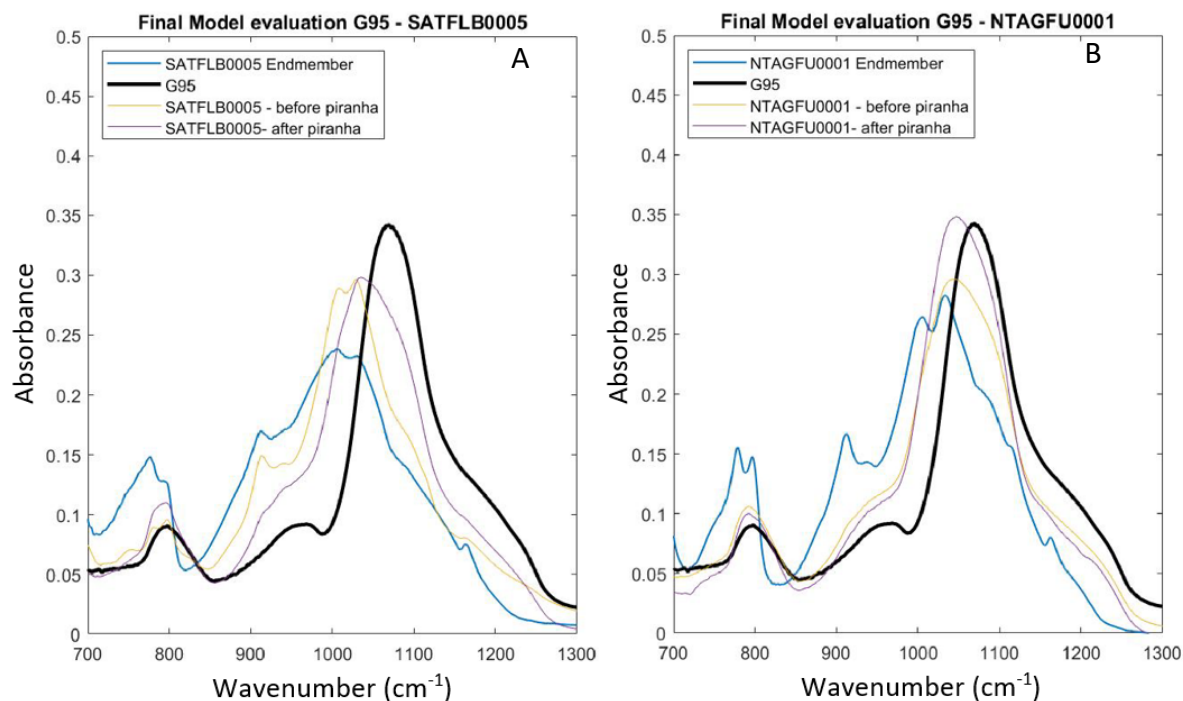


Figure 4 FTIR model comparing soil endmember (blue lines) to phytolith standard (G95 – black lines). Samples after initial extraction (yellow lines) and again after piranha solution treatment (purple lines).

### 3.4 Soil vs climate

The oxygen isotope values of soil phytoliths showed no statistically significant correlation with the  $RH_{\text{annual}}$  ( $r = -0.09$ ,  $p = 0.75$ ) (Figure 5.A) and a moderate negative correlation with the  $T_{\text{annual}}$  ( $r = -0.57$ ,  $p = 0.02$ ) (Figure 5.B). There was a statistically significant moderate negative correlation with the 2 year  $RH_{T_{\text{max-warm}}}$  (Figure 5.C) or 5 year  $RH_{T_{\text{max-warm}}}$  (Figure 5.D). The 5 year  $RH_{T_{\text{max-warm}}}$  showed the highest Pearson's correlation value ( $r = -0.65$  and  $p = 0.006$ ).



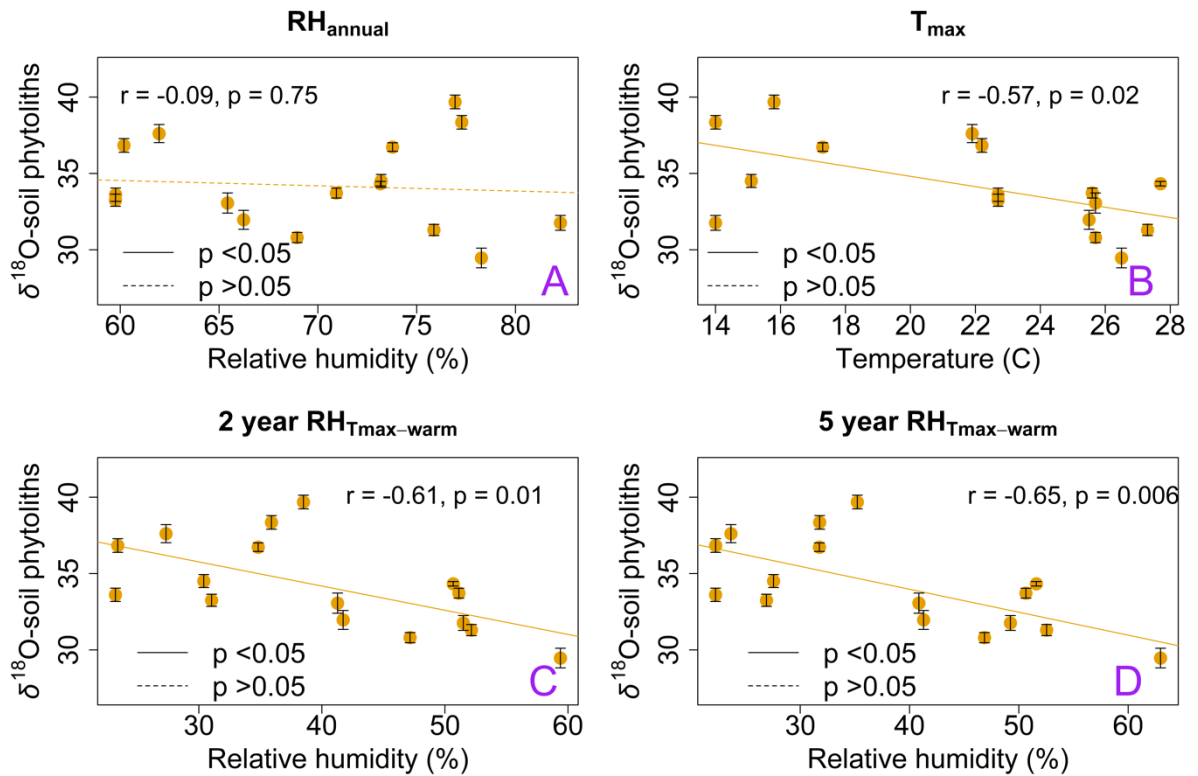


Figure 5 Soil phytoliths compared to (A) long term mean annual relative humidity ( $RH_{\text{annual}}$ ), (B) long term mean annual temperature ( $T_{\text{max}}$ ), (C) mean two year warmest quarter relative humidity at the daily maximum temperature (2 year  $RH_{T_{\text{max-warm}}}$ ), and (D) mean five year warmest quarter relative humidity at the daily maximum temperature (5 year  $RH_{T_{\text{max-warm}}}$ ). (Number of data points = 16).

### 3.5 Plants vs soil

There was no statistically significant correlation between the measured  $\delta^{18}\text{O}$  values of phytoliths from plants and soils ( $r = 0.17$   $p = 0.40$ ). The oxygen isotope values of phytoliths extracted from grasses were up to 12 ‰ lower than the phytoliths from soil at the same site (Table 3), except for one location (NTADAC0001) which had the highest relative humidity (Table 2).

### 3.6 Modelled source water and phytolith $\delta^{18}\text{O}$ values

There were no statistically significant correlations between the measured  $\delta^{18}\text{O}$  values of phytoliths extracted from either plant or soil with any of the modelled leaf water  $\delta^{18}\text{O}$  values (Supplementary Table S.8, Appendix 3). The modelled leaf water  $\delta^{18}\text{O}$  values strongly correlated with the 5 year  $\text{RH}_{\text{Tmax-warm}}$  (Figure 6) with an  $r$  value of  $-0.82$  ( $p < 0.001$ ). The oxygen isotope values of precipitation from Hollins et al. (2018) isoscape showed no statistically significant correlation with the 5 year  $\text{RH}_{\text{Tmax-warm}}$ . The modelled source water  $\delta^{18}\text{O}$  values were all lower than the measured  $\delta^{18}\text{O}$  values of phytolith from both plants and soils.

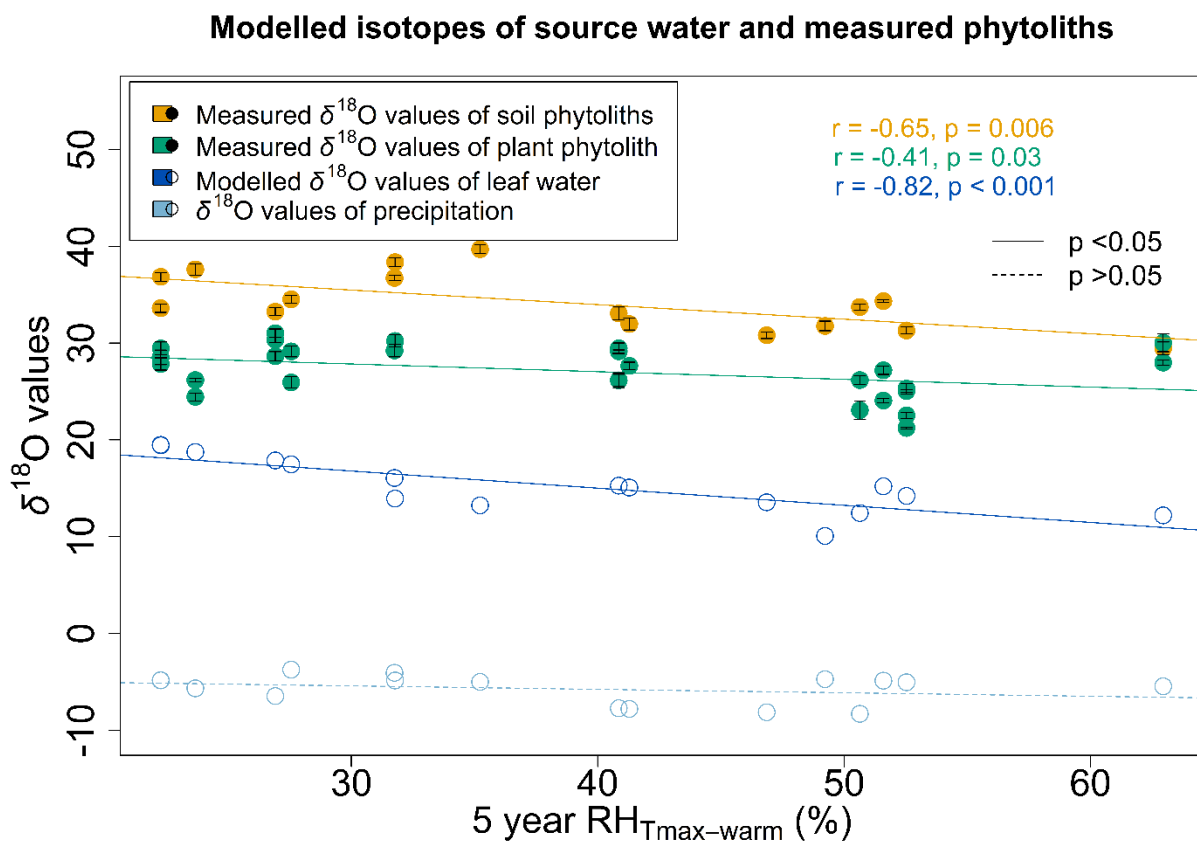


Figure 6 Measured plant and soil phytolith oxygen isotope values and modelled annual mean oxygen isotope values of precipitation (Hollins et al., 2018) and leaf water versus the mean

five year warmest quarter relative humidity at the daily maximum temperature (5 year  $RH_{T_{max-warm}}$ ).

Modelled  $\delta^{18}O$  values of phytoliths precipitating from 100% precipitation (Supplementary Table S.8, Appendix 3) plotted close to measured  $\delta^{18}O$  values of plant phytoliths with a similar trendline with mean relative humidity at the maximum temperate of the warmest period that was slightly offset from the trendline for plant phytoliths (Figure 7). Modelled  $\delta^{18}O$  values of phytolith precipitating from the 100% leaf water plotted higher than measured  $\delta^{18}O$  values of phytoliths extracted from both soil and plants. The trendline of modelled phytoliths with 100% leaf water with mean relative humidity at the maximum temperate of the warmest period was steeper than those of the measured plant and soil phytolith  $\delta^{18}O$  values.

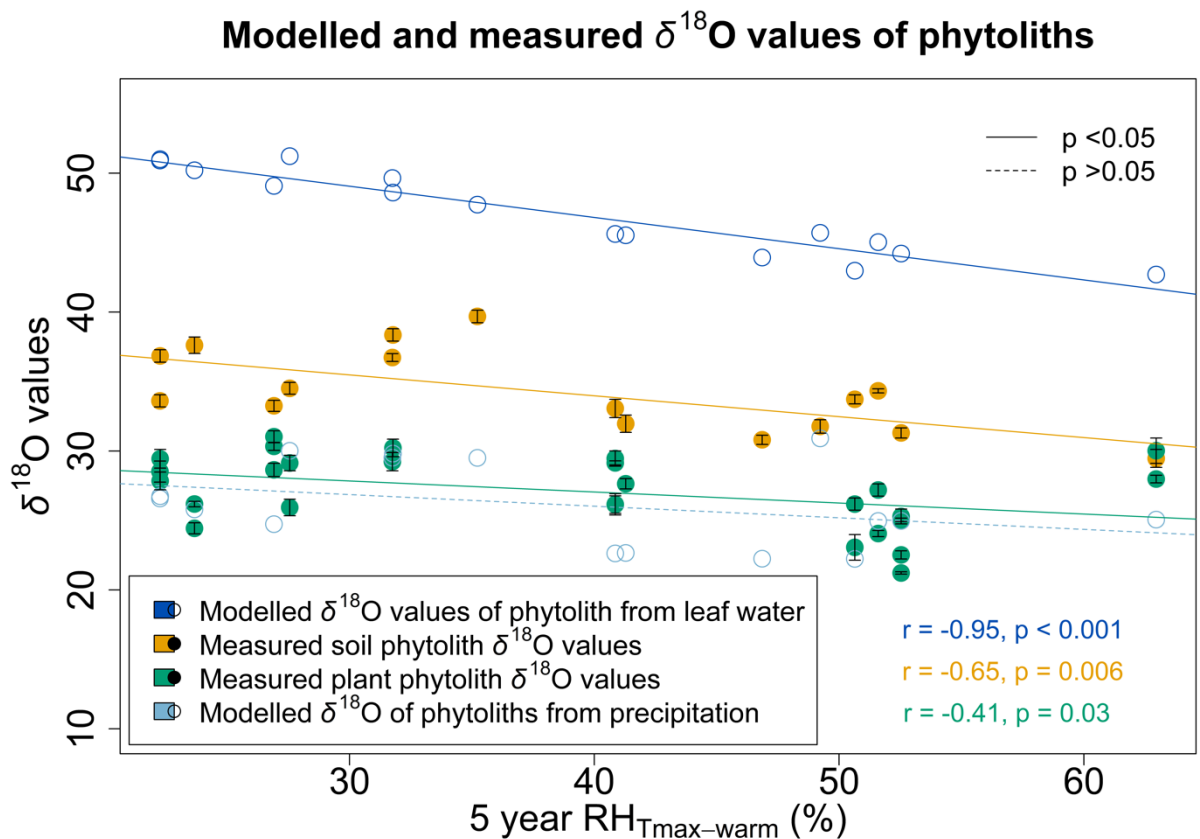


Figure 7 Scatterplot of measured isotope composition of phytoliths extracted from plants (green) and soils (yellow), and modelled isotope composition of phytoliths precipitating from 100% precipitation (light blue) and 100% leaf water (dark blue) compared to mean five year warmest quarter relative humidity at the daily maximum temperature (5 year  $RH_{T_{max-warm}}$ ).

Mass balance modelling that best matched the measured  $\delta^{18}O$  values of phytolith from plants indicated that on average 8% of the plant phytolith isotope composition derives from leaf water, with the remaining 92% deriving from precipitation (Figure 8). The trendline for the  $\delta^{18}O$  values of predicted plant phytoliths against 5 year  $RH_{T_{max-warm}}$  using 8% leaf water and was very similar to that of the measured isotope values of plant phytoliths against 5 year  $RH_{T_{max-warm}}$  (Figure 8).

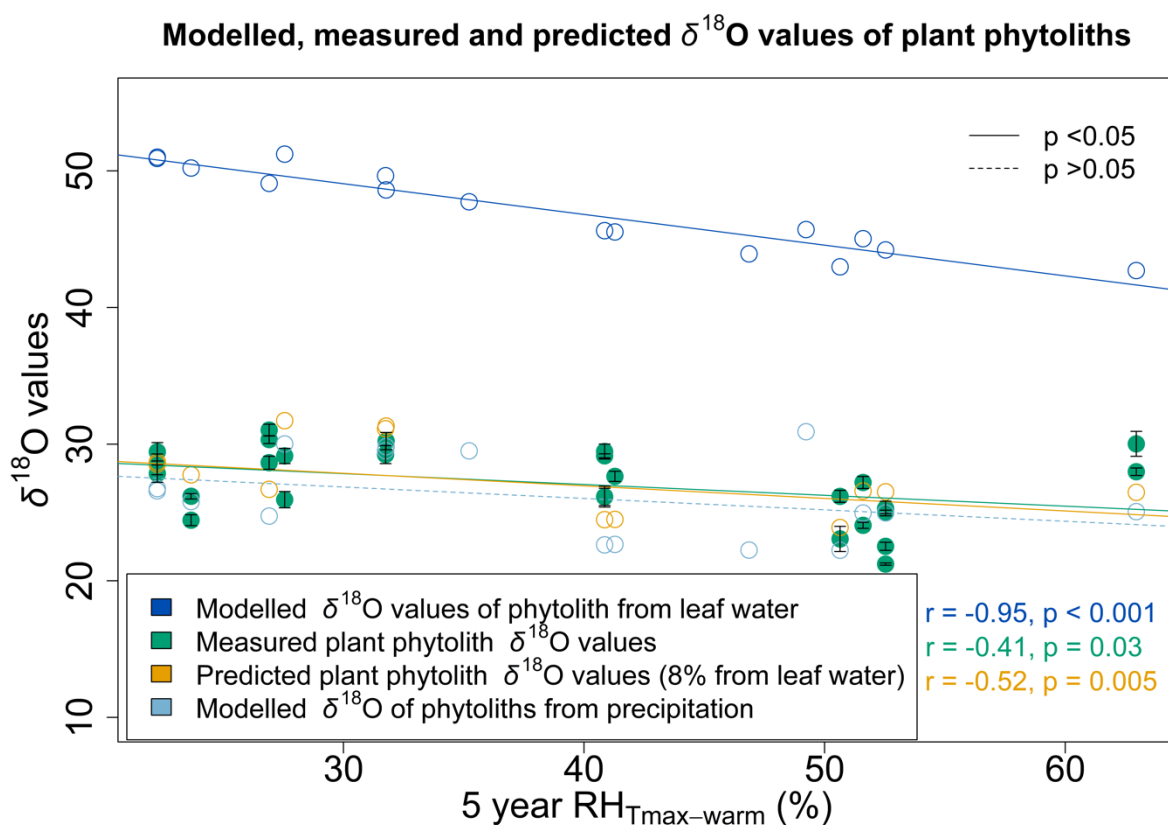


Figure 8 Measured isotope composition of phytoliths extracted from plants (green) and modelled isotope composition of plant phytoliths (yellow), and modelled isotope composition of phytoliths precipitating from 100% precipitation (light blue) and 100% leaf

water (dark blue) versus the mean five year warmest quarter relative humidity at the daily maximum temperature (5 year  $RH_{T_{max-warm}}$ )

Mass balance modelling for predicting measured  $\delta^{18}O$  values of phytolith extracted from soils indicated that 38% derives from leaf water, with the remaining 62% from precipitation (Figure 9). As with the predicted plant phytoliths, the trendline for the  $\delta^{18}O$  values of predicted soil phytoliths against 5 year  $RH_{T_{max-warm}}$  was very similar than that of the measured isotope values of soil phytoliths against 5 year  $RH_{T_{max-warm}}$ .

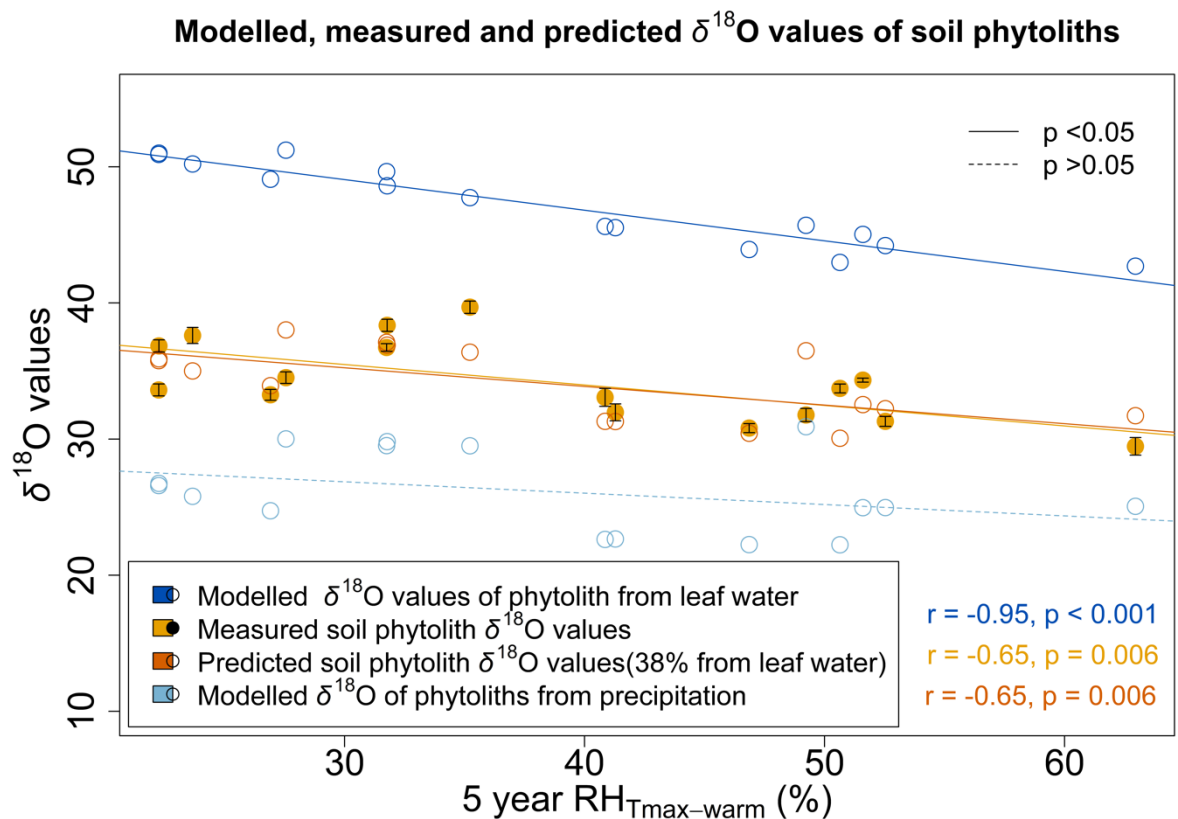


Figure 9 Measured isotope composition of phytoliths extracted from soils (yellow) and modelled isotope composition of soil phytoliths (orange), and modelled isotope composition of phytoliths precipitating from 100% precipitation (light blue) and 100% leaf water (dark blue) versus the mean five year warmest quarter relative humidity at the daily maximum temperature (5 year  $RH_{T_{max-warm}}$ ).

Predicted  $\delta^{18}\text{O}$  values of phytoliths for both plants and soils were plotted on Q-Q plots, both showed the data fell along a 1:1 line and the tails of the data did not skew up or down (Supplementary Figure S.9 and S.10, Appendix 3). This indicated that the data has a normal distribution and is suitable for regression analysis and residual plots. The residual plots had a 50-50 split between data points, there were no outliers, and no patterns or shapes were observed indicating that the model is a good fit (Supplementary Figure S.11 and S.12, Appendix 3).

The data for predicted  $\delta^{18}\text{O}$  values of phytoliths for both plants and soils were plotted against the measured values (Figure 10). Pearson's correlation for the measured and predicted soil phytolith  $\delta^{18}\text{O}$  values showed a moderate correlation ( $r = 0.64$ ,  $p = 0.008$ , RMSE = 2.33) while the plant phytoliths did not have a statistically significant correlation, as indicated by a high p-value ( $r = 0.27$ ,  $p = 0.18$ , RMSE 2.94).

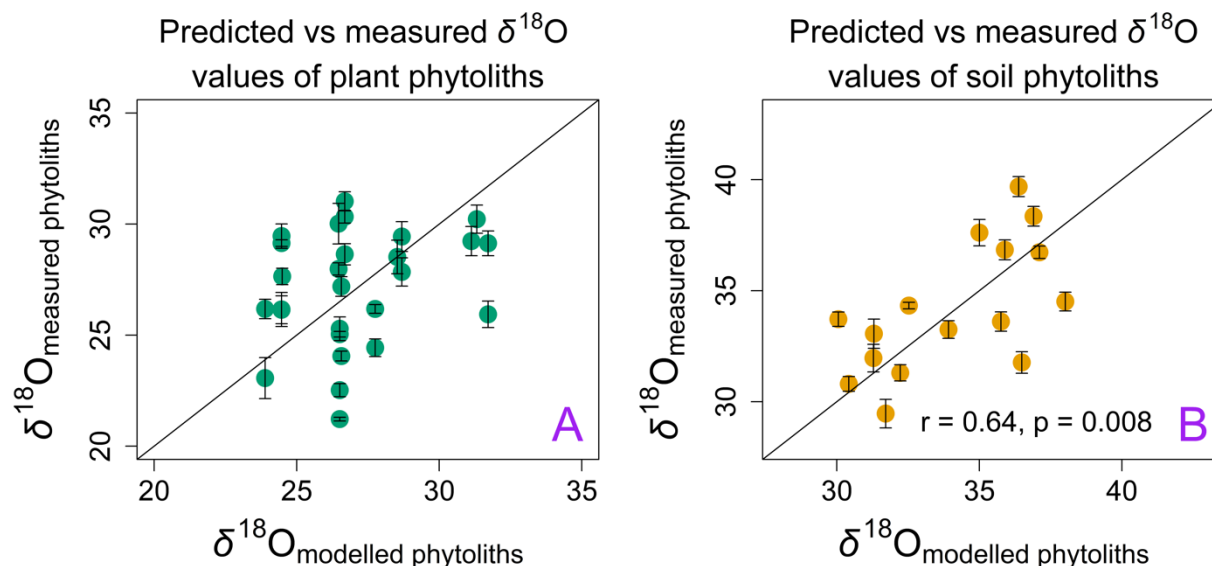


Figure 10 Modelled versus measured  $\delta^{18}\text{O}$  values of phytoliths from plants (A) and soils (B).

## 4 Discussion

### 4.1 Variability of plant phytolith oxygen isotope ratios within a site

It was hypothesized [H1] that the  $\delta^{18}\text{O}$  values of phytoliths from species growing at the same sites would not vary because environmental conditions should be controlling fractionation.

However, there was substantial variation of between 1.6 and 4.1 ‰ for grass phytoliths from the same site. The variation did not appear to be related to species, as at site NTAGFU0017

*Aristida holathera* had a higher value (26.2 ‰, Table 3) than *Chrysopogon fallax* (23.1 ‰)

whereas at NTAGFU0031 it was the opposite with *Aristida holathera* having the lower value

(22.5 ‰, Table 3) than *Chrysopogon fallax* (25.3 ‰). The variation amongst plants may be

due to microclimates (Webb and Longstaffe, 2000), though varying ages of the grass samples

could provide a better explanation. The grasses used in this study were mostly perennials,

and the ages of the plants are unknown. Samples could be from plants that are only a couple

of weeks old to several years old thus recording different time periods. It is likely that most

sampled plants were older than a year as the  $\delta^{18}\text{O}$  values of the plants correlated best with

the two-year time period rather than shorter or longer periods (Figure 3.C-D, Supplementary

Table S.7, Appendix 3). Alternative explanations for differences in the  $\delta^{18}\text{O}$  values of

phytoliths in species at the same site include methodological uncertainties such as sampling

some non-transpiring tissue instead of transpiring tissue, especially in smaller specimens,

which could lead to different  $\delta^{18}\text{O}$  values as non-transpiring tissue will have a lower value

than transpiring tissue. Additionally, the plants were dried and stored in teabags on top of

silica gel (White et al., 2012). There is a small possibility that silica dust may have stuck to the

outside of the plant and was not cleaned off properly in the pre-rinse, thus altering the

overall isotopic composition. This is unlikely though, and as the plant samples from the same

site were stored in the same box it would be expected that any contamination would result

in smaller rather than larger variations between samples. Differences in the isotopic composition of the source water could also be an explanation for the isotopic difference of plants from the same site. Different plants could take up water from different soil depths, which may have contrasting isotope values due to differences between soil water and ground water. While this could be an issue, generally grasses roots do not extend to the water table, so it is expected that all the grasses at a site are using the same or similar source water (soil water near the surface). If the comparison had been comparing grasses to trees, then this could have been an issue (Renée Brooks et al., 2010; Von Freyberg et al., 2020) because, while fractionation within leaves should be the same across species, the initial source water oxygen isotope value would be different, with soil water value exhibiting larger variations than deeper ground water (Kendall and McDonnell, 2012).

#### 4.2 Oxygen isotope ratios of phytoliths compared to climate along the transect

##### 4.2.1 Plant phytolith oxygen isotope ratios vs climate

To test for climatic controls in plant phytoliths (H2), the  $\delta^{18}\text{O}$  values of phytoliths extracted from modern grasses growing naturally in Australia were compared to climate data. The  $\delta^{18}\text{O}$  values of phytoliths from plants did not show a strong correlation to any of the annual average climate parameters, which may indicate that phytoliths in plants are not continuously recording daytime averages throughout their lifetimes.  $\delta^{18}\text{O}$  values of modern grass phytoliths did show a moderate correlation with both the  $\text{RH}_{\text{Tmax-warm}}$  and the  $\text{T}_{\text{max}}$ , which could be due to the relative humidity being lower during the warmer period, leading to higher  $\delta^{18}\text{O}$  values of phytoliths when they are produced. Shahack-Gross et al. (1996) found that phytoliths from non-transpiring tissue correlated with temperature and was able to reconstruct the temperatures during the growing season from the  $\delta^{18}\text{O}$  values of phytoliths extracted from plants grown in controlled conditions in Israel. They found the



$\delta^{18}\text{O}$  value of phytoliths from transpiring tissue did not correlate with the relative humidity and assumed the relative humidity was too variable to correlate to  $\delta^{18}\text{O}$  value. However, this lack of correlation with relative humidity could be because they did not consider the relative humidity of the warmest period. Webb and Longstaffe (2000) also found that the  $\delta^{18}\text{O}$  values of phytoliths from non-transpiring tissue of grasses grown in Canada correlated with temperature but in addition, they found that the  $\delta^{18}\text{O}$  values of phytoliths extracted from transpiring tissue correlated with the relative humidity of the summer months, like the findings in this study. This was despite the phytoliths coming from two species of grass that had different periods of peak plant growth. Our findings are consistent with the results of Webb and Longstaffe (2000) showing that the  $\delta^{18}\text{O}$  values of phytoliths from grasses have a moderate correlation with the relative humidity of the summer months.

Species of the genus *Aristida* were collected from eight separate locations and the  $\delta^{18}\text{O}$  values of the phytoliths extracted from these specimens showed a strong correlation with both  $T_{\text{max}}$  and the  $\text{RH}_{T_{\text{max-warm}}}$ . When other species were compared against the *Aristida* line of best fit with  $\text{RH}_{T_{\text{max-warm}}}$ , it became evident that all the other plant taxa fit well along the line except two data points (Figure 3.C and Figure 3.D). These two samples (P24 and P25) are from the same location (NTADAC0001). This site is the only site where the  $\delta^{18}\text{O}$  values of phytoliths from plants and soils were similar. Moreover, the  $\delta^{18}\text{O}$  value of the soil phytoliths was the lowest of all the soil samples. This site is the most humid of all the locations (Table 1) so we would expect there to be less  $^{18}\text{O}$  enrichment than the other sites, which would lead to the lowest  $\delta^{18}\text{O}$  values for both plants and soils. However, while the soils match the expectation, the plant phytolith values from this site are not among the lowest when compared to the other plants. It was furthermore noted the collection date at this site was quite different to the other samples. All other samples were collected between November

2011 and November 2012, and the samples from site NTADAC0001 was collected at the end of May 2013. There were successive La Niña events recorded in Australia between 2010 and 2012 (Falster et al., 2021). La Niñas are characterized by larger amounts of precipitation than normal, which leads to lower  $\delta^{18}\text{O}$  values for precipitation so the plant source water could be significantly lower than non-La Niña periods (Bowen et al., 2019; Dansgaard, 1964; Hollins et al., 2018; Lachniet and Patterson, 2009; Rozanski et al., 1993; Tang and Feng, 2001). As a result of lower source water  $\delta^{18}\text{O}$  values, the phytoliths extracted from grass at the sites collected in 2011 and 2012 could be lower than normal  $\delta^{18}\text{O}$  values, and the NTADAC0001 grass phytolith samples would have  $\delta^{18}\text{O}$  values that are more consistent with longer term trends at the site.

#### 4.2.2 Soil phytolith oxygen isotope ratios vs climate

To test for climatic controls in soil phytoliths (H2), similar comparisons were made as for plant phytoliths. The  $\delta^{18}\text{O}$  values of phytoliths from soils correlate moderately with  $T_{\text{annual}}$  (Figure 5) and correlate strongly with the  $\text{RH}_{\text{Tmax-warm}}$ . Like the plants, there was not a correlation with the  $\delta^{18}\text{O}$  values with the mean annual relative humidity. The soil phytoliths correlated best with the 5-year times period (Figure 5.D) and had stronger correlation with climate than did the phytoliths from plants (Figure 3.D). Alexandre et al. (2012) used the  $\delta^{18}\text{O}$  values of phytoliths from soils in a rainforest to reconstruct temperature where 80% of the phytoliths were from non-transpiring tissue. They found that while they were able to reconstruct temperature, the relative humidity signal was still quite strong in the soil phytoliths. They tried to correlate the  $\delta^{18}\text{O}$  values to the annual mean relative humidity but were unsuccessful, which in the light of the findings of this study, may be ascribed to the stronger correlation to the relative humidity of the warmest period.

One of the biggest concerns with soil phytoliths is taphonomy causing bias in the record. Post-depositional processes can result in the altering and dissolution of phytoliths or transportation in and out of the system (Crifò and Strömberg, 2020; Piperno, 2006; Prentice and Webb, 2016; Strömberg et al., 2018). Aeolian and hydrological processes have both been shown to move phytoliths around (Cary et al., 2005; Funk et al., 2022; Piperno, 2006). Premathilake et al. (2022) indicated a loss of approximately 25% of the soil phytoliths from the modern-day topsoil and the older deeper deposits. A preliminary assessment of the reliability of soil phytoliths at different depths of soil as a true representation of phytolith assemblages was conducted by Crifò and Strömberg (2020). While only testing phytoliths in a rainforest and dry forest, it was noted that there were fewer phytoliths in the lower A-horizon versus the upper A-horizon which was attributed to taphonomic processes. They concluded that despite this, the morphology of phytoliths in a single sample from the lower A-horizon was still a good representation of modern-day samples. Several of the phytolith samples used in this study were from site locations close to each other and reported similar climate parameters and oxygen isotope values, suggesting that taphonomic processes have not had a great effect on the results. How this biased preservation of phytoliths at depth might alter the oxygen isotopes needs to be investigated. It is unknown whether variations in soil conditions, for example pH or average water content, effect the oxygen isotope composition of phytoliths. Dissolution and oxygen exchange of biogenic silica is a known issue in laboratory conditions (Akse et al., 2020; Menicucci et al., 2017; Tyler et al., 2017). Phytoliths in soils are not sitting continually in water, so these laboratory comparisons are not directly relevant to phytoliths in soils, and more realistic experiments are needed. Charcoal was found in most soil samples and while phytolith extraction methods removed most of the charcoal, it could not be eliminated completely. Charcoal removal is a known

issue, though it is thought that as charcoal is mostly carbon, it will not affect the oxygen isotope ratios (Alexandre et al., 2012; Bryant and Holloway, 2009; Riding, 2021). However, the two samples with high amounts of charcoal (SATFLB0015 and SATKAN0002) showed large standard deviations indicating that charcoal can be an issue and should be kept to below the 3% residual concentration to prevent imprecise readings (Leng and Sloane, 2008). This might be explained by oxygen being released from the charcoal or interference of the charcoal with the microfluorination process. It is likely that the charcoal would have released oxygen during dehydroxylation which involved heating samples to at least 1100°C, but with such a large volume of charcoal, the small amount of oxygen being released may have been more than that being released from the silica (Conesa et al., 2000). SATFLB0015 had a standard deviation of 1.9 ( $1\sigma$ , N = 9) and SATKAN0002 had a standard deviation of 3.4 ( $1\sigma$ , N = 16). These high standard deviations may be a specific issue with the micro-fluorination process used in this study. The process relies on combusted fluorine physically touching the beads of silica and substantial amounts of charcoal could inhibit this from occurring (Menicucci et al., 2013). The two soil samples with significant volume of charcoal took longer to clear the silica out of the reaction tube, indicating that the charcoal was inhibiting the ability for the fluorine to reduce the silica.

The amount of residual charcoal in the two samples, along with visibly darkened and black phytoliths, suggest recent high temperature fires. It is unknown how high temperature fires affect the oxygen isotopes of phytoliths already in the soil, but it is known that morphological features of phytoliths in burned material are affected by fire and these are deposited into the soils (Devos et al., 2021). The residual charcoal may not have been the cause of the low values and high standard deviation of the samples, but rather the phytoliths themselves, may have had their oxygen isotopes changed due to the high temperature fires.

### 4.3 Phytolith oxygen isotope ratios from soil vs plant

It was expected that phytoliths from plants would have similar  $\delta^{18}\text{O}$  values to those of topsoil at the same location [H3] however they did not, with up to 12 ‰ difference between the two (Table 3). Both plant (Figure 3.C and D) and soil (Figure 5.C and D) phytolith  $\delta^{18}\text{O}$  values are negatively correlated with the  $\text{RH}_{\text{Tmax-warm}}$ , which suggests that the relative humidity signal in the  $\delta^{18}\text{O}$  values of phytoliths in plants is being transferred to the soil. The soils manifest a stronger correlation than the plants, which could be due to longer term trends being recorded in the soil phytoliths. The  $\delta^{18}\text{O}$  values of phytoliths extracted from soils were consistently higher than those from plants from the same sites (Figure 6), which contrasts with the model  $\delta^{18}\text{O}$  values of phytoliths from soils by Webb and Longstaffe (2002) which produced values lower than the  $\delta^{18}\text{O}$  values of transpiring tissue from plants. Soil phytolith  $\delta^{18}\text{O}$  values were expected to follow the previous modelling for a two main reasons: 1) Transpiring tissue has the highest abundance of phytoliths and highest  $\delta^{18}\text{O}$  values while the rest of the plant has fewer phytoliths with lower values. It is expected that phytoliths from soils are a mix of these two pools of phytoliths so the  $\delta^{18}\text{O}$  values will be between the  $\delta^{18}\text{O}$  values of these two pools. 2) If there was oxygen exchange in the phytoliths after being transferred to the soil, it would be exchanging oxygen with soil water which has a much lower  $\delta^{18}\text{O}$  value than the phytoliths, thus decreasing the  $\delta^{18}\text{O}$  value (Gehrels et al., 1998).

There are other possible explanations for the lower  $\delta^{18}\text{O}$  values of phytoliths extracted from the grass samples. There has not been a comparison of phytoliths from plants that have died and decomposed naturally versus those that have been picked and digested. It is possible that at the end of life of the grass the plant water is fractionated as it dries out and the last of the silica is precipitating in greatly enriched water. These phytoliths could have

significantly higher values than the rest of the phytoliths in the plant, an issue that could be compounded by the mass dying of plants during the end of summer. The overabundance of higher values in these phytoliths could hide the signal of the rest of the phytoliths. There is also evidence that plants growing in lower relative humidity produce more phytoliths and these phytoliths have higher  $\delta^{18}\text{O}$  values than the plants growing in higher relative humidity (Webb and Longstaffe, 2002). Periods of lower relative humidity could therefore mask the signals of not just the lower phytolith values in the plants, but also the lower phytolith values from previous years. The relative humidity at each site for the 10 years before collection was tested to see if there were any anomalies in relative humidity, but none were observed.

#### 4.4 Craig Gordon modelling and predicted phytolith $\delta^{18}\text{O}$ values

To test if the process controlling the oxygen isotope composition of phytoliths is understood, Craig-Gordon modelling of the environmental controls on leaf water oxygen isotope ratio, combined with temperature-sensitive fractionation during silica precipitation was used to predict phytolith oxygen isotope ratios in plants and soils [H4]. Modelled  $\delta^{18}\text{O}$  values of phytoliths precipitating from 100% unfractionated rainfall plotted around the same values as the measured  $\delta^{18}\text{O}$  values of plant phytoliths, whilst at some locations, the modelled  $\delta^{18}\text{O}$  values of phytoliths plotted higher than the measured values. Since the rainfall values used within the model are interpolated from climate stations up to 200 km away, and the derived 5 year  $T_{\text{max}}$  was used in the temperature fractionation equation, variance from the long-term values of modelled  $\delta^{18}\text{O}$  values is to be expected (Hollins et al., 2018; Shahack-Gross et al., 1996). The enrichment of oxygen that would result from surface water evaporation is also not considered in the modelled  $\delta^{18}\text{O}$  values (Allison et al., 1983; Webb and Longstaffe, 2000). While there is room for improvement, this modelling assuming 100% rainfall as source water provides a reasonable starting point and a minimum isotopic composition that

can be expected at these sites because the modelling uses the average maximum temperature and does not take evaporation into account, both of which would produce lower  $\delta^{18}\text{O}$  values. As previously discussed, the phytoliths extracted from plants in this study have lower  $\delta^{18}\text{O}$  values than expected, which may be related to La Niña conditions during the sampling period. If the measured  $\delta^{18}\text{O}$  values of plant phytoliths have been affected by a lower initial  $\delta^{18}\text{O}$  value of precipitation due to larger amounts of rain, this would explain why the values plot close to or slightly lower than the modelled  $\delta^{18}\text{O}$  values of phytoliths from long-term average precipitation instead of plotting between the measured  $\delta^{18}\text{O}$  values of soil phytoliths and the modelled  $\delta^{18}\text{O}$  values of phytoliths from leaf water (Figure 7).

The modelled  $\delta^{18}\text{O}$  values of phytoliths from 100% leaf water are expected to have the very highest values of phytoliths in plants. This is because the leaf water was calculated using the  $\text{RH}_{\text{Tmax}}$ , which results in the lowest relative humidity and the highest leaf water values (Cernusak et al., 2016; Cernusak et al., 2022).

The measured  $\delta^{18}\text{O}$  values of soil phytoliths plot in between the two sets of modelled  $\delta^{18}\text{O}$  values of phytoliths from the two end member source waters, which is consistent with modelled  $\delta^{18}\text{O}$  values of soil phytoliths in Webb and Longstaffe (2000).

The predicted plant phytolith  $\delta^{18}\text{O}$  values, with an assumed 8% of leaf water and 92% of source water, show good agreement with the measured plant phytolith  $\delta^{18}\text{O}$  values (Figure 10) considering each site has only one predicted value, whilst the measured plant  $\delta^{18}\text{O}$  values showed large variations. However, the 8% of the phytolith oxygen coming from leaf water does not seem realistic, especially considering the measured plant phytolith  $\delta^{18}\text{O}$  values are lower than soil phytoliths instead of higher (Figure 8, section 4.3). The modelling could be redone using a set of phytoliths extracted from plants grown in controlled

conditions where the different variables (temperature and relative humidity) are known and maintained. This will allow a better constraint on the percentage of leaf water and precipitation being recorded in the plants.

The predicted  $\delta^{18}\text{O}$  of phytoliths from soils, with assumed 38% phytoliths from transpiring tissue (leaf water oxygen source) and 62% from non-transpiring tissue (precipitation oxygen source), agrees well with previous soil phytolith modelling (Webb and Longstaffe, 2000). The previous study, which created the model from the  $\delta^{18}\text{O}$  values of phytoliths from different parts of grass and the weighted averages of phytoliths from transpiring and non-transpiring tissue, suggested that soil phytoliths should comprise approximately 40 to 45% of phytoliths from strongly transpiring tissue.

While there are many things affecting the  $\delta^{18}\text{O}$  values of phytoliths, it is possible to predict the values using estimate  $\delta^{18}\text{O}$  values of precipitation, climate data and an estimation of the mixing between potential source water for phytolith formation. The ability to predict the soil phytolith values with a RMSE of 2.33 indicates that the main processes controlling the oxygen isotopes of phytoliths in soil are understood. This opens the possibility of using  $\delta^{18}\text{O}$  values of phytoliths in sedimentary deposits as proxy for temperature or relative humidity. For this to be done, another proxy to constrain one of the climate parameters would be needed. For example, carbonate clumped isotopes, tree rings or glacial record could be used to reconstruct the temperature or constrain if the temperature has increased or decreased. (Green et al., 2018; Mann et al., 2008). The  $\delta^{18}\text{O}$  values of precipitation could be considered stable, and then the relative humidity could be reconstructed.



## 5 Conclusions

The oxygen isotope composition of phytoliths extracted from plants and bulk topsoil across a latitudinal transect of Australia were compared to climate data and then modelled. This study showed that the oxygen isotope ratios of phytoliths in plants at the same location showed a large variation with no trends noticed amongst different species. This is most likely an outcome of plants being of different ages. The  $\delta^{18}\text{O}$  values of phytoliths from plants and bulk topsoil reflect the combined effects of relative humidity on leaf water isotope ratios and temperature on silica-water isotope fractionation during phytolith formation. In particular, the oxygen isotope ratios of phytoliths from both plants and soils correlated with the  $\text{RH}_{\text{Tmax-warm}}$  not the  $\text{RH}_{\text{annual}}$ . The  $\delta^{18}\text{O}$  values of grasses did not have similar  $\delta^{18}\text{O}$  values to those of topsoil at the same location except at one site. The soil phytolith oxygen isotope ratios were successfully modelled using interpolated oxygen isotopes of precipitation,  $T_{\text{max}}$ ,  $\text{RH}_{\text{Tmax}}$ , the Craig-Gordon model, temperature dependent fractionation and a two-pool mass balance mixing model. It is not possible to reconstruct accurate relative humidity from the bulk phytoliths without knowing either temperature or the  $\delta^{18}\text{O}$  of precipitation, however combined with other proxies for these parameters, a quantitative relative humidity proxy could be developed.

## 6 References

- Akse S. P., Middelburg J. J., King H. E. and Polerecky L. (2020) Rapid post-mortem oxygen isotope exchange in biogenic silica. *Geochimica et Cosmochimica Acta* **284**, 61-74.
- Alexandre A., Crespin J., Sylvestre F., Sonzogni C. and Hilbert D. W. (2012) The oxygen isotopic composition of phytolith assemblages from tropical rainforest soil tops (queensland, australia): Validation of a new paleoenvironmental tool. *Climate of the Past* **8**, 307-324.
- Alexandre A., Webb E., Landais A., Piel C., Devidal S., Sonzogni C., Couapel M., Mazur J.-C., Pierre M., Prié F., Vallet-Coulomb C., Outrequin C. and Roy J. (2019) Effects of leaf length and development stage on the triple oxygen isotope signature of grass leaf water and phytoliths: Insights for a proxy of continental atmospheric humidity. *Biogeosciences* **16**, 4613-4625.

- Alexandre A., Landais A., Vallet-Coulomb C., Piel C., Devidal S., Pauchet S., Sonzogni C., Couapel M., Pasturel M., Cornuault P., Xin J., Mazur J.-C., Prié F., Bentaleb I., Webb E., Chalié F. and Roy J. (2018) The triple oxygen isotope composition of phytoliths as a proxy of continental atmospheric humidity: Insights from climate chamber and climate transect calibrations. *Biogeosciences* **15**, 3223-3241.
- Allison G. B., Barnes C. J. and Hughes M. W. (1983) The distribution of deuterium and  $^{18}\text{O}$  in dry soils 2. Experimental. *Journal of Hydrology* **64**, 377-397.
- Bird M.I., Wynn J.G., Saiz G., Wurster C.M., McBeat, A., (2015) The Pyrogenic Carbon Cycle. *Annual Review of Earth and Planetary Sciences* **43**, 273-298.
- Bowen G. J., Cai Z., Fiorella R. P. and Putman A. L. (2019) Isotopes in the water cycle: Regional- to global-scale patterns and applications. *Annual Review of Earth and Planetary Sciences* **47**, 453-479.
- Bryant V. M. and Holloway R. G. (2009) Reducing charcoal abundance in archaeological pollen samples. *Palynology* **33**, 63-72.
- Cary L., Alexandre A., Meunier J.-D., Boeglin J.-L. and Braun J.-J. (2005) Contribution of phytoliths to the suspended load of biogenic silica in the nyong basin rivers (cameroon). *Biogeochemistry* **74**, 101-114.
- Cernusak L. A., Barbour M. M., Arndt S. K., Cheesman A. W., English N. B., Feild T. S., Helliker B. R., Holloway-Phillips M. M., Holtum J. A. M., Kahmen A., McInerney F. A., Munksgaard N. C., Simonin K. A., Song X., Stuart-Williams H., West J. B. and Farquhar G. D. (2016) Stable isotopes in leaf water of terrestrial plants. *Plant, Cell & Environment* **39**, 1087-1102.
- Cernusak L. A., Barbeta A., Bush R. T., Eichstaedt R., Ferrio J. P., Flanagan L. B., Gessler A., Martín-Gómez P., Hirl R. T., Kahmen A., Keitel C., Lai C.-T., Munksgaard N. C., Nelson D. B., Ogée J., Roden J. S., Schnyder H., Voelker S. L., Wang L., Stuart-Williams H., Wingate L., Yu W., Zhao L. and Cuntz M. (2022) Do  $^2\text{H}$  and  $^{18}\text{O}$  in leaf water reflect environmental drivers differently? *New Phytologist* **235**, 41-51.
- Chapligin B., Meyer H., Friedrichsen H., Marent A., Sohns E. and Hubberten H. W. (2010) A high-performance, safer and semi-automated approach for the  $\delta^{18}\text{O}$  analysis of diatom silica and new methods for removing exchangeable oxygen. *Rapid Commun Mass Spectrom* **24**, 2655-2664.
- Conesa J. A., Sakurai M. and Antal M. J. (2000) Synthesis of a high-yield activated carbon by oxygen gasification of macadamia nut shell charcoal in hot, liquid water. *Carbon* **38**, 839-848.
- Crifò C. and Strömberg C. A. E. (2020) Small-scale spatial resolution of the soil phytolith record in a rainforest and a dry forest in costa rica: Applications to the deep-time fossil phytolith record. *Palaeogeography, Palaeoclimatology, Palaeoecology* **537**.
- Dansgaard W. (1964) Stable isotopes in precipitation. *Tellus* **16**, 436-468.
- Devos Y., Hodson M. J. and Vrydaghs L. (2021) Auto-fluorescent phytoliths: A new method for detecting heating and fire. *Environmental Archaeology* **26**, 388-405.
- Falster G., Konecky B., Madhavan M., Stevenson S. and Coats S. (2021) Imprint of the pacific walker circulation in global precipitation  $\delta^{18}\text{O}$ . *Journal of Climate* **34**, 8579-8597.
- Funk R., Busse J., Siegmund N., Sommer M., Iturri L. A., Panebianco J. E., AVECILLA F. and Buschiazzi D. E. (2022) Phytoliths in particulate matter released by wind erosion on arable land in la pampa, argentina. *Frontiers in Environmental Science* **10**.
- Gehrels J. C., Peeters J. E. M., De Vries J. J. and Dekkers M. (1998) The mechanism of soil water movement as inferred from  $^{18}\text{O}$  stable isotope studies. *Hydrological Sciences Journal* **43**, 579-594.

- Geis J. W. (1973) Biogenic silica in selected species of deciduous angiosperms. *Soil science* **116**, 113-130.
- Green D. R., Smith T. M., Green G. M., Bidlack F. B., Tafforeau P. and Colman A. S. (2018) Quantitative reconstruction of seasonality from stable isotopes in teeth. *Geochimica et Cosmochimica Acta* **235**, 483-504.
- Hollins S. E., Hughes C. E., Crawford J., Cendón D. I. and Meredith K. T. (2018) Rainfall isotope variations over the Australian continent – implications for hydrology and isoscape applications. *Science of The Total Environment* **645**, 630-645.
- Howard S., McInerney F. A., Caddy-Retalic S., Hall P. A. and Andrae J. W. (2018) Modelling leaf wax n-alkane inputs to soils along a latitudinal transect across Australia. *Organic Geochemistry* **121**, 126-137.
- Jeffrey S. J., Carter J. O., Moodie K. B. and Beswick A. R. (2001) Using spatial interpolation to construct a comprehensive archive of Australian climate data. *Environmental Modelling & Software* **16**, 309-330.
- Kendall C. and McDonnell J. J. (2012) *Isotope tracers in catchment hydrology*. Elsevier.
- Kita I., Taguchi S. and Matsubaya O. (1985) Oxygen isotope fractionation between amorphous silica and water at 34–93°C. *Nature* **314**, 83-84.
- Kottek M., Grieser J., Beck C., Rudolf B. and Rubel F. (2006) World map of the Köppen-Geiger climate classification updated.
- Lachniet M. S. and Patterson W. P. (2009) Oxygen isotope values of precipitation and surface waters in northern Central America (Belize and Guatemala) are dominated by temperature and amount effects. *Earth and Planetary Science Letters* **284**, 435-446.
- Leng M. J. and Sloane H. J. (2008) Combined oxygen and silicon isotope analysis of biogenic silica. *Journal of Quaternary Science* **23**, 313-319.
- Mann M. E., Zhang Z., Hughes M. K., Bradley R. S., Miller S. K., Rutherford S. and Ni F. (2008) Proxy-based reconstructions of hemispheric and global surface temperature variations over the past two millennia. *Proceedings of the National Academy of Sciences* **105**, 13252-13257.
- McInerney F.A., Gerber C., Dangerfield E., Cernusak L.A., Puccini A., Szarvas S., Singh T., Welti N., (2023) Leaf water  $\delta^{18}\text{O}$ ,  $\delta^2\text{H}$  and d-excess isoscapes for Australia using region-specific plant parameters and non-equilibrium vapour. *Hydrological Processes* **37**(5), e14878.
- Menicucci A. J., Matthews J. A. and Spero H. J. (2013) Oxygen isotope analyses of biogenic opal and quartz using a novel microfluorination technique. *Rapid Communications in Mass Spectrometry* **27**, 1873-1881.
- Menicucci A. J., Thunell R. C. and Spero H. J. (2020) 220 year diatom  $\delta^{18}\text{O}$  reconstruction of the Guaymas basin thermocline using microfluorination. *Paleoceanography and Paleoclimatology* **35**, e2019PA003749.
- Menicucci A. J., Spero H. J., Matthews J. and Parikh S. J. (2017) Influence of exchangeable oxygen on biogenic silica oxygen isotope data. *Chemical Geology* **466**, 710-721.
- Outrequin C., Alexandre A., Vallet-Coulomb C., Piel C., Devidal S., Landais A., Couapel M., Mazur J.-C., Peugeot C., Pierre M., Prié F., Roy J., Sonzogni C. and Voigt C. (2021) The triple oxygen isotope composition of phytoliths, a new proxy of atmospheric relative humidity: Controls of soil water isotope composition, temperature,  $\text{CO}_2$  concentration and relative humidity. *Climate of the Past* **17**, 1881-1902.
- Piperno D. R. (2006) *Phytoliths: A comprehensive guide for archaeologists and paleoecologists*. Academic Press, San Diego.

- Premathilake R., Akhilesh K., Anupama K., Prasad S., Gunnell Y., Orukaimani G. and Pappu S. (2022) Issues of phytolith taphonomy at palaeolithic sites: Investigation and results from attirampakkam, india. *Journal of Archaeological Science: Reports* **42**, 103357.
- Prentice A. J. and Webb E. A. (2016) The effect of progressive dissolution on the oxygen and silicon isotope composition of opal-a phytoliths: Implications for palaeoenvironmental reconstruction. *Palaeogeography, Palaeoclimatology, Palaeoecology* **453**, 42-51.
- Qi H., Coplen T. B. and Wassenaar L. I. (2011) Improved online  $\delta^{18}\text{O}$  measurements of nitrogen- and sulfur-bearing organic materials and a proposed analytical protocol. *Rapid Communications in Mass Spectrometry* **25**, 2049-2058.
- R Core Team (2021) R: A language and environment for statistical computing. R foundation for statistical computing, vienna, austria. 2012.
- Renée Brooks J., Barnard H. R., Coulombe R. and McDonnell J. J. (2010) Ecohydrologic separation of water between trees and streams in a mediterranean climate. *Nature Geoscience* **3**, 100-104.
- Riding J. B. (2021) A guide to preparation protocols in palynology. *Palynology* **45**, 1-110.
- Rozanski K., Araguás-Araguás L. and Gonfiantini R. (1993) Isotopic patterns in modern global precipitation. In *Climate change in continental isotopic records*. pp. 1-36.
- Schober P., Boer C. and Schwarte L. A. (2018) Correlation coefficients: Appropriate use and interpretation. *Anesthesia & Analgesia* **126**.
- Shahack-Gross R., Shemesh A., Yakir D. and Weiner S. (1996) Oxygen isotopic composition of opaline phytoliths: Potential for terrestrial climatic reconstruction. *Geochimica et Cosmochimica Acta* **60**, 3949-3953.
- Shemesh A., Charles C. D. and Fairbanks R. G. (1992) Oxygen isotopes in biogenic silica: Global changes in ocean temperature and isotopic composition. *Science* **256**, 1434-1436.
- Snelling A. M., Swann G. E. A., Leng M. J. and Pike J. (2012) A micro-manipulation technique for the purification of diatoms for isotope and geochemical analysis. *Silicon* **5**, 13-17.
- Strömberg C. A. E., Dunn R. E., Crifò C. and Harris E. B. (2018) Phytoliths in paleoecology: Analytical considerations, current use, and future directions. In *Methods in paleoecology: Reconstructing cenozoic terrestrial environments and ecological communities* (eds. D. A. Croft, D. F. Su and S. W. Simpson). Springer International Publishing, Cham. pp. 235-287.
- Tang K. and Feng X. (2001) The effect of soil hydrology on the oxygen and hydrogen isotopic compositions of plants' source water. *Earth and Planetary Science Letters* **185**, 355-367.
- Tyler J. J., Sloane H. J., Rickaby R. E. M., Cox E. J. and Leng M. J. (2017) Post-mortem oxygen isotope exchange within cultured diatom silica. *Rapid Communications in Mass Spectrometry* **31**, 1749-1760.
- Urban M. A., Romero I. C., Sivaguru M. and Punyasena S. W. (2018) Nested cell strainers: An alternative method of preparing palynomorphs and charcoal. *Review of Palaeobotany and Palynology* **253**, 101-109.
- Von Freyberg J., Allen S. T., Grossiord C. and Dawson T. E. (2020) Plant and root-zone water isotopes are difficult to measure, explain, and predict: Some practical recommendations for determining plant water sources. *Methods in Ecology and Evolution* **11**, 1352-1367.

- Webb E. A. and Longstaffe F. J. (2000) The oxygen isotopic compositions of silica phytoliths and plant water in grasses: Implications for the study of paleoclimate. *Geochimica et Cosmochimica Acta* **64**, 767-780.
- Webb E. A. and Longstaffe F. J. (2002) Climatic influences on the oxygen isotopic composition of biogenic silica in prairie grass. *Geochimica et Cosmochimica Acta* **66**, 1891-1904.
- Webb E. A. and Longstaffe F. J. (2003) The relationship between phytolith- and plant-water  $\delta^{18}O$  values in grasses. *Geochimica et Cosmochimica Acta* **67**, 1437-1449.
- White A., Sparrow B., Leitch E., Foulkes J., Flitton R., Lowe A. and Caddy-Retalic S. (2012) *Ausplots rangelands survey protocols manual*, V. 1.2.9 ed. The University of Adelaide Press, Adelaide, South Australia.
- Xu T. and Hutchinson M. F. (2013) New developments and applications in the anuclim spatial climatic and bioclimatic modelling package. *Environmental Modelling & Software* **40**, 267-279.

## Chapter 5:

## Conclusion

## Conclusion

In this master's thesis, it has been shown that the oxygen isotope ratios of phytoliths extracted from plants and bulk topsoil can be related to the combined effects of relative humidity on leaf water isotope ratios and temperature on silica-water isotope fractionation. This outcome provides new, promising results of relevance to the previously understudied field of phytolith oxygen isotope ratios as a palaeoclimate proxy (Alexandre et al., 2012; Alexandre et al., 2019; Alexandre et al., 2018; Hodson et al., 2008; Outrequin et al., 2021; Shahack-Gross et al., 1996; Webb and Longstaffe, 2000; Webb and Longstaffe, 2002, 2003; Webb and Longstaffe, 2006). Throughout this master's research it became apparent that not only is not enough known about the processes controlling the oxygen isotope signal being recorded in the phytoliths, but also the methods of extracting and analysing the phytoliths also need more research. Indeed, the difficulty in extracting and analysing the isotopic composition of phytoliths may be part of the reason that there are so few publications.

Chapter two compared and contrasted a number of different extraction methods and confirmed the utility of FTIR, SEM and other methods for quantifying contamination. FTIR analysis and modelling can be used to check for the types of contamination in a sample, which enabled identification of how some contaminants (e.g., organic matter) can impede the removal of other contaminants (e.g., clay). Thus, while the modelling was unable to accurately quantify the amount of contamination, it proved to be a valuable tool for identifying types of contaminants. It was possible to remove the residual organic contamination in phytoliths extracted from soils using Piranha solution (sulfuric acid and hydrogen peroxide solution), which is normally reserved for phytolith extractions from plant material. Then a repeat of the density separation and filtration steps resulted in phytolith samples with the required purity (Chapter 2, 'Chemical 4'). Chapter two also investigated the

use of non-thermal ambient air radio frequency plasma ashing as a method of extracting phytoliths for oxygen isotopes. For fresh plant samples that were ball milled, the phytoliths could successfully be extracted with the purity needed for subsequent oxygen isotope analyses using the plasma ashing.

Chapter three focused on developing a dehydroxylation method that could be completed online, using existing high temperature pyrolysis and elemental analyser equipment coupled to a mass spectrometer, thus avoiding the need for an offline tube furnace dehydroxylation method, which is commonly used but which requires additional peripheral equipment (Chapligin et al. 2010; Menicucci et al. 2013). The new online method resulted in the successful dehydroxylation of reference biogenic silica material of a known composition using a standard TC/EA-IRMS set up. It also showed that the microflourination method of Menicucci et al. (2013), previously used on diatoms, also works on phytoliths. Though analysis takes longer than in the tube dehydroxylation method, the new EAD method makes the analyses of oxygen isotope ratios of biogenic silica such as diatoms and phytoliths more accessible in a standard stable isotope laboratory. The sensitivity of the IRMS used in this study allowed as little as 600 ug (4 replicates of 150 +/- 10%) of biogenic silica to be analysed with precision and accuracy. This will assist in research analysing the oxygen isotopes of biogenic silica extracted from sediments, for which sample size can often be prohibitive. It is hoped that by developing more efficient and cost-effective methods for the extraction and dehydroxylation of biogenic silica, research in the field of oxygen isotopes of phytoliths can expand faster. Using the methods developed here for extracting, dehydroxylating and analysing the oxygen isotope ratios of phytoliths from plants and soils, the central aims of this masters was addressed.



Chapter four was the first study to assess the oxygen isotope ratios of phytoliths from plants and soils at the same location and how the signal in the oxygen isotope ratios is passed from plant to soil. It was expected that phytoliths from different species of grass at the same location would have similar  $\delta^{18}\text{O}$  values to one another because they are growing in the same conditions and there is no known 'vital effect' on the production of phytoliths (Webb and Longstaffe, 2000). However, it was discovered there was large variability of oxygen isotopes from phytoliths in plants of different species growing at the same location. It was also expected that the  $\delta^{18}\text{O}$  values of phytoliths extracted from transpiring tissue would be similar to the  $\delta^{18}\text{O}$  values of phytoliths from the topsoil at the same site, though they would be slightly higher as the soil phytoliths would also have a mix of phytoliths from non-transpiring tissue which have lower  $\delta^{18}\text{O}$  values (Webb and Longstaffe, 2000). The phytoliths from the plants had lower  $\delta^{18}\text{O}$  values than the phytoliths from soils at the same location. Despite this, both the plant and soil phytolith oxygen isotope ratios showed a negative correlation with the relative humidity of the warmest months and with the mean annual temperature (Chapter 4). This signal was stronger in soils than plants, which could be accredited to the short-term variability of the plant phytolith oxygen isotope values and the long-term accumulation of phytoliths in soils.

The oxygen isotope ratios of phytoliths from plants and soils were predicted using Craig-Gordon leaf water modelling and a previously defined, temperature dependent silica-water oxygen isotope fractionation equation (Chapter 4). The modelling was able to predict the oxygen isotopes with a root-mean-square-error of 2.93 for plant phytoliths, and 2.33 for soil phytoliths. This model essentially had 4 variables: oxygen isotope ratios of precipitation, temperature, relative humidity, and a mass balance percentage for the resulting endmembers representing phytoliths from transpiring and non-transpiring tissue (based on the measured phytolith oxygen isotope ratios: 8% from transpiring tissue for plant phytoliths

and 38% for soil phytoliths). If it were to be assumed that the percentage of phytoliths coming from the two endmembers (transpiring vs non-transpiring) are consistent, then there are only three environmental variables that are likely to change. In regard to reconstructing past climates using the oxygen isotope values of phytoliths from sediments, there may be locations where reconstructing these three variables with the aid of phytolith oxygen isotopes is achievable. Long term averages of oxygen isotopes of precipitation can be constrained by isotope analysis of ice cores, speleothems, or ancient wood. Temperature can be inferred from a range of proxies, including tree ring widths, clumped isotopes in carbonates and various organic biomarker tracers Bradley (1999). With these constrained, the relative humidity signal could be isolated to provide either quantitative or qualitative records of the relative humidity of the warmest periods. Originally it was thought that the soils would offer insight into the annual average relative humidity, but a proxy for relative humidity during the warmest period has the potential to be more important in research investigating future climate change.

## Future research

### 1. Extraction methods

During the establishment of a method for extracting phytolith samples with residual contamination to the purity required for oxygen isotope analysis, it became obvious that the chemical 4 treatment (Chapter 2) could be streamlined by rearranging to eliminate duplicated treatment steps (Appendix 1). Time constraints prevented this method from being tested so a trial still needs to be completed.

Plasma ashing shows potential as a useful method for phytolith extraction and needs more research. The suggestions in chapter 2 on how to make the process more efficient need to be tested, such as cooling the airflow to allow for increased power or starting with a low

power and then increasing the power after the bulk of the organic matter has been removed. The next trials should focus on three aspects of phytolith extractions for subsequent oxygen isotope analyses. Firstly, and most importantly for the field of oxygen isotopes of phytoliths, this process should be tested to see if the oxygen isotope ratios of biogenic silica are affected by plasma, since other methods can affect the oxygen isotope ratios (Crespin et al., 2008; Tyler et al., 2017). This has not yet been tested but the absence of alteration of isotope ratios in carbonates treated with plasma ashing is encouraging (Adlan et al., 2020). Secondly, this process should be tested on soils to see if the resistant older organic matter found in soils can be successfully removed. Plasma ashing for the extraction of biogenic silica was only tested on fresh organic matter (Chapter 2), which can be easier to oxidise. For non-biogenic silica, plasma ashing has been used on older organic matter in a set up very different to the one used in this study (Bird et al., 2010). While most of the organic matter was removed, not all was eliminated, which would be an issue for subsequent oxygen isotope analyse (Chapter 2). Thirdly, plasma ashing should be tested on plant material to see if it is possible to separate phytoliths from epidermal layers. Epidermal layers are generally transpiring tissue, it may be a new way to analyse the oxygen isotopes of transpiring vs non transpiring tissue (Alexandre et al., 2018).

## 2. Dehydroxylation

The new method of dehydroxylation, where the dehydroxylation, microflourination and oxygen isotope analyses are all done online in one process offers the potential for the analysis of the weakly bonded, exchangeable oxygen within the silica matrix (Chapter 3). However, the setup used in this laboratory used traps that captured released hydroxyl and water molecules, making the reading imprecise. With alterations to the system, the exchangeable oxygen may be analysed which may assist in our understanding of how laboratory procedures are affecting the oxygen isotope ratios of both molecular and loosely

bound oxygen atoms. This could be done by using laboratory waters of different isotopic composition to test how both the exchangeable and non-exchangeable oxygen is affected by temperature or see if the exchangeable oxygen remains stable over time.

### 3. Phytolith oxygen isotope analysis

Research has become increasingly focused on the oxygen isotopic composition of phytoliths in plants to better understand the complexity of the processes of the isotopic controls (Alexandre et al., 2019; Alexandre et al., 2018; Outrequin et al., 2021). The oxygen isotope ratios of phytoliths in sediments will likely be a low resolution proxy where temperature and relative humidity could only be constrained over longer periods of time as phytoliths are time averaged. Perhaps the research into phytolith oxygen isotope ratio as a proxy for climate should be more focused on the bigger processes at play. A deeper understanding of how the oxygen isotope ratios of phytoliths in different parts of a single leaf is not going to help us understand the proxy record. To date, there are no publications of the oxygen isotope composition of phytoliths from a whole plant, nor are there any showing how the oxygen isotope ratios of phytoliths are transferred from plant to soil. Are the oxygen isotopes of the phytoliths from plants in this study an outlier due to lower than usual oxygen isotope ratios of La Nina effected precipitation, or is the oxygen isotope ratio of phytoliths in plants, on the whole, usually lower than those found in soil due to some process we are not aware of simply because we have not actually compared them before? The amount of research needed in this field at a bigger scale is endless. To start:

Are the oxygen isotope ratios of phytoliths in a whole plant effected by death and diagenesis? A simple greenhouse experiment could be done to test this. Grow 20 annual plants of the same species in controlled conditions. Collect 10 plants, allow the other 10 to die naturally. Extract the phytolith from the two groups in bulk and analyse them in bulk

with a number of replicates. Are the isotope values the same or do the plants that died naturally have a higher value?

Repeat testing of the oxygen isotope ratios of phytoliths from soils and plants from the same locations over a number of years would be helpful to see how much of the isotopic signal is attributed to new influxes of phytoliths and if variation of precipitation oxygen isotope ratios are strong enough to be seen in the soil phytolith signal. It would also indicate if the lower oxygen isotope ratios of phytoliths extracted from plants is an anomaly or not.

As phytoliths transferred from soils can be preserved in sediments, it is expected that their original isotopic composition will also be preserved. The ability to predict the oxygen isotope ratios of phytoliths with modelling indicates that there is enough knowledge to at least start analysing the oxygen isotope ratios of phytoliths from sedimentary deposits and seeing if a change in climate is indeed visible, and with the right location, this may even be quantified.

## Summary

This research presents improvements in the extractions of phytoliths in preparation for oxygen isotope analysis and a new alternative method for the dehydroxylation of biogenic silica which does not rely on additional pieces of equipment beyond those required for isotope analysis. The climate-isotope relationship across a large geographic transect was investigated and it was found that the  $\delta^{18}\text{O}$  values of bulk phytoliths from topsoils reflect the mean annual temperature and relative humidity at the maximum temperature of the warmest period. Quantitative modelling was used predict the oxygen isotope ratios of phytoliths. This thesis represents a significant step in advancing research on phytolith oxygen isotopes in Australia, and comparable environments worldwide.

## References

- Adlan Q., Davies A. J. and John C. M. (2020) Effects of oxygen plasma ashing treatment on carbonate clumped isotopes. *Rapid Commun Mass Spectrom* **34**, e8802.
- Alexandre A., Crespin J., Sylvestre F., Sonzogni C. and Hilbert D. W. (2012) The oxygen isotopic composition of phytolith assemblages from tropical rainforest soil tops (Queensland, Australia): validation of a new paleoenvironmental tool. *Clim Past* **8**, 307-324.
- Alexandre A., Webb E., Landais A., Piel C., Devidal S., Sonzogni C., Couapel M., Mazur J.-C., Pierre M., Prié F., Vallet-Coulomb C., Outrequin C. and Roy J. (2019) Effects of leaf length and development stage on the triple oxygen isotope signature of grass leaf water and phytoliths: insights for a proxy of continental atmospheric humidity. *Biogeosciences* **16**, 4613-4625.
- Alexandre A., Landais A., Vallet-Coulomb C., Piel C., Devidal S., Pauchet S., Sonzogni C., Couapel M., Pasturel M., Cornuault P., Xin J., Mazur J.-C., Prié F., Bentaleb I., Webb E., Chalié F. and Roy J. (2018) The triple oxygen isotope composition of phytoliths as a proxy of continental atmospheric humidity: insights from climate chamber and climate transect calibrations. *Biogeosciences* **15**, 3223-3241.
- Bird M. I., Charville-Mort P. D. J., Ascough P. L., Wood R., Higham T. and Apperley D. (2010) Assessment of oxygen plasma ashing as a pre-treatment for radiocarbon dating. *Quat Geochronol* **5**, 435-442.
- Bradley R. S. (1999) *Paleoclimatology: reconstructing climates of the Quaternary*. Elsevier.
- Crespin J., Alexandre A., Sylvestre F., Sonzogni C., Paillès C. and Garreta V. (2008) IR Laser Extraction Technique Applied to Oxygen Isotope Analysis of Small Biogenic Silica Samples. *Analytical Chemistry* **80**, 2372-2378.
- Hodson M. J., Parker A. G., Leng M. J. and Sloane H. J. (2008) Silicon, oxygen and carbon isotope composition of wheat (*Triticum aestivum* L.) phytoliths: implications for palaeoecology and archaeology. *J Quaternary Sci* **23**, 331-339.
- Menicucci A. J., Matthews J. A. and Spero H. J. (2013) Oxygen isotope analyses of biogenic opal and quartz using a novel microfluorination technique. *Rapid Communications in Mass Spectrometry* **27**, 1873-1881.
- Outrequin C., Alexandre A., Vallet-Coulomb C., Piel C., Devidal S., Landais A., Couapel M., Mazur J.-C., Peugeot C., Pierre M., Prié F., Roy J., Sonzogni C. and Voigt C. (2021) The triple oxygen isotope composition of phytoliths, a new proxy of atmospheric relative humidity: controls of soil water isotope composition, temperature, CO<sub>2</sub> concentration and relative humidity. *Clim Past* **17**, 1881-1902.
- Shahack-Gross R., Shemesh A., Yakir D. and Weiner S. (1996) Oxygen isotopic composition of opaline phytoliths: Potential for terrestrial climatic reconstruction. *Geochim Cosmochim Acta* **60**, 3949-3953.
- Tyler J. J., Sloane H. J., Rickaby R. E. M., Cox E. J. and Leng M. J. (2017) Post-mortem oxygen isotope exchange within cultured diatom silica. *Rapid Communications in Mass Spectrometry* **31**, 1749-1760.
- Webb E. A. and Longstaffe F. J. (2000) The oxygen isotopic compositions of silica phytoliths and plant water in grasses: implications for the study of paleoclimate. *Geochim Cosmochim Acta* **64**, 767-780.
- Webb E. A. and Longstaffe F. J. (2002) Climatic influences on the oxygen isotopic composition of biogenic silica in prairie grass. *Geochim Cosmochim Acta* **66**, 1891-1904.
- Webb E. A. and Longstaffe F. J. (2003) The relationship between phytolith- and plant-water  $\delta^{18}\text{O}$  values in grasses. *Geochim Cosmochim Acta* **67**, 1437-1449.
- Webb E. A. and Longstaffe F. J. (2006) Identifying the  $\delta^{18}\text{O}$  signature of precipitation in grass cellulose and phytoliths: Refining the paleoclimate model. *Geochim Cosmochim Acta* **70**, 2417-2426.

# Appendix 1

Supplementary for Chapter 2: Phytolith extraction  
for oxygen isotope analysis: Method development

## HAZARD MANAGEMENT – SAFE OPERATING PROCEDURE (SOP)


**Only to be completed where required as a control measure under a Risk Assessment**

<p>A document setting out the requirements to carry out the work in a safe and healthy manner and in a logical sequence.</p> <p>It must be able to be easily read by those who need to know what has been planned.</p> <p>It is relevant to the following people:</p> <ul style="list-style-type: none"> <li>the worker carrying out the work; and</li> <li>the person who has management and control over the work.</li> </ul>	<p>A SOP, if identified as a control measure, is to:</p> <ul style="list-style-type: none"> <li>identify the work;</li> <li>specify/address the identified hazards relating to the work;</li> <li>describe the measures to be implemented to control the risks;</li> <li>take into account the circumstances at the workplace that may affect the way in which the work is carried out;</li> <li>take into account emergency management arrangements where applicable; and</li> <li>be communicated to all workers who carry out the work.</li> </ul>
---	---






<b>NAME OF THE TASK/ACTIVITY</b>	<b>WET DIGESTION OF PLANT LEAVES USING PIRANHA SOLUTION AND HCL</b>	<b>DATE:</b> 11\01\2023
<b>LOCATION</b>	MAWSON LABORATORIES, ROOM G34A	
<b>RISK ASSESSMENT (RA) NAME</b>		
<b>Residual risk rating on the RA</b>	<input type="checkbox"/> Low <input checked="" type="checkbox"/> Medium <input type="checkbox"/> High <input type="checkbox"/> Very High	
<b>Hazards identified on the RA</b>	<p><b>Equipment:</b> Hot plate, centrifuge, glass</p> <p><b>Chemicals:</b> Piranha Solution (Sulfuric acid (H<sub>2</sub>SO<sub>4</sub>) and Hydrogen peroxide (H<sub>2</sub>O<sub>2</sub> 30%))</p> <div style="text-align: center;">  </div> <p><b>Signal word;</b> <b>DANGER</b></p> <p><b>Hazard statements:</b>                      H331 Toxic if inhaled.                      H314 Causes severe skin burns and eye damage.                      H350 May cause cancer.                      H272 May intensify fire; oxidiser.</p> <p><b>Precautionary statement(s) Prevention</b>                      P201 Obtain special instructions before use.                      P210 Keep away from heat, hot surfaces, sparks, open flames and other ignition sources. No smoking.                      P260 Do not breathe mist/vapours/spray.                      P271 Use only outdoors or in a well-ventilated area.</p> <p><b>Precautionary statement(s) Response</b>                      P301+P330+P331 <b>IF SWALLOWED:</b> Rinse mouth. Do NOT induce vomiting.                      P303+P361+P353 <b>IF ON SKIN (or hair):</b> Take off immediately all contaminated clothing. Rinse skin with water [or shower].                      P305+P351+P338 <b>IF IN EYES:</b> Rinse cautiously with water for several minutes. Remove contact lenses, if present and easy to do. Continue rinsing.                      P308+P313 <b>IF exposed or concerned:</b> Get medical advice/attention.</p> <p><b>Precautionary statement(s) Storage</b></p>	

HSW Handbook	Hazard Management	Effective Date:	1 December 2020	Version 4.0
Authorised by	Chief Operating Officer (University Operations)	Review Date:	1 December 2023	Page 1 of 7
Warning	This process is uncontrolled when printed. The current version of this document is available on the HSW Website.			



	<p><b>P403+P233</b> Store in a well-ventilated place. Keep container tightly closed.  <b>P405</b> Store locked up.</p> <p><b>Precautionary statement(s) Disposal</b>  <b>P501</b> Dispose of contents/container to authorised hazardous or special waste collection point in accordance with any local regulation.</p> <p><b>Hydrochloric acid ( HCl 10%)</b></p> <div style="text-align: center;">  </div> <p><b>Hazard statements:</b>  <b>H331</b> Toxic if inhaled.  <b>H314</b> Causes severe skin burns and eye damage.  <b>H302</b> Harmful if swallowed.  <b>H413</b> May cause long lasting harmful effects to aquatic life.</p> <p><b>Precautionary statement(s) Prevention</b>  <b>P260</b> Do not breathe mist/vapours/spray.  <b>P271</b> Use only outdoors or in a well-ventilated area.  <b>P280</b> Wear protective gloves, protective clothing, eye protection and face protection.  <b>P270</b> Do not eat, drink or smoke when using this product.</p> <p><b>Precautionary statement(s) Response</b>  <b>P301+P330+P331 IF SWALLOWED:</b> Rinse mouth. Do NOT induce vomiting.  <b>P303+P361+P353 IF ON SKIN (or hair):</b> Take off immediately all contaminated clothing. Rinse skin with water [or shower].  <b>P305+P351+P338 IF IN EYES:</b> Rinse cautiously with water for several minutes. Remove contact lenses, if present and easy to do. Continue rinsing.  <b>P310</b> immediately call a POISON CENTER/doctor/physician/first aider.</p> <p><b>Precautionary statement(s) Storage</b>  <b>P403+P233</b> Store in a well-ventilated place. Keep container tightly closed.  <b>P405</b> Store locked up.</p> <p><b>Precautionary statement(s) Disposal</b>  <b>P501</b> Dispose of contents/container to authorised hazardous or special waste collection point in accordance with any local regulation.</p>	
--	---	--

HSW Handbook	Hazard Management	Effective Date:	1 December 2020	Version 4.0
Authorised by	Chief Operating Officer (University Operations)	Review Date:	1 December 2023	Page 2 of 7
Warning	This process is uncontrolled when printed. The current version of this document is available on the HSW Website.			

PERSONAL PROTECTIVE EQUIPMENT (BE SPECIFIC AND SPECIFY PPE TO BE WORN DURING THE TASK) (DELETE THE ROW IF NOT APPLICABLE)	
	Eye protection: <input checked="" type="checkbox"/> Safety glasses <input type="checkbox"/> Eye shields <input type="checkbox"/> Safety goggles <input type="checkbox"/> Other: Safety glasses with unperforated side shields must be worn, even if wearing spectacles.
	Face protection: <input type="checkbox"/> Dust goggles <input checked="" type="checkbox"/> Face shield <input type="checkbox"/> Visor <input type="checkbox"/> Face mask <input type="checkbox"/> Dust mask <input type="checkbox"/> Other: Face shield must be worn if fume hood sash is not down as a barrier between solution and face
	Hand protection: <input type="checkbox"/> Rubber <input type="checkbox"/> Cut resistant <input type="checkbox"/> Leather <input type="checkbox"/> Vinyl <input checked="" type="checkbox"/> Neoprene <input type="checkbox"/> Nitrile <input type="checkbox"/> Barrier creams <input type="checkbox"/> Other: Elbow length neoprene gloves in good condition.
	<input checked="" type="checkbox"/> Enclosed footwear: <input checked="" type="checkbox"/> Footwear that is resistant to spills of hazardous substances <input type="checkbox"/> Boots with steel caps <input type="checkbox"/> Other:
	Protective clothing: <input checked="" type="checkbox"/> Lab coat <input type="checkbox"/> Gown <input type="checkbox"/> Long sleeves <input checked="" type="checkbox"/> Long pants <input type="checkbox"/> High visibility <input type="checkbox"/> Helmet <input type="checkbox"/> Sun protection <input checked="" type="checkbox"/> Other: PVC apron over lab coat. Long pants or overalls must be worn outside of boots
DESCRIBE, IN SEQUENCE, STEPS TO COMPLETE THE ACTIVITY SAFELY	
<p><b>Pre-operational checks</b></p> <p><b>Equipment</b></p> <ul style="list-style-type: none"> <li>• Hot plate</li> <li>• Centrifuge</li> <li>• Fume cupboard</li> <li>• Glass beakers</li> <li>• Glass pipette</li> <li>• Glass stirrer</li> <li>• 50ml Centrifuge tubes</li> <li>• Large waste container</li> </ul> <p><b>Reagents and chemicals</b></p> <ul style="list-style-type: none"> <li>• Sodium hexametaphosphate</li> <li>• Sodium polytungstate (SPT) at 2.38 g cm<sup>-3</sup>, 2.34 g cm<sup>-3</sup>, 2.30 g cm<sup>-3</sup>, 2.20 g cm<sup>-3</sup></li> <li>• Sulfuric acid (100%)</li> <li>• Hydrogen peroxide (30%)</li> <li>• Hydrochloric acid (10%)</li> <li>• Ice</li> <li>• Lime (Sodium hydroxide)</li> </ul> <p><b>Operational checks/steps to complete the activity from start to finish (including transport and waste disposal where relevant)</b></p> <p style="text-align: center;"><b><u>Stage 1: Sample preparation – sediment</u></b></p> <ol style="list-style-type: none"> <li>1. Lightly crush soil - tap, do not grind.</li> <li>2. Wet sieve using 2mm sieve and Milli-Q (MQ) water.</li> <li>3. Dry samples (air or freeze dry. Or oven at max temp of 50 degrees)</li> <li>4. Add at least 5 g of soil to 50ml test tube labelled with appropriate information on both side of tube and on the lid. Printed label stuck on with clear tape works best for the side. Sharpie is fine for the lid.</li> </ol> <p style="text-align: center;"><b><u>Stage 2: Removal of carbonates</u></b></p> <ol style="list-style-type: none"> <li>5. Add 10-12ml of HCl (5%) to each sample and leave overnight.</li> <li>6. Pipette liquid to waste beaker, empty beaker into appropriate waste container.</li> <li>7. Add 10 ml of MQ water and centrifuge (2000 rpm, 5 mins, brake 0), remove water and repeat two more times.</li> </ol> <p style="text-align: center;"><b><u>Stage 3: Deflocculant and gravity sedimentation</u></b></p> <ol style="list-style-type: none"> <li>8. Add sodium hexametaphosphate (5%) buffered at pH 7 to test tube. Shake well to mix. Leave for 5 day (Can be overnight, but 5 days is optimum and shortens the number of times you need to do the next step). Pipette off solution.</li> <li>9. Top up test tube with MQ water, shake and centrifuge at 2000 rpm, 5 mins, brake 0, remove water with pipette and repeat two more times.</li> <li>10. Sieve through a 250 µm sieve into a labelled beaker using MQ water in a squeeze bottle. Let sample settle for 1 hour and then slowly pour off top half of the liquid. Repeat until supernatant is clear</li> <li>11. Label 15 ml centrifuge tubes with sample name and the letter "A"</li> <li>12. Transfer samples to labelled centrifuge tubes (2000 rpm, 5 mins, brake 0) and remove as much liquid as possible with a pipette.</li> </ol>	

HSW Handbook	Hazard Management	Effective Date:	1 December 2020	Version 4.0
Authorised by	Chief Operating Officer (University Operations)	Review Date:	1 December 2023	Page 3 of 7
Warning	This process is uncontrolled when printed. The current version of this document is available on the HSW Website.			

#### Stage 4: Heavy liquid separation (initial)

13. Add 4 ml of 2.38 g cm<sup>-3</sup> SPT to samples and shake to combine well.
14. Centrifuge samples (2500 rpm, 20 mins, brake 0).
15. Phytolith will be at the top of the liquid. Add a little bit of MQ water. Use a new pipette for each sample, suck up the water and a little bit of the SPT. Put this in a new test tube labelled appropriately, these test tubes need "B".
16. Add MQ water to the original test tube ("A") and remove most of the liquid to SPT waste.
17. Repeat the previous 4 steps on the original test tube ("A").
18. Add 5 ml MQ water to the original test tube and shake, then (2000 rpm, 5 mins, brake 0). Syphon liquid to SPT waste
19. Add 10 ml water to original test tube, shake and centrifuge (2000 rpm, 5 mins, brake 0). Syphon liquid down sink and archive the test tube.
20. Add MQ water up to the 12 ml line on the new test tube ("B") and shake, centrifuge (2000 rpm, 5 mins, brake 0). Syphon liquid into SPT waste
21. Repeat steps 15-23 with the new test tube, this time using 2.34 g cm<sup>-3</sup> SPT (Labelled "C"), and then 2.30 (into 50 ml centrifuge tube Labelled "D").
22. Rinse final tube ("D") sample 3 times with centrifuge (2000 rpm, 5 mins, brake 0) and MQ water.
23. Freeze-dry sample

#### Stage 5: Piranha solution to remove organic matter.

- **IMPORTANT:**
- **The following steps must be completed in a fume cupboard.**
- **Smaller batches are recommended to decrease the risk of explosion in case of a large spill.**
- **Never have both Sulfuric acid and hydrogen peroxide bottles in the fume cupboard at the same time.**
- **Lower the fume cupboard sash as low as practical to avoid fumes or splashes.**
- **Wear a face shield if you cannot lower sash enough to protect face.**
- **DO NOT use paper towel to clean up spills as it can combust – flush with water.**

24. Ensure full spill kit is nearby and locate emergency shower in case of large spills.
25. Place plant or material into GLASS beaker
26. Carefully pour sulfuric acid (100%) into beaker until sample material is covered.
27. Heat to 70 degrees and let it sit until only black sludge remains – approximately 2 to 4 hours. Do not leave unattended while heat is on.
28. Cool to room temperature (overnight is fine).
29. Ensure sulfuric acid bottle and any other containers of organic compounds (e.g. acetone) are removed from fume cupboard.
30. Put warning sign on fume cupboard "DANGER – Sulfuric Acid + Hydrogen Peroxide SOLUTION (a.k.a. Piranha Solution) – CORROSIVE AND EXPLOSIVE HAZARD – DO NOT USE" along with contact details of person responsible.
31. Inform supervisor(s), other lab users and lab managers (if relevant) that you are carrying out this procedure, specifying when you will be finished.
32. Once sulfuric acid bottle has been taken away and sign is on fume cupboard, bring hydrogen peroxide to fume cupboard.
33. **Very slowly** add 30% hydrogen peroxide with a pipette, stirring solution with a glass stirrer between additions. Solution will bubble and get very hot (over 100°C). Wait until bubbling has stopped before adding more Hydrogen peroxide. Continue to slowly add hydrogen peroxide until liquid becomes clear and colourless (solution should have a ratio of hydrogen peroxide to sulfuric acid of less than 1/3, never go more than 1/2 or an explosion can occur).
34. Once clear and no longer bubbling, Heat to 70 degrees and allow to sit for 2 hours. Do not leave unattended while heat is on. Stirring occasionally with glass stirrer or glass pipette.
35. Allow to sit for one hour without stirring. Do not leave unattended while heat is on. If the reaction appears to be too vigorous, turn off the heat and close the fume hood sash. If it is safe to do so, transfer the beakers from the hotplate into a Pyrex tray to cool down. If samples bubble over, advise other users to stay clear and discuss cleanup strategy with supervisor(s).
36. Remove from heat, transfer beakers into a Pyrex tray, cover each beaker with a watch glass ensuring gases can escape and allow to sit for 24 hours.
37. Decant supernatant reagent slowly into a large waste beaker using a glass pipette, ensuring sample remains in the bottom of the beaker.
38. Transfer residual samples to 50ml centrifuge tubes, rinse beakers with Milli Q water into the centrifuge tubes.
39. Fill centrifuge tube with MQ water and centrifuge at 2000 rpm, 5 mins, brake 0. Remove supernatant to waste. Rinse three times.
40. Let removed waste solution sit in fume cupboard for a further 24 hours in an open container.

#### Stage 6: HCl to remove carbonate residue.

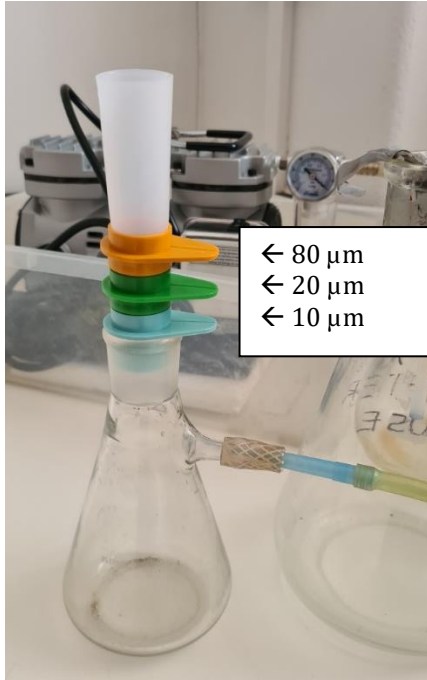
41. To the sample, add 10-12ml of HCl, shake and centrifuge at 2000 rpm, 5 mins, brake 0. Pipette HCl to a clean waste beaker.
42. Centrifuge with MQ water at 2000 rpm, 5 mins, brake 0. Pipette supernatant liquid to the HCl waste beaker, retaining sample pellet at the bottom of the tube. Repeat three times.
43. Dispose of waste beaker contents to HCl waste container.

#### Stage 7: Nested filtration

44. Connect 10 µm, 20 µm, 80 µm cell strainers and funnel together and sit on filtration flask connected to vacuum trap and vacuum pump. Pour sample into the funnel and turn on vacuum pump. Once liquid has been drawn out, fill the funnel with MQ water from a squeeze bottle

HSW Handbook	Hazard Management	Effective Date:	1 December 2020	Version 4.0
Authorised by	Chief Operating Officer (University Operations)	Review Date:	1 December 2023	Page 4 of 7
Warning	This process is uncontrolled when printed. The current version of this document is available on the HSW Website.			

ensuring phytoliths are agitated and float up into the water. Repeat this at least 5 times. If there are a lot of phytoliths, you may want to remove the 85 µm cell strainer and repeat the rinse on the smaller fractions to ensure any clay particles can get through before the phytoliths block all the holes.



45. Once sample has been filtered, back flush each filter into the same labelled 50 ml centrifuge tubes (e.g., combine the three fractions back together). The 3 different size filters prevent the smaller sized filters clogging up and trapping the fine clay particles)
46. Put each cell strainer upside down on to the flask and use filtration system to back flush each of the cell strainers to make sure there are no phytoliths left. Mark the strainers with a permanent marker. We reuse the smaller strainers maximum 5 times.
47. Freeze dry sample.

#### Stage 7: Heavy liquid separation (Final)

48. Add 4 ml of 2.30 g cm<sup>-3</sup> SPT to samples and shake to combine well.
49. Centrifuge samples (2500 rpm, 20 mins, break 0).
50. Phytoliths will be at the top of the liquid. Add a little bit of MQ water. Use a new pipette for each sample, suck up the water and a little bit of the SPT. Put this in a new test tube labelled appropriately, these test tubes need "E".
51. Add MQ water to the original test tube ("D") and remove most of the liquid to SPT waste.
52. Repeat the previous 4 steps on the original test tube ("D").
53. Add 5 ml MQ water to the original test tube and shake, then (2000 rpm, 5 mins, brake 0). Syphon liquid to SPT waste
54. Add 10 ml water to original test tube, shake and centrifuge (2000 rpm, 5 mins, brake 0). Syphon liquid down sink and archive the test tube.
55. Add MQ water up to the 12 ml line on the new test tube ("E") and shake, centrifuge (2000 rpm, 5 mins, brake 0). Syphon liquid into SPT waste.
56. Rinse final tube ("E") sample 3 times with centrifuge (2000 rpm, 5 mins, brake 0) and MQ water.

#### Stage 8: Store

57. Having removed supernatant water from final sample, freeze dry sample.
58. It is now read for any contamination tests and oxygen isotope analysis

#### Stage 9: Waste neutralization

59. After waste beaker with Piranha solution has sat for 24 hours, it is ready to be neutralized. Get another large container and put 5 times the volume of ice in it. If ice is not available, add 10 times the volume of cold water instead.
60. Put on full PPE.
61. Pour waste solution over ice or into water.
62. Slowly add sodium hydroxide to waste solution in small batches until pH reaches 8
63. Pour neutralized solution into labelled waste container.
64. Remove warning sign from fume cupboard.

HSW Handbook	Hazard Management	Effective Date:	1 December 2020	Version 4.0
Authorised by	Chief Operating Officer (University Operations)	Review Date:	1 December 2023	Page 5 of 7
Warning	This process is uncontrolled when printed. The current version of this document is available on the HSW Website.			

On completion of work – steps to make safe (including clean up, any waste disposal & service/maintenance requirements)

Waste-

- Piranha solution – leave in a large open beaker for 24 hours in fume cupboard then put in glass waste bottle labelled according to regulations with a ventilated lid. Only pipette a drop into bottle first, if no reaction then pour in.
- HCl - waste container banded and labelled according to regulations.
- Waste containers must be disposed of at chemical facility when full.
- Empty chemical containers need to be cleaned and rinsed 3-4 times before going out for recycling and label either needs to be removed or covered.
- Broken glassware or containers need to be placed into broken glassware container and sealed.

Emergency and Spill Procedures, Transport or storage requirements (where relevant), First aid/Medical

Spills inside fume cupboards

- Small spills (less than 100 ml) within the fume hood must be thoroughly flushed with water into the sink.
- Large spills (more than 100 ml) neutralize acid with the spill kit. Transfer precipitates to a plastic container using plastic scoop and scraper and then flush using water from a plastic jug, Arrange appropriate disposal of the container, plastic scoop and scraper as hazards waste.
- In both cases, alert supervisor(s) and lab managers.

Spills outside the fume cupboard

- Small spills (less than 500ml) – if you have not been exposed then treat with spill kit
- Large spills (more than 500ml) – Restrict access to the area and evacuate the laboratory. Call emergency services – fire on (0) 000
- In both cases, alert supervisor (s) and lab managers.

**First aid/Medical**

Eye contact:

- Immediately hold eyelids apart and flush the eye continuously with running water. Ensure complete irrigation of the eye by keeping eyelids apart and away from eye and moving the eyelids by occasionally lifting the upper and lower lids.
- Continue flushing until advised to stop by the Poisons Information Centre or a doctor, or for at least 15 minutes.
- Transport to hospital or doctor without delay.
- Removal of contact lenses after an eye injury should only be undertaken by skilled personnel.

Skin contact:

- Immediately flush body and clothes with large amounts of water, using safety shower if available.
- Quickly remove all contaminated clothing, including footwear.
- Wash skin and hair with running water. Continue flushing with water until advised to stop by the Poisons Information Centre.
- Transport to hospital, or doctor.

Inhalation:

- If fumes or combustion products are inhaled remove from contaminated area.
- Lay patient down. Keep warm and rested.
- Prosthesis such as false teeth, which may block airway, should be removed, where possible, prior to initiating first aid procedures.
- Apply artificial respiration if not breathing, preferably with a demand valve resuscitator, bag-valve mask device, or pocket mask as trained. Perform CPR if necessary.
- Transport to hospital, or doctor, without delay.
- Inhalation of vapours or aerosols (mists, fumes) may cause lung oedema.
- Corrosive substances may cause lung damage (e.g. lung oedema, fluid in the lungs).
- As this reaction may be delayed up to 24 hours after exposure, affected individuals need complete rest (preferably in semi-recumbent posture) and must be kept under medical observation even if no symptoms are (yet) manifested.
- Before any such manifestation, the administration of a spray containing a dexamethasone derivative or beclomethasone derivative may be considered.

**This must definitely be left to a doctor or person authorised by him/her.**

Ingestion:

- For advice, contact a Poisons Information Centre or a doctor at once.
- Urgent hospital treatment is likely to be needed.
- **If swallowed do NOT induce vomiting.**
- If vomiting occurs, lean patient forward or place on left side (head-down position, if possible) to maintain open airway and prevent aspiration.
- Observe the patient carefully.
- Never give liquid to a person showing signs of being sleepy or with reduced awareness; i.e. becoming unconscious.

HSW Handbook	Hazard Management	Effective Date:	1 December 2020	Version 4.0
Authorised by	Chief Operating Officer (University Operations)	Review Date:	1 December 2023	Page 6 of 7
Warning	This process is uncontrolled when printed. The current version of this document is available on the HSW Website.			

- Give water to rinse out mouth, then provide liquid slowly and as much as casualty can comfortably drink.
- Transport to hospital or doctor without delay.

**Prepared by**

People involved in the drafting of this SOP: Kimberley Edwards, Francesca McInerney, Jonathan Tyler, Alexander Francke

Person authorising the SOP

Name: Jonathan Tyler

Signature

Position: Senior Lecturer, lab area supervisor

**This SOP must be reviewed after any incident/injury associated with this activity or when a Risk assessment is reviewed.**

File your completed SOP as instructed by the Supervisor/Person in control of the area/activity and retain the SOP in accordance with the State Records of SA, General disposal [Schedule](#) No. 30 issued under the State Records Act 1997. (Contact the University's [Records Management Office](#) for further assistance/information if required.)

HSW Handbook	Hazard Management	Effective Date:	1 December 2020	Version 4.0
Authorised by	Chief Operating Officer (University Operations)	Review Date:	1 December 2023	Page 7 of 7
Warning	This process is uncontrolled when printed. The current version of this document is available on the HSW Website.			

## Appendix 2

Supplementary for Chapter 3: Phytolith extraction  
for oxygen isotope analysis: Method development

Supplementary information and data

## S.2 Preliminary testing of EA tube dehydroxylation

Variations of method included:

- Different sample weights (100  $\mu\text{g}$  – 1000  $\mu\text{g}$ )
- Teflon + graphite mix weight (1000-4000  $\mu\text{g}$ )
- Using Teflon alone instead of the Teflon mixed with graphite
- Mixing graphite in with the sample.

Results:

- Different variations of sample weight (100  $\mu\text{g}$  – 1000  $\mu\text{g}$ )
  - 100  $\mu\text{g}$  – frequently got  $\delta^{18}\text{O}$  values that were too low and peak areas (indicative of the how much sample was being reacted) too small. 150 - 400 got the same results, more than 200  $\mu\text{g}$  of sample needed extra drops of Teflon to clear the column of biogenic silica. 1000  $\mu\text{g}$  needed 20 Teflon drops to stop getting a signal.
- Teflon + graphite mix weight (1-4mg)
  - Similar results, occasionally the signal from 1 mg was very small, 1.5-4 mg showed no increase in accuracy or precision. 2 mg was chosen as that was the easiest amount to weigh out using the spatula we had.
- Using Teflon alone instead of the Teflon mixed with graphite.
  - Worked well in a freshly packed column, but after a few days the signal decreased, adding graphite to the sample or to the Teflon both improved the signal. Premixing the Teflon and graphite to add after the sample was dehydroxylated was deemed the most efficient way to proceed.
- Mixing graphite in with the sample.
  - Helped get a better signal when using just Teflon, especially when the sample was 100  $\mu\text{g}$ . Made no noticeable different when using Teflon + graphite mix.



### S.3 Individual analysis results for reference material

Reference material	$\delta^{18}\text{O}$ values								Mean	SD	SE	Number of replicates
BFC	29.0	29.0	29.0	28.9	29.2	28.9	29.2	28.8	28.9	0.3	0.1	22
	28.9	28.4	29.0	29.4	28.8	29.1	28.7	28.8				
	28.9	28.5	28.7	29.0	28.5	28.5						
G95	36.3	35.9	36.9	36.9	37.3				36.7	0.5	0.2	5
NBS28	9.4	10.1	10.0	9.5	10.2	9.9	9.7	9.3	9.6	0.3	0.1	23
	10.1	9.2	9.6	9.4	9.9	9.6	9.6	9.4				
	9.4	10.0	9.6	9.2	9.4	9.3	9.6					

## Appendix 3

Supplementary for Chapter 4: Oxygen isotope ratios of phytoliths from modern grasses and soil along a latitudinal transect of Australia and their correlation with climate

Supplementary data and figures

#### S.4 Temperature (T) data used in Chapter 4

Site	annual mean T (1960-2014)	1 month mean maximum T	3 month mean maximum T	6 month mean maximum T	Annual mean maximum T (1 year before collection)	Annual mean maximum T (2 years before collection)	Annual mean maximum T (5 years before collection)	Warmest period mean maximum T (1 year before collection)	Warmest period mean maximum T (2 year before collection)	Warmest period mean maximum T (5 year before collection)
NTADAC0001	26.5	32.5	32.5	32.9	32.6	32.3	32.4	33.3	33.1	32.2
NTAGFU0031	27.3	28.5	30.1	32.6	33.4	33.1	33.8	35.7	34.8	34.9
NTAGFU0040	27.7	29.9	30.5	32.8	34.0	33.6	34.3	36.3	35.3	35.2
NTAGFU0017	25.6	30.3	31.9	33.5	31.9	31.7	32.3	35.1	34.3	34.5
NTAGFU0010	25.7	31.2	33.1	34.4	32.3	32.1	32.7	36.0	35.0	35.3
NTAGFU0008	25.5	33.7	34.8	35.4	32.1	31.8	32.5	36.7	35.6	35.9
NTAGFU0001	25.7	33.5	35.5	35.8	32.3	32.0	32.8	37.0	35.9	36.1
NTABRT0004	22.7	37.8	35.8	32.5	30.1	29.3	30.4	36.4	36.2	36.6
NTAFIN0019	21.9	33.1	31.2	26.8	29.3	28.5	29.7	36.5	36.3	36.7
NTAFIN0022	21.7	32.4	31.6	27.3	29.2	28.4	29.6	36.2	36.0	36.7
SAASTP0004	22.7	20.2	24.6	30.1	29.9	29.0	29.8	37.4	37.5	37.5
SAASTP0001	22.2	19.9	25.0	30.1	29.5	28.6	29.4	36.9	37.1	37.1
SATFLB0005	16.0	16.2	15.5	20.6	24.6	24.1	24.6	32.1	32.5	33.0
SATFLB0008	15.1	15.3	14.5	19.3	23.3	22.8	23.3	30.4	30.9	31.3
SATFLB0010	17.3	15.9	15.4	19.8	23.6	23.2	23.8	30.2	30.6	31.1
SATFLB0014	14.0	24.3	20.3	16.3	20.5	20.5	20.7	27.6	27.8	28.5

Site	annual mean T (1960-2014)	1 month mean maximum T	3 month mean maximum T	6 month mean maximum T	Annual mean maximum T (1 year before collection)	Annual mean maximum T (2 years before collection)	Annual mean maximum T (5 years before collection)	Warmest period mean maximum T (1 year before collection)	Warmest period mean maximum T (2 year before collection)	Warmest period mean maximum T (5 year before collection)
<b>SATFLB0012</b>	15.8	23.4	19.4	16.6	20.8	20.8	21.2	27.5	27.4	28.0
<b>SATFLB0015</b>	13.7	21.8	17.9	14.6	18.5	18.5	18.8	25.1	25.1	25.6
<b>SATKAN0002</b>	14.1	12.5	12.5	16.6	19.1	18.6	19.3	24.7	24.5	25.1
<b>SATKAN0001</b>	14.0	12.5	12.6	16.3	18.1	17.6	18.0	22.8	22.6	23.0

#### S.5 Relative humidity (RH) data used in Chapter 4. (T – temperature)

Site	annual mean RH (1960-2014)	1 month mean RH at max T	3 month mean RH at max T	6 month mean RH at max T	Annual mean RH at max T (1 year before collection)	Annual mean RH at max T (2 years before collection)	Annual mean RH at max T (5 years before collection)	Annual mean RH at max T (1976-2013)	Warmest period mean RH at max T (1 year before collection)	Warmest period mean RH at max T (2 year before collection)	Warmest period mean RH at max T (5 year before collection)	Warmest period mean RH at max T (1976-2013)
<b>NTADAC0001</b>	78	49	55	57	48	48	49	51	59	59	63	64
<b>NTAGFU0031</b>	76	34	42	47	44	45	43	45	49	52	53	53
<b>NTAGFU0040</b>	73	30	37	43	41	42	41	41	47	51	52	50
<b>NTAGFU0017</b>	71	42	48	47	40	41	38	38	47	51	51	49
<b>NTAGFU0010</b>	69	39	44	43	37	38	35	34	42	47	47	45
<b>NTAGFU0008</b>	66	32	38	38	32	34	31	30	36	42	41	39

Site	annual mean RH (1960-2014)	1 month mean RH at max T	3 month mean RH at max T	6 month mean RH at max T	Annual mean RH at max T (1 year before collection)	Annual mean RH at max T (2 years before collection)	Annual mean RH at max T (5 years before collection)	Annual mean RH at max T (1976-2013)	Warmest period mean RH at max T (1 year before collection)	Warmest period mean RH at max T (2 year before collection)	Warmest period mean RH at max T (5 year before collection)	Warmest period mean RH at max T (1976-2013)
<b>NTAGFU0001</b>	65	39	37	37	32	34	31	30	36	41	41	39
<b>NTABRT0004</b>	60	22	25	21	29	32	26	25	30	31	27	26
<b>NTAFIN0019</b>	62	28	24	27	29	32	26	25	29	27	24	22
<b>NTAFIN0022</b>	62	25	23	27	30	32	26	25	28	28	24	22
<b>SAASTP0004</b>	60	34	29	27	26	30	27	25	20	23	22	21
<b>SAASTP0001</b>	60	35	29	27	27	31	27	25	21	23	22	21
<b>SATFLB0005</b>	68	41	45	40	33	36	34	34	26	27	24	24
<b>SATFLB0008</b>	73	47	51	44	37	40	38	38	29	30	28	28
<b>SATFLB0010</b>	74	51	54	48	41	43	41	41	34	35	32	31
<b>SATFLB0014</b>	77	30	39	51	45	46	46	45	34	36	32	32
<b>SATFLB0012</b>	77	35	45	54	47	49	47	48	37	38	35	36
<b>SATFLB0015</b>	80	38	48	59	52	54	53	52	41	43	40	40
<b>SATKAN0002</b>	80	67	67	59	53	55	53	53	43	46	42	44
<b>SATKAN0001</b>	82	69	70	63	58	60	58	59	50	51	49	51

S.6 Individual analysis results for all samples (Chapter 4). Results in red are from samples removed from this study due to high levels of residual contamination.

Sample	$\delta^{18}\text{O}$ values									Mean	SD	SE	No. of replicates
NTADAC0001	29.9	29.4	29.7	29.9	28.8	28.5	29.1	30.4		29.5	0.6	0.2	8
NTAGFU0031	31.7	31.6	31.3	31.6	31.2	30.6	31.2	31.2		31.3	0.4	0.1	8
NTAGFU0040	34.2	34.5	34.3							34.3	0.1	0.1	3
NTAGFU0017	33.5	33.5	34.1	33.8						33.7	0.3	0.2	4
NTAGFU0010	30.9	30.4	31.1							30.8	0.3	0.2	3
NTAGFU0008	31.8	31.6	31.6	32.9						32.0	0.6	0.3	4
NTAGFU0001	32.2	32.3	33.4	33.9	33.3	33.2				33.1	0.7	0.3	6
NTABRT0004	33.0	33.9	32.9	33.1	33.0	33.6				33.2	0.4	0.2	6
NTAFIN0019	37.6	38.0	38.2	37.3	38.7	37.2	37.4	37.3	36.8	37.6	0.6	0.2	9
SAASTP0004	33.2	34.4	33.7	34.0	33.3	34.0	33.2	33.1	33.5	33.6	0.4	0.1	9
SAASTP0001	37.0	36.3	37.5	36.6	36.8					36.8	0.4	0.2	5
SATFLB0005	29.4	29.0	28.7							29.0	0.4	0.2	3
SATFLB0008	34.8	34.2	35.0	34.1						34.5	0.4	0.2	4
SATFLB0010	36.8	36.7	36.4	37.0						36.7	0.3	0.1	4
SATFLB0014	37.8	38.6	38.7							38.4	0.4	0.3	3
SATFLB0012	39.5	39.2	39.4	40.5	40.1	40.1	39.5	39.8	39.2	39.7	0.4	0.1	9
SATFLB0015	23.2	26.4	27.0	23.7	23.2	28.0	23.4	24.0	23.6	24.7	1.9	0.6	9
SATKAN0002	16.6	17.2	16.5	26.4	22.3	22.4	22.2	17.2	18.4	18.3	3.4	0.9	16
SATKAN0002 (continued)	17.9	16.6	16.1	17.0	16.1	17.7	12.0						
SATKAN0001	31.4	31.7	31.8	32.0	31.9	30.7	31.9	32.4	32.2	31.8	0.5	0.2	9
P24	27.6	28.0	27.7	27.8	28.4	28.0	28.3	28.0		28.0	0.3	0.1	8

Sample	$\delta^{18}\text{O}$ values						Mean	SD	SE	No. of replicates	
P25	29.0	30.3	30.8				30.0	0.9	0.5	3	
P18	25.0	25.0	25.2				25.0	0.1	0.1	3	
P19	21.1	21.3	21.2				21.2	0.1	0.0	3	
P20	24.7	25.8	25.3				25.3	0.5	0.3	3	
P21	22.2	22.5	22.4	22.9			22.5	0.3	0.1	4	
P22	24.2	23.8	24.2				24.1	0.2	0.1	3	
P23	26.8	27.2	27.6				27.2	0.4	0.3	3	
P15	26.4	25.6	26.6	26.2			26.2	0.4	0.2	4	
P38	22.1	23.2	23.9				23.1	0.9	0.5	3	
P13	27.6	27.9	27.1	27.5	28.1		27.6	0.4	0.2	5	
P07	26.0	27.3	26.1	25.6	26.3	25.3	26.4	26.1	0.6	0.2	7
P09	29.1	29.7	29.3	30.2	28.9			29.5	0.5	0.2	5
P10	25.9	25.6	27.0					26.2	0.8	0.4	3
P12	29.0	29.1	29.3					29.1	0.1	0.1	3
P05	30.7	31.1	30.9	30.5	31.7	31.5	30.7	31.0	0.4	0.2	7
P06	30.0	30.4	30.4	29.9	30.6	30.7	30.4	30.3	0.3	0.1	7
P41	28.1	28.8	28.7	28.1	29.2	29.0		28.6	0.5	0.2	6
P01	24.3	23.9	24.7	24.8				24.4	0.4	0.2	4
P02	26.3	25.9	26.1	26.3				26.2	0.2	0.1	4
P37	29.1	28.8	28.8	27.4				28.5	0.8	0.4	4
P31	29.4	28.6	30.3	29.4				29.4	0.7	0.3	4
P32	27.6	28.6	27.3					27.8	0.6	0.4	3
P26	25.4	26.6	25.8					25.9	0.6	0.3	3
P30	28.8	28.8	29.0	30.0				29.1	0.6	0.3	4
P36	29.7	28.4	29.6	29.9	28.6			29.2	0.7	0.3	5
P27	29.5	30.7	30.5					30.2	0.6	0.4	3

S.7 Pearson's product-moment correlation coefficient values.

Parameter	Aristida ( $\delta^{18}\text{O}$ )	Plants ( $\delta^{18}\text{O}$ )	Soil ( $\delta^{18}\text{O}$ )	Modelled phytoliths from 100% precipitation ( $\delta^{18}\text{O}$ )	Modelled phytoliths from 100% leaf water ( $\delta^{18}\text{O}$ )	Predicted plant phytolith ( $\delta^{18}\text{O}$ )	Predicted soil phytolith ( $\delta^{18}\text{O}$ )
<b>Temperature</b>							
<b>annual mean (1960-2014)</b>	r = -0.81, p = 0.001	r = -0.43, p = 0.03	r = -0.57, p = 0.02	r = -0.82, p = <0.001	r = -0.77, p = <0.001	r = -0.84, p = <0.001	r = -0.36, p = 0.17
<b>1 month mean maximum</b>	r = 0.34, p = 0.29	r = -0.02, p = 0.93	r = -0.29, p = 0.27	r = -0.77, p = <0.001	r = -0.47, p = 0.01	r = -0.77, p = <0.001	r = 0.94, p = <0.001
<b>3 month mean maximum</b>	r = 0.33, p = 0.30	r = -0.09, p = 0.66	r = -0.43, p = 0.09	r = -0.91, p = <0.001	r = -0.54, p = 0.004	r = -0.90, p = <0.001	r = -0.59, p = 0.02
<b>6 month mean maximum</b>	r = -0.09, p = 0.79	r = -0.20, p = 0.32	r = -0.60, p = 0.01	r = -0.93, p = <0.001	r = -0.62, p = <0.001	r = -0.93, p = <0.001	r = -0.51, p = 0.04
<b>Annual mean maximum (1 year before collection)</b>	r = -0.80, p = 0.002	r = -0.41, p = 0.03	r = -0.53, p = 0.04	r = -0.83, p = <0.001	r = -0.70, p = <0.001	r = -0.85, p = <0.001	r = -0.49, p = 0.06
<b>Annual mean maximum (2 years before collection)</b>	r = -0.78, p = 0.003	r = -0.43, p = 0.03	r = -0.53, p = 0.04	r = -0.84, p = <0.001	r = -0.75, p = <0.001	r = -0.86, p = <0.001	r = -0.77, p = <0.001
<b>Annual mean maximum (5 years before collection)</b>	r = -0.76, p = 0.004	r = -0.42, p = 0.03	r = -0.51, p = 0.04	r = -0.85, p = <0.001	r = -0.71, p = <0.001	r = -0.86, p = <0.001	r = -0.85, p = <0.001



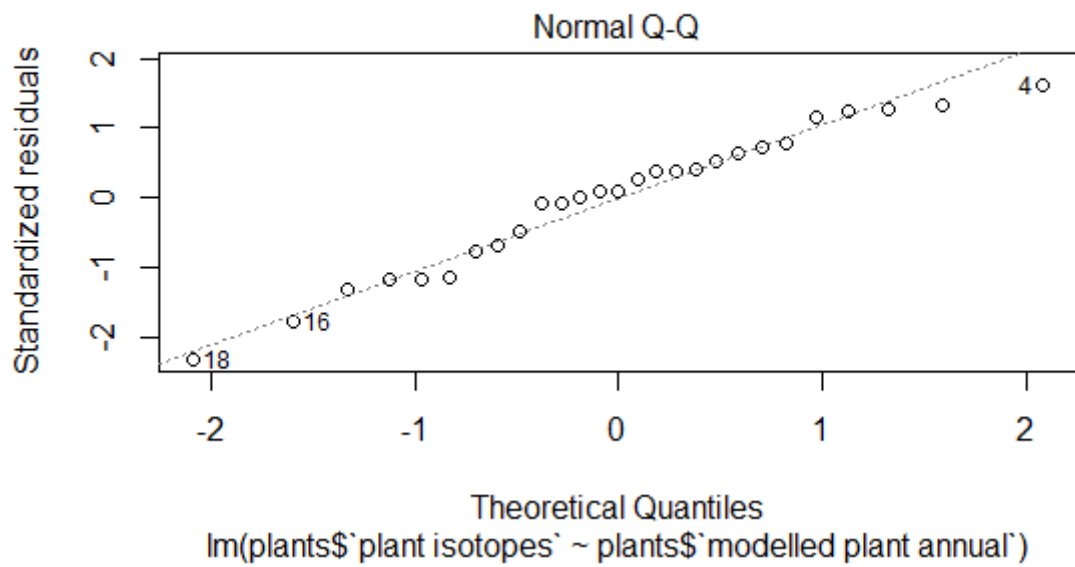
<b>Warmest period mean maximum (1 year before collection)</b>	r = 0.43, p = 0.17	r = -0.21, p = 0.29	r = -0.27, p = 0.31	r = -0.74, p = <0.001	r = -0.16, p = 0.43	r = -0.70, p = <0.001	r = 0.85, p = <0.001
<b>Warmest period mean maximum (2 year before collection)</b>	r = 0.68, p = 0.01	r = -0.12, p = 0.55	r = -0.22, p = 0.42	r = -0.62, p = <0.001	r = 0.01, p = 0.97	r = -0.57, p = 0.002	r = 0.86, p = <0.001
<b>Warmest period mean maximum (5 year before collection)</b>	r = 0.78, p = 0.003	r = -0.12, p = 0.57	r = -0.16, p = 0.55	r = -0.59, p = 0.001	r = 0.09, p = 0.66	r = -0.54, p = 0.004	r = 0.81, p = <0.001
<b>Relative humidity</b>							
<b>annual mean (1960-2014)</b>	r = -0.90, p = <0.001	r = -0.33, p = 0.09	r = -0.09, p = 0.75	r = 0.21, p = 0.30	r = -0.58, p = 0.001	r = 0.13, p = 0.52	r = 0.08, p = 0.76
<b>1 month mean at maximum temperature</b>	r = -0.38, p = 0.22	r = 0.00, p = 0.98	r = -0.29, p = 0.27	r = 0.18, p = 0.36	r = -0.24, p = 0.24	r = 0.15, p = 0.47	r = 0.79, p = <0.001
<b>3 month mean at maximum temperature</b>	r = -0.68, p = 0.01	r = -0.15, p = 0.46	r = -0.31, p = 0.25	r = 0.15, p = 0.44	r = -0.50, p = 0.009	r = 0.09, p = 0.65	r = -0.51, p = 0.05
<b>6 month mean at maximum temperature</b>	r = -0.80, p = 0.002	r = -0.28, p = 0.15	r = -0.14, p = 0.61	r = 0.09, p = 0.66	r = -0.65, p = <0.001	r = 0.02, p = 0.94	r = -0.61, p = 0.01
<b>Annual mean at maximum temperature (1 year before collection)</b>	r = -0.87, p = <0.001	r = -0.32, p = 0.10	r = -0.11, p = 0.68	r = 0.12, p = 0.56	r = -0.66, p = <0.001	r = 0.04, p = 0.85	r = -0.65, p = 0.006
<b>Annual mean at maximum temperature (2 years before collection)</b>	r = -0.86, p = <0.001	r = -0.30, p = 0.12	r = -0.09, p = 0.74	r = 0.18, p = 0.36	r = -0.61, p = <0.001	r = 0.10, p = 0.60	r = 0.20, p = 0.46

<b>Annual mean at maximum temperature (5 years before collection)</b>	r = -0.89, p = <0.001	r = -0.28, p = 0.16	r = -0.10, p = 0.71	r = 0.18, p = 0.36	r = -0.61, p = <0.001	r = 0.11, p = 0.59	r = 0.09, p = 0.74
<b>Annual mean at maximum temperature (1976-2013)</b>	r = -0.90, p = <0.001	r = -0.30, p = 0.13	r = -0.12, p = 0.67	r = 0.19, p = 0.35	r = -0.61, p = <0.001	r = 0.11, p = 0.58	r = -0.61, p = 0.01
<b>Warmest period mean at maximum temperature (1 year before collection)</b>	r = -0.82, p = 0.001	r = -0.41, p = 0.04	r = -0.56, p = 0.02	r = -0.34, p = 0.08	r = -0.91, p = <0.001	r = -0.41, p = 0.03	r = 0.95, p = <0.001
<b>Warmest period mean at maximum temperature (2 year before collection)</b>	r = -0.81, p = 0.001	r = -0.42, p = 0.03	r = -0.61, p = 0.01	r = -0.45, p = 0.02	r = -0.96, p = <0.001	r = -0.52, p = 0.006	r = 0.97, p = <0.001
<b>Warmest period mean at maximum temperature (5 year before collection)</b>	r = -0.82, p = <0.001	r = -0.41, p = 0.03	r = -0.65, p = 0.006	r = -0.45, p = 0.02	r = -0.96, p = <0.001	r = -0.52, p = 0.005	r = 0.96, p = <0.001
<b>Warmest period mean at maximum temperature (1976-2013)</b>	r = -0.84, p = <0.001	r = -0.41, p = 0.04	r = -0.63, p = 0.009	r = -0.40, p = 0.04	r = -0.94, p = <0.001	r = -0.47, p = 0.01	r = -0.65, p = 0.006
<b>D18O_plants_measured</b>				r = 0.24, p = 0.22	r = 0.41, p = 0.04	r = 0.27, p = 0.18	r = 0.86, p = <0.001
<b>D18O_soil_measured</b>	r = 0.31, p = 0.32	r = 0.17, p = 0.40		r = 0.49, p = 0.01	r = 0.72, p = <0.001	r = 0.53, p = 0.005	r = 0.84, p = <0.001

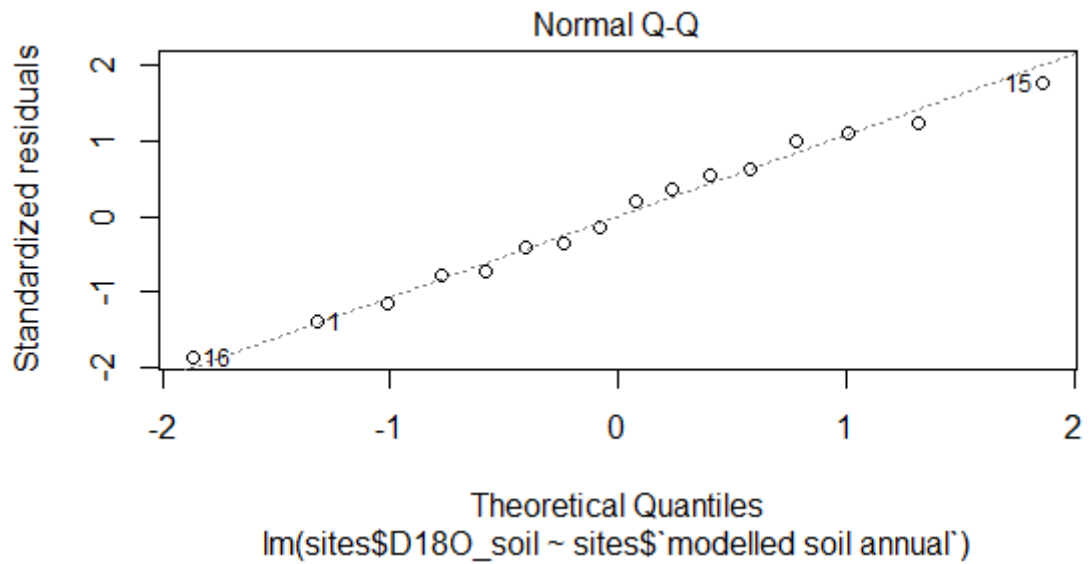
## S.8 Oxygen isotope values used in Chapter 4 modelling

Site	$\delta^{18}\text{O}$ from Hollins Isoscape ‰ (precipitation)	$\delta^{18}\text{O}$ leaf water 5_yr_avg (Craig Gordan Model)	Modelled $\delta^{18}\text{O}$ phytoliths 100% from precipitation	Modelled $\delta^{18}\text{O}$ phytoliths 100% from leaf water	Predicted $\delta^{18}\text{O}$ phytoliths from soil	Predicted $\delta^{18}\text{O}$ phytoliths from plants
NTADAC0001	-5.46	12.19	25.06	42.70	31.71	26.47
NTAGFU0031	-5.05	14.20	24.97	44.21	32.23	26.51
NTAGFU0040	-4.88	15.19	24.96	45.03	32.53	26.57
NTAGFU0017	-8.31	12.44	22.23	42.98	30.05	23.89
NTAGFU0010	-8.14	13.55	22.24	43.93	30.42	23.98
NTAGFU0008	-7.80	15.07	22.66	45.53	31.28	24.49
NTAGFU0001	-7.73	15.27	22.63	45.62	31.30	24.47
NTABRT0004	-6.48	17.87	24.73	49.08	33.92	26.69
NTAFIN0019	-5.67	18.74	25.80	50.21	35.00	27.75
NTAFIN0022	-5.56	18.79	25.93	50.28	35.12	27.88
SAASTP0004	-4.85	19.48	26.58	50.91	35.76	28.53
SAASTP0001	-4.83	19.43	26.74	51.00	35.89	28.69
SATFLB0005	-3.94	18.40	29.34	51.69	37.77	31.14
SATFLB0008	-3.74	17.47	30.01	51.22	38.01	31.71
SATFLB0010	-4.07	16.06	29.51	49.64	37.11	31.13
SATFLB0014	-4.86	13.93	29.81	48.61	36.90	31.32
SATFLB0012	-5.01	13.23	29.50	47.74	36.38	30.96
SATFLB0015	-5.01	11.60	30.35	46.96	36.62	31.69
SATKAN0002	-4.66	11.88	30.53	47.07	36.77	31.86
SATKAN0001	-4.73	10.07	30.91	45.71	36.49	32.09

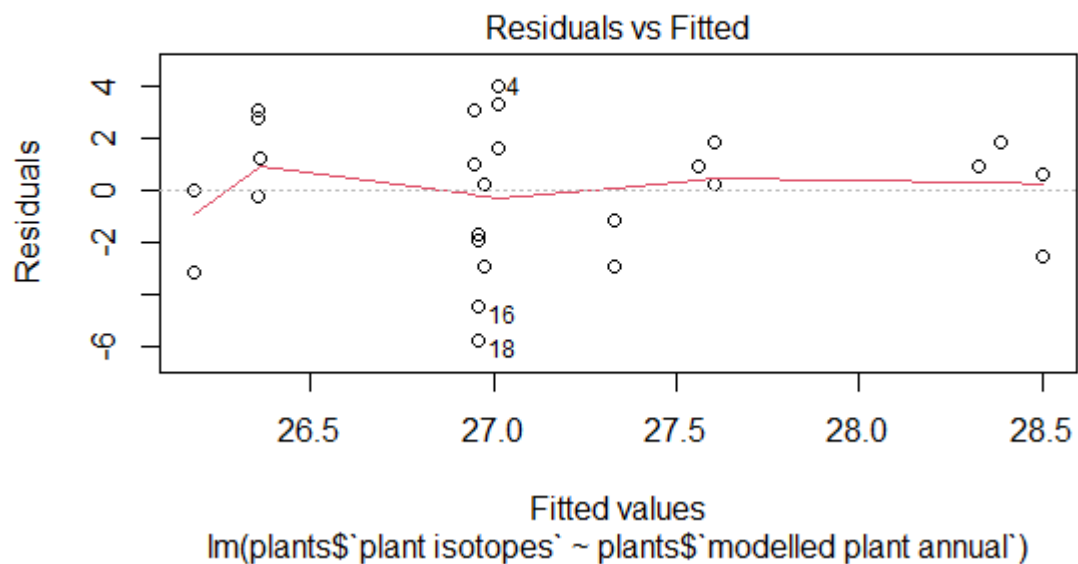
S.9 Q-Q plot for measured vs predicted  $\delta^{18}\text{O}$  values of plant phytoliths



S.10 Q-Q plot for measured vs predicted  $\delta^{18}\text{O}$  values of soil phytoliths



S.11 residual plot for measured vs predicted  $\delta^{18}\text{O}$  values of plant phytoliths



S.12 residual plot for measured vs predicted  $\delta^{18}\text{O}$  values of soil phytoliths

